

**Schlaganfall bei Normotensiven und Hypertensiven Ratten:
Effekte von Lithium und Hemmstoffen des
Renin-Angiotensin-Systems**

Dissertation

zur Erlangung des Doktorgrades

der Mathematisch-Naturwissenschaftlichen Fakultät

der Christian-Albrechts-Universität zu Kiel

vorgelegt von

Jihong Xu

Kiel,

im September 2002

**Stroke in Normotensive and Hypertensive Rats:
Effects of Lithium and Inhibitors of the Renin-Angiotensin System**

Thesis submitted for the degree of Doctor of Philosophy

by

Jihong Xu

Institute of Pharmacology

Christian-Albrechts-University of Kiel

September 2002

Referee:

Co-referee:

Date of oral examination:

Admitted for printing: Kiel,

Prof. Dr. A. Ziegler

Prof. Dr. W. Hänsel

01. November 2002

06. November 2002

gez.:

Prof. Dr. A. Irle

Stellvertreter Dekan

Statement of Originality

I declare that this thesis has not been submitted in any form for another degree or diploma at any university. Results discussed in this thesis are my own work, and information derived from the literature or unpublished work of others has been acknowledged in the text and a list of references provided.

CONTENTS

	Page	
1	Introduction	1
1.1	Stroke and animal models of stroke	1
1.1.1	Stroke-prone spontaneously hypertensive rats	1
1.1.2	Intraluminal thread model of focal cerebral ischemia	2
1.2	Cell death and focal cerebral ischemia	2
1.3	Microglial responses and focal cerebral ischemia	4
1.4	The renin-angiotensin system and stroke	5
1.5	Neuroprotective effects of lithium	7
1.6	Aims of the study	9
2	Materials and Methods	11
2.1	Preparation of solutions and reagents	11
2.1.1	Solutions and reagents for immunohistochemistry and perfusion	11
2.1.2	Solutions for drug treatment	12
2.1.3	Solutions and reagents for albumin measurement	13
2.1.4	Solutions and reagents for plasma renin activity (PRA) measurement	14
2.2	Animals	14
2.3	Stroke prevention in SHRSP	14
2.3.1	Experimental protocol	14
2.3.2	Systolic blood pressure (SBP) measurement	15
2.3.3	Determination of salt and water intake	15
2.3.4	Urine collection	16
2.3.5	Blood collection	16
2.3.6	Determination of urinary and plasma sodium, potassium and lithium concentrations	16
2.3.7	Determination of urinary albumin concentration	16
2.3.8	Determination of plasma renin activity	17
2.3.9	Cresyl violet staining	17
2.3.10	TUNEL staining	17
2.4	Intraluminal thread model of focal cerebral ischemia	18

2.4.1	Preparation of the occluding thread	18
2.4.2	Surgery	18
2.4.3	Regional cerebral blood flow (rCBF) monitored by Laser-Doppler flowmetry	18
2.4.4	Experimental design	19
2.4.5	Implantation of the femoral artery catheter	21
2.4.6	Measurement of mean arterial blood pressure (MAP)	21
2.4.7	Blood collection for the measurement of blood parameters	21
2.4.8	Evaluation of neurological deficits	21
2.4.8.1	A grading scale of 0-3 developed by Bederson et al. (1986)	22
2.4.8.2	A grading scale of 3-18 developed by Garcia et al. (1995b)	22
2.4.9	Tissue processing	24
2.4.10	Measurement of the infarction size	25
2.4.11	Immunohistochemistry	26
2.4.11.1	TUNEL staining	26
2.4.11.2	Activated Caspase-3	27
2.4.11.3	Activated microglia	27
2.5	Statistical analysis	28
3	Results	30
3.1	Stroke prevention in SHRSP	30
3.1.1	Survival rate	30
3.1.2	Systolic blood pressure	32
3.1.3	Body weight	34
3.1.4	Water intake and urinary volume	36
3.1.5	The concentrations of sodium and potassium in plasma and their urinary excretions	40
3.1.6	Lithium concentration in plasma and urine	44
3.1.7	Daily urinary excretion of albumin	46
3.1.8	Plasma renin activity	47
3.1.9	Neurological signs	48
3.1.10	Histopathologic studies	48
3.1.11	TUNEL staining	49
3.2	Intraluminal thread model of focal cerebral ischemia	56

3.2.1	Physiological parameters	56
3.2.1.1	Mean arterial blood pressure (MAP)	56
3.2.1.2	Blood parameters	58
3.2.2	Measurement of regional cerebral blood flow	63
3.2.3	Neurological evaluation	64
3.2.4	Total infarct volume, serial infarct sizes and edema volume	67
3.2.5	TUNEL staining	72
3.2.6	Activated caspase-3 immunoreactivity	75
3.2.7	Activated Microglia	78
3.2.8	Li ⁺ -concentration in plasma	81
4	Discussion	82
4.1	Stroke development in salt-loaded SHRSP	82
4.2	Effects of captopril and captopril plus lithium on stroke prevention in salt-loaded SHRSP	83
4.3	Effects of telmisartan and telmisartan plus lithium on stroke prevention in salt-loaded SHRSP	87
4.4	Effects of lithium on focal cerebral ischemia in normotensive rats	89
4.5	Effects of captopril and captopril plus lithium on focal cerebral ischemia in normotensive rats	92
4.6	Effects of telmisartan and telmisartan plus lithium on focal cerebral ischemia in normotensive rats	95
5	Summary	99
6	Zusammenfassung	101
	References	104
	Acknowledgements	126
	Curriculum Vitae	127

Abbreviations

ACE	angiotensin-converting enzyme
Ang I	angiotensin I
Ang II	angiotensin II
AP-1	activator protein-1
AT1	angiotensin II receptor type 1
AT2	angiotensin II receptor type 2
BSA	Bovine Serum Albumin
CCA	common carotid artery
CE	converting enzyme
CSF	cerebrospinal fluid
CAMP	adenosine 3', 5'-cyclic monophosphate
CBF	cerebral blood flow
ECA	external carotid artery
EDTA	ethylenediaminetetraacetic acid
ICA	internal carotid artery
IL-1 β	interleukin-1 β
IL-6	interleukin-6
IP-3	inositol 1,4,5-triphosphate
ITFs	inducible transcription factors
LDF	laser-Doppler flowmetry
MAP	mean arterial blood pressure
MCA	middle cerebral artery
MCAO	middle cerebral artery occlusion
MCP-1	monocyte chemoattractant protein-1
NF- κ B	nuclear factor κ B
NGS	normal goat serum
NMDA	N-methyl-D-aspartate
PARP	cleavage of poly (ADP-ribose) polymerase
PB	Phosphate Buffer
PBS	Phosphate Buffered Saline
PRA	plasma renin activity

RAS	renin-angiotensin system
rCBF	regional cerebral blood flow
RT	room temperature
SAH	subarachnoid hemorrhage
SBP	systolic blood pressure
SHR	spontaneously hypertensive rat
SHRSP	stroke-prone spontaneously hypertensive rat
TUNEL	Terminal deoxynucleotidyl transferase-mediated dUTP nick-end labeling
VSMC	vascular smooth muscle cells

1 Introduction

1.1 Stroke and animal models of stroke

Stroke is a cardiovascular disease affecting the blood vessels that supply oxygen and nutrients to the brain. A stroke occurs when a blood vessel within the brain or leading to the brain ruptures or is clogged e.g. by a thrombus. Four types of stroke can be distinguished. The first two, cerebral thrombosis and cerebral embolism, are caused by blood vessel occlusion and account for almost 80 % of all strokes. The other two types, subarachnoid hemorrhage and intracerebral hemorrhage, are caused by bleeding or hemorrhage, often as a result of an aneurysm in the brain or a head injury, and are classified as hemorrhagic strokes.

Stroke is the third most common cause of death in most western populations after coronary-heart disease and cancer. It is also an important cause of serious, long-term disability in patients who survive and experience the physical and mental consequences of insult for many years thereafter.

The development of reliable animal models of stroke based on similarities with syndromes of human cerebrovascular disease would allow the study of the pathophysiology of this disease as well as the efficacy of various treatment modalities. In the present studies, we used two different animal models of stroke namely the stroke-prone spontaneously hypertensive rat (SHRSP) and a model of focal cerebral ischemia induced by the temporal occlusion of the middle cerebral artery.

1.1.1 Stroke-prone spontaneously hypertensive rats

In 1963, spontaneously hypertensive rats (SHR) were isolated from a Wistar-Kyoto rat colony by Okamoto and Aoki (Okamoto and Aoki, 1963). Later, the SHR colony was further separated by Okamoto and his colleagues into several sublines (Okamoto et al., 1972), some of which had a tendency to develop cerebrovascular lesions (cerebral hemorrhage and/or infarction) and are named stroke-prone SHR. The SHRSP is a genetic model of severe hypertension in which the incidence of cerebral disorders and spontaneous stroke is very high (Okamoto et al., 1974). Because of the similarity between the cerebrovascular lesions observed in SHRSP and those observed in humans, SHRSP have long been used for the investigation of preventive therapies for stroke.

It is well known that high blood pressure is one of the causative factors of stroke in humans and that abnormally high salt intake results in an elevation of the blood pressure. In SHRSP increased salt intake accelerated the development of hypertension and the occurrence of

stroke. When maintained on a 1% NaCl drinking solution and supplemented with a special so-called “japan diet”, these rats rapidly develop malignant hypertension and stroke (Nagaoka et al., 1976 and Stier et al., 1988).

1.1.2 Intraluminal thread model of focal cerebral ischemia

Animal models of focal cerebral ischemia are generally intended to replicate features of human focal ischemic stroke produced by occlusion of a single cerebral artery. Thus, the vast majority of animal models of focal cerebral ischemia employ middle cerebral artery occlusion (MCAO). This is surgically feasible in primate, cats, and rodents, especially rats. The most frequently used procedures to achieve occlusion are coagulation of the MCA through a temporal craniectomy (Tamura et al., 1981; Coyle, 1982; Bederson et al., 1986) and intraluminal thread occlusion without craniectomy via a cervical carotid approach (Koizumi et al., 1986; Longa et al., 1989; Nagasawa and Kogure, 1989). The intraluminal occlusion method has become an increasingly popular tool for studying the pathophysiology and treatment of stroke since its original description (Koizumi et al., 1986). The greatest advantage of this model is the ease with which recirculation can be commenced simply by pulling out the thread and re-exposing the origin of the MCA.

Regardless of the species or technique of MCA occlusion, the resulting ischemia exhibits several important features germane to its neuropathology: a gradient of cerebral blood flow (CBF) decrement which is lowest (typically 10-20% of control, or below) in the ischemic core, a zone destined to develop infarction, and somewhat higher (20-40% of control) in the surrounding penumbral zone, whose fate depends upon multiple factors. The final stage of infarct development in focal cerebral ischemia is pan-necrosis, in which the neuronal death is accompanied by glial and vascular cell death and loss of cellular elements (Lipton, 1999).

Animal models of focal cerebral ischemia have provided some insights into the dynamic events involved in ischemic brain injury, and were widely used in preclinical trials. It is thus essential to strive for lesion reproducibility, physiological controls, and rigorous assessment of outcome by means of quantitative histopathology and secondarily by behavioral outcome measures.

1.2 Cell death and focal cerebral ischemia

In recent years it became clear that hypoxic neurons die by two different modes: necrosis and apoptosis (Okamoto et al., 1993; Ferrer et al., 1994). Apoptosis is an active process of cell destruction characterized by cell shrinkage and chromatin aggregation followed by

fragmentation, while the integrity of the cell membrane and mitochondria is still preserved. Apoptotic cell death is energy dependent and not associated with inflammation and damage to the neighboring tissue (Wyllie et al., 1980; Savill et al., 1993; Cohen, 1993). Necrosis is instead characterized by passive cell swelling, intense mitochondrial damage and membrane dysfunction. Necrosis usually causes an inflammatory response and injury to the surrounding tissue (Choi, 1992).

Linnik et al. (1993) were the first to implicate apoptosis in focal brain ischemia. By application of the protein synthesis inhibitor cycloheximide, they were able to reduce the size of focal cerebral infarction by 70 %, which indicated that neuronal loss induced by ischemia was dependent on de novo protein synthesis. Moreover, DNA fragmentation was shown in extracts of ischemic brains indicating programmed cell death (Linnik et al., 1993, Tominaga et al., 1993). These initial findings were extended by several groups (Manev et al., 1994; Li et al., 1995a,b; Braun et al., 1996; Charriaut-Marlange et al., 1996). Li et al. (1995a,b) identified apoptotic cells, mostly neurons, by electron microscopy in the inner boundary zone of infarction of rats subjected to transient (2 h) focal ischemia. Apoptotic neurons increased in number as early as 0.5 h, peaked at 24-48 h, and persisted for 4 weeks after the onset of reperfusion. The presence of apoptotic neurons several days after ischemia suggests that cell death after ischemia is a dynamic process and not simply caused by the initial ischemic insult. In focal ischemia, the central lesion or core is conventionally considered necrotic (Garcia et al., 1995a,b; Lipton, 1999), whereas the bordering area, or penumbra, recruits apoptotic mechanisms (Linnik et al., 1993; Li et al., 1995a,b; Charriaut-Marlangue et al., 1996). However, a large body of evidence has been accumulated, which suggests that the both mechanisms may just represent extremes of a potentially continuous spectrum of possibilities for a cell population to die. In tissue, apoptosis and necrosis may either co-exist or be a sequential phenomena. The mode of cell death may be influenced by the intensity or exposure time toward insults (Bonfoco et al., 1995; Dybpukt et al., 1995).

DNA fragmentation in the brain after focal ischemia can be detected by Terminal deoxynucleotidyl transferase-mediated dUTP nick-end labeling (TUNEL) (Chen et al., 1997). This is not an unambiguous identification of apoptosis because it labels both nucleosomal and non-nucleosomal fragments (Portera-Cailliau et al., 1995). The latter are formed during necrotic cell death.

Caspases are implicated in the control of apoptosis (Li and Yuan, 1999; Hengartner, 2000). Given the number and diversity of caspase targets, most, if not all, of the morphological features described for apoptosis are caspase-dependent. Caspases do not appear to be

associated with necrotic death (Armstrong et al., 1997; Gottron et al., 1997). They participate in cascades that include initiator and effector caspases (Friedlander et al., 1997; Fink et al., 1998), which are both activated by ischemia (Schielke et al., 1998; Plesnila and Moskowitz, 2000). Caspase-3 is one of the key executioners of apoptosis (Cohen, 1997).

The penumbra area has been considered a therapeutic target in focal cerebral ischemia (Ginsberg and Pulsinelli, 1994; Hossmann, 1994). In the present study, we examined the effect of different treatment regimens on activated caspase-3 immunoreactivity and subsequent DNA fragmentation on the cortical penumbral area of rats with transient focal ischemia following 2 days of reperfusion.

1.3 Microglial responses and focal cerebral ischemia

Microglia are a class of mononuclear phagocytes intrinsic to the CNS. These cells are the principal immune effector elements of the brain and are associated with diverse clinical problems including cerebrovascular disease (Giulian, 1992). Four forms of microglia can be defined on the basis of developmental and pathophysiological studies. They include (1) the amoeboid microglia, found predominantly in the white matter perinatally, (2) the ramified microglia, found in the gray and white matter postnatally, (3) the activated microglia, found in areas of secondary reaction due to nerve transection and CNS inflammation, and (4) the reactive (phagocytic) microglia, found in areas of trauma, ischemic injury, or neuronal degeneration (Hickey et al., 1992; Jordan and Thomas, 1988; Perry and Gordon, 1988; Streit et al., 1988). Virtually all microglia of the mature CNS are found as quiescent, ramified cells with no recognized function. During CNS injury, ramified microglia retract processes, become more amoeboid-like, and transform into the activated or reactive microglia (del Rio-Hortega, 1932).

In transient (2 h) MCAO, Zhang et al. (1997) described the temporal profile of the microglia response. Round and amoeboid cells became predominant in the ischemic core lesion and were mingled with highly ramified microglia in the boundary zone at 22 h of reperfusion. A high number of ramified microglia was found in an adjacent area containing morphologically intact neurons. Round and amoeboid cells were localized to the inner boundary of the ischemic lesion surrounding the infarct zone at 46 h of reperfusion. From 70-166 h of reperfusion round and amoeboid cells were present throughout the entire ischemic lesion in the infarct zone. Similar results were reported by Kato et al. (1996) and by Lehrmann et al. (1997). It remains unclear from these studies what proportion of phagocytes was microglia-derived or recruited from the circulation. Since microglia and macrophages not only share

heritage (Hickey et al., 1992), but also surface and endocellular markers (Flaris et al., 1993), they become virtually indistinguishable under pathological conditions (Stoll et al., 1989; Perry et al., 1993; George and Griffin, 1994).

There is some evidence that delayed neuronal and functional losses after ischemic injury are the results of neurotoxic inflammatory cells (Giulian 1997). First, neuronal poisons, including Ntox, can be only detected in tissues heavily infiltrated with reactive microglia or macrophages. The levels of neurotoxic activity found in CNS injured by ischemia correlate with the number of mononuclear phagocytes at the lesion sites. Importantly, no toxic activity was detected in neighboring non-inflamed tissues. Second, drugs that reduce inflammatory cell numbers also reduce the amount of Ntox released by damaged tissue. Third, active mononuclear phagocytes appear at a time of a delayed loss of neurons and deterioration in neurological function. Fourth, suppression of CNS inflammation improves both motor neuron survival and preserves motor functions. And fifth, isolation of specific cell populations confirmed that reactive mononuclear phagocytes are the principal source of neuron-killing factors in damaged CNS.

The surrounding penumbra, appears to be a suitable target for immunosuppressive therapies during the acute phase of ischemic injury. In the present study, we measured the density of activated microglia or macrophages in the cortical penumbral area of rats with transient focal ischemia following 2 days reperfusion, in order to evaluate the effects of different treatment regimens on inflammation after brain ischemia.

1.4 The renin-angiotensin system and stroke

The renin-angiotensin system (RAS) is a major physiological regulator of body fluid volume, electrolyte balance and blood pressure (Goodfriend et al., 1996; Griendling et al., 1996; Matsukawa and Ichikawa, 1997; Ardaillou, 1999). Angiotensin II (Ang II) is a potent vasoconstrictor hormone and is produced via the renin-angiotensin enzymatic cascade. Renin converts angiotensinogen into the decapeptide Ang I and angiotensin-converting enzyme (ACE) cleaves Ang I to form the active octapeptide Ang II (Ellis and Patterson, 1996; Edling et al., 1995). The major actions of Ang II are mediated by two subtypes of G-protein-coupled angiotensin receptors, the AT₁- and AT₂-receptors. Most of the classical actions of Ang II on fluid and blood pressure homeostasis are mediated by AT₁-receptors (de Gasparo et al., 2000). The renin-angiotensin system has been implicated in the development of end-organ damage, including strokes, in clinical and experimental situations. ACE inhibitor and Ang II AT₁-receptor antagonists have been shown to prevent the occurrence of stroke and mortality in

SHRSP (Stier et al., 1989; Stier et al., 1991; Vacher et al., 1993; Richer et al., 1994; Camargo et al., 1991; Fornes et al., 1993). Many experimental studies showed that both ACE inhibitors and AT₁ antagonists produced an anti-stroke effect independent of a change in blood pressure. It has been suggested that such treatment may protect against vascular damage produced by the elevations in plasma Ang II. A reduction in neutrophil chemoattraction to vascular endothelium, decreased vascular smooth muscle hypertrophy and hyperplasia, decreased vascular permeability, lowered plasma aldosterone levels, and a reduction in the incidence of cerebrovascular fibrinoid necrosis have all been suggested as possible beneficial mechanisms that could act to retard stroke development in response to the inhibition of the effects of Ang II through ACE inhibitor or AT₁ receptor antagonist treatment (Camargo et al., 1991; Stier et al., 1991; Stier et al., 1989; Camargo et al., 1993; Inada et al., 1995; Lee et al., 1994; Stier et al., 1993; MacLeod et al., 1997). However, not all of the effects of ACE inhibition can be explained by the decrease in Ang II generation. Some of them, especially with respect to organ protection, have also been attributed to bradykinin potentiation (Gohlke et al., 1996). Ischemic stroke can be caused by a number of monogenic disorders, and the ACE gene is probably the most extensively investigated candidate gene in ischemic stroke (Hassan and Markus, 2000). ACE gene deletion polymorphism can result in a high serum level of ACE, which was shown to increase the risk and severity of the ischemic lesions (Catto et al., 1996; Doi et al., 1997). In animal models of cerebral ischemia ACE inhibitors or AT₁ receptor antagonists improved the neurological outcome and reduced the infarct volume (Werner et al., 1991; Dai et al., 1999; Ravati et al., 1999; Nishimura et al., 2000). Recently Walther et al. (2002) demonstrated a direct correlation between brain Ang II and the severity of ischemic injury in transgenic mice after focal cerebral ischemia. Angiotensinogen-overexpressing mice had an enlarged infarct size and a much smaller penumbra area, and AT₁ receptor knockout mice had a smaller lesion size and a much larger penumbra area compared with their wild-type litter-mates, after 1 or 24 h of permanent MCAO. Ischemic stroke results from a transient or permanent reduction or interruption of cerebral blood flow, and the autoregulation of cerebral blood flow is impaired during brain ischemia. The neuroprotective effects of ACE inhibitors and AT₁ receptor antagonists, or transgene-induced suppression of AT₁ receptor, may partly be related to the normalization of cerebrovascular autoregulation (Culman et al., 2001; Walther et al., 2002). ACE inhibitors and AT₁ receptor antagonists were shown to shift the upper and lower limits of cerebral blood flow autoregulation to lower blood pressure levels and result in decreased neuronal injury (Paulson et al., 1988; Vraamark et al., 1995; Nishimura et al., 2000; Saavedra et al., 2001). Further mechanisms are involved in the

beneficial effect of AT₁ receptor antagonists in brain ischemia. Long-term blockade of central AT₁ receptors has been shown to reduce the expression of c-Fos and c-Jun in response to cerebral ischemia. Activation of ITFs (inducible transcription factors) after hypoxia-ischemia represents one of the links between the extracellular signals and the initiation of intracellular genomic metabolic events that are associated with regeneration and survival or lead to a selective delayed neuronal death. Focal cerebral ischemia has been shown to induce the expression of gene products of the c-Fos and c-Jun families in the nervous system. c-Jun in particular is believed to initiate degeneration via de novo protein synthesis of apoptotic effectors (Dai et al., 1999). The involvement of AT₁ stimulation in apoptosis caused by Ang II has been shown in myocytes (Leri et al., 1998) and endothelial cells in vitro (Li et al., 1999) and in rat blood vessels in vivo (Diep et al., 1999). Some ACE inhibitors attenuated cardiomyocyte apoptosis in SHR (Diez et al., 1997). These data suggested that ACE inhibitors and AT₁ receptor antagonists could have a beneficial influence on cellular apoptosis which is thought to play a role in the pathology of several neurodegenerative diseases such as amyotrophic lateral sclerosis, multiple sclerosis, Parkinson's and Alzheimer's disease as well as stroke (Bredesen, 1995).

In contrast, several findings indicate a benefit from Ang II in brain ischemia. Infusion of Ang II or AT₂ receptor stimulation has been shown to decrease the mortality rate in gerbils with unilateral carotid ligation (Fernandez et al., 1986; Fernandez et al., 1994). Moreover, the ACE inhibitor, enalaprilat, and the non-selective Ang II receptor antagonist, saralasin, were shown to increase the mortality in the same gerbil model of brain ischemia (Kaliszewski et al., 1988). The promotion of angiogenesis and recruitment of pre-existing collateral circulation by Ang II in case of acute ischemia have been suggested as a possible mechanism of this benefit (Fournier et al., 2000).

1.5 Neuroprotective effects of lithium

For almost half a century, lithium has been the most widely used treatment for manic depressive illness. Its clinical profile includes the anti-manic and anti-depressant actions as well as prophylaxis of both mania and depression by reducing the frequency of the bipolar episodes (Goodwin and Jamison, 1990; Birch, 1991).

Increasing evidence supports the notion that lithium has neuroprotective effects both in vitro and in vivo. Lithium has been shown to protect against the toxic effects of a variety of insults including glutamate, NMDA receptor activation, low potassium and toxic concentrations of anticonvulsants in rat cerebellar granule cells (D'Mello et al., 1994; Nonaka et al., 1998a, b).

The protective effects of lithium against the deleterious actions of glutamate and NMDA receptor activation have also been demonstrated to occur in hippocampal and cortical neurons in culture (Nonaka et al., 1998a). Other in vitro studies have indicated that lithium induces the survival of PC12 cells after serum/nerve growth factor deprivation (Volonte and Rukenstein, 1993), and protects both PC12 cells and human neuroblastoma SH-SY5Y cells from ouabain toxicity (Li et al., 1994). Several studies have provided evidence for neuroprotective effects of lithium in vivo. Inouye et al. (1995) demonstrated that lithium pre-treatment delayed radiation-induced apoptosis in the cells of the external granular layer after newborn mice were exposed to gamma irradiation. Other studies have demonstrated that lithium attenuated both the behavioral deficits and the reduction in choline acetyl transferase activity induced by forebrain cholinergic system lesions (Pascual and Gonzalez, 1995) as well as the kainic acid-induced reduction in glutamate decarboxylase levels and [³H]D-aspartate up-take (Sparapani et al., 1997). In a rat model of ischemia, chronic lithium administration at higher doses markedly reduced brain infarction and neurological deficits induced by occlusion of the middle cerebral artery (Nonaka and Chuang, 1998).

In an attempt to elucidate the molecular mechanisms underlying the neuroprotection induced by lithium, it has been shown that long-term treatment with lithium increases the expression of the anti-apoptotic gene bcl-2. Lithium markedly increased the levels of bcl-2 in rat frontal cortex, hippocampus, and striatum in Wistar rats at therapeutically relevant concentrations (Manji et al., 1999). Similar to the situation observed in rat brain in vivo, lithium produced a marked increase in bcl-2 levels in SH-SY5Y cells and rat cerebellar granular cells (Chen and Chuang, 1999). Moreover, lithium reduced the levels of the pro-apoptotic protein p53 both in cerebellar granule cells (Chen and Chuang, 1999) and SH-SY5Y cells (Lu et al., 1999).

The effects of lithium on signaling pathways and transcription factors may contribute to its neuroprotective effects. A bimodal mechanism of action of lithium is proposed. This model describes the critical effect of lithium as that of a stabilizer of the magnitude of fluctuations of signaling processes. This is achieved by balancing positive and negative regulators of signaling processes which results in raising basal activities and diminishing maximal activities, thereby stabilizing signaling activities within an optimal range and preventing fluctuations either above or below this optimum. This model is applicable to many published results concerning the activation of AP-1 DNA binding and cyclic AMP production (Jope, 1999). It is important to emphasize that in addition to its neuroprotective effects, lithium is well known to exert toxic effects at higher concentration in a variety of experimental conditions (Hasegkar et al., 1996; Madiehe et al., 1995) as well as in humans (Goodwin and

Jamison, 1990; Lenox and Manji, 1998). In general, the lithium toxicity is related to dose, maturity of the cells, and interactions with other pharmacologic agents such as neuroleptics, cholinomimetics and ACE inhibitors (D'Mello et al., 1994; Jope et al., 1986; Lenox and Manji, 1998; Finley et al., 1996).

1.6 Aims of the study

A number of actions of lithium have been described which support the hypothesis of a synergistic interaction with RAS inhibitors such as ACE inhibitors. Lithium has been shown to decrease blood pressure in SHR, possibly related to a decrease in plasma ACE activity (Das and Bhargava, 1985). Synergistic effects may occur between lithium and ACE inhibitors at the level of the intracellular phosphatidylinositol signaling system, particularly inositol 1,4,5-triphosphate (IP-3). Lithium causes noncompetitive inhibition of monophosphatase, thus reducing the breakdown of inositol phosphate to inositol and causing depletion of IP-3 in the long-term. On the other hand, most of the AT₁ receptor-mediated effects of Ang II are mediated, at least in part, via IP-3. Lowering of IP-3 concentrations is seen at therapeutic lithium concentrations. This effect may be particularly important in the central nervous system because the inositol supply of neural cells is dependent on the local breakdown, in contrast to extraneural cells that may use inositol from nutrients (Lehmann and Ritz, 1995). ACE inhibitors reduce sympathetic transmission and facilitate parasympathetic nervous transmission. Lithium acts in a similar fashion and would tend to act synergistically with ACE inhibitors (Shionoiri, 1993; Matussek, 1972). Co-medication of lithium and ACE inhibitor (high dose) can increase toxicity.

Recently we have demonstrated synergistic interactions between lithium and the ACE inhibitor, captopril, in the prevention of stroke in SHRSP. Treatment of these rats with a low dose of captopril (25 mg/kg per day) doubled the life expectancy when compared to control rats although blood pressure was only slightly reduced. The addition of a low dose of lithium (1 mmol/kg) to captopril dramatically increased survival when compared to captopril treatment alone without an additional effect on blood pressure.

The present study was designed:

(1) to investigate whether a higher dose of captopril (50 mg/kg/day) can further increase survival in salt-loaded SHRSP and whether the synergistic effect between lithium and the ACE inhibitor on survival was preserved under these conditions.

(2) to investigate whether the AT₁ receptor antagonist, telmisartan can prolong survival in

salt-loaded SHRSP and whether the addition of lithium to the AT₁ receptor antagonist has synergistic effect on survival in these animals.

(3) to investigate the effects of chronic treatment of normotensive Wistar rats with lithium, the ACE inhibitor captopril or a combination of both drugs on neurological deficits, infarct volume as well as apoptotic and inflammatory events following acute focal ischemia induced by unilateral middle cerebral artery occlusion with two days of reperfusion.

(4) to investigate the effects of chronic treatment of normotensive Wistar rats with the AT₁ receptor antagonist, telmisartan and a combination of lithium and telmisartan on neurological deficits, infarct volume as well as apoptotic and inflammatory events following acute focal ischemia.

2 Materials and Methods

2.1 Preparation of solutions and reagents

2.1.1 Solutions and reagents for immunohistochemistry and perfusion

10×PB (Phosphate Buffer): 11.5 g $\text{Na}_2\text{HPO}_4 \cdot 2\text{H}_2\text{O}$ (Merck), 2 g KH_2PO_4 (Merck) and 2 g KCl (Merck) were dissolved in 800 ml distilled water. The pH was adjusted to 7.4 and a final volume of 1000 ml was achieved by adding distilled water.

PBS (Phosphate Buffered Saline): 8 g NaCl (Merck) were dissolved in 800 ml distilled water. After addition of 100 ml PB (10×) solution, the pH was adjusted to 7.4 and a final volume of 1000 ml was achieved by adding distilled water.

PBST: 5 ml Triton X-100 (Sigma) was added to 995 ml PBS (1×, pH 7.4)

30% Sucrose solution: 30g sucrose (Merck) was dissolved in 80 ml distilled water, then the volume was adjusted to 100 ml.

4% Paraformaldehyde solution: 40 g paraformaldehyde (Merck) was dissolved in 900 ml PB (1×, pH 7.4) at 60°C, then the volume was adjusted to 1000ml.

0.1% Paraformaldehyde solution: 10 ml 4% paraformaldehyde was added in 390 ml PBS (1×, pH 7.4), and mixed.

0.1% Cresyl violet solution: 1g cresyl violet acetate (9-amino-5-imino-5H-benzo [α]-phenoxazine acetate salt, Sigma) was added to 1000 ml distilled water. The solution was vortexed for 2 days and filtered through filterpaper.

Acidic alcohol: 100 ml 10% acetic acid (Merck) was added in 900 ml 100% ethanol (Sigma), and mixed.

0.1% Triton X-100 in 0.1% sodium citrate: 1 g sodium citrate (Merck) was dissolved in 1000 ml distilled water, then 1 ml Triton X-100 was added in the above solution, and mixed.

5% Normal goat serum (NGS) in PBST: 50 µl normal goat serum (Vector) was added in 950 µl PBST, and mixed.

1% Bovine serum albumin (BSA) in PBST: 1 g BSA (Sigma) was dissolved in 100 ml PBST, and mixed.

0.3% Hydrogen peroxide: 10 µl 30% H₂O₂ (Merck) was added in 990 µl methanol (Merck), and mixed.

3% Hydrogen peroxide: 100 µl 30% H₂O₂ was added in 900 µl methanol, and mixed.

ABC solution: VECTASTAIN[®] ELITE ABC Reagent (Vector): Two drops of reagent A were added to 5 ml PBS. After the addition of 2 drops of reagent B, the solution was mixed immediately. The solution was ready for use after 30 min.

DAB Reagent: 3, 3'-diaminobenzidine tablet sets (Sigma): Each Sigma Fast DAB tablets set contains the following when dissolved in 5 ml deionized water: D 9292 DAB: 0.7 mg/ml; U 1380 Urea hydrogen peroxide: 0.2 mg/ml and Tris buffer: 0.06 M.

TUNEL reaction solution: 50 µl TUNEL reaction solution included: 10 µl 5×TdT buffer; 2 µl CoCl₂; 1µl terminal transferase (nucleoside-triphosphate: DNA deoxynucleotidylexotransferase, TdT enzyme) and 37 µl TUNEL label (Nucleotide mix, containing fluorescein-dUTP and dNTP). All of these reagents were purchased from Roche Diagnostics GmbH.

2.1.2 Solutions for drug treatment

Lithium chloride solution: LiCl (Sigma) was solubilized in 0.9% saline. The concentration of the LiCl solution was dependent on the weight of the rat and the application volume (1 mmol/kg, 0.5 ml/rat).

Captopril solution: Captopril (Wörwag GmbH & Co., Böblingen, Germany) was solubilized in 0.9% saline. The concentration of the captopril solution was dependent on the weight of

the rat and the application volume (50 mg/kg in SHRSP and 25 mg/kg in Wistar rats, 0.5 ml/rat).

Telmisartan solution: Telmisartan (Boehringer Ingelheim, Biberach an der Riss, Germany) was solubilized in 0.9% saline with a few drops of 1 M NaOH (Merck), and the pH of the solution was adjusted to pH 9.5. The concentration of the telmisartan solution was dependent on the weight of the rat and the application volume (0.3 mg/kg, 0.5 ml/rat) .

Captopril + LiCl solution: LiCl and captopril were solubilized to 0.9% saline. The concentration of this solution was dependent on the weight of the rat and the application volume (captopril: 50 mg/kg in SHRSP and 25 mg/kg in Wistar rats; LiCl: 1.0 mmol/kg, 0.5 ml/rat).

Telmisartan + LiCl solution: Telmisartan was solubilized in 0.9% saline with a few drops of 1 M NaOH, then LiCl was added to the solution and the pH of the solution was adjusted to pH 9.5. The concentration of this solution was dependent on the weight of the rat and the application volume (telmisartan: 0.3 mg/kg; LiCl: 1.0 mmol/kg, 0.5 ml/rat).

2.1.3 Solutions and reagents for albumin measurement

Buffer A: 3.2 g diethylmalonic acid (Aldrich), 8.77g NaCl , 1 ml 0.1 M EDTA (Roth) and 1 ml Tween 20 (Sigma) were dissolved in 800 ml distilled water. The PH was adjusted to 7.4 by 1 M KOH (Merck) and a final volume of 1000 ml was achieved by adding distilled water. 5g gelatine (Sigma) was added to the above solution, and mixed at 37 °C.

Rat serum albumin (RSA) stock solution: 1g rat albumin (Sigma) was dissolved in 1000 ml 0.1 M NaHCO₃ (Aldrich).

Coating solution: RSA stock solution was diluted 1:5000 with 0.1 M NaHCO₃.

Conjugate solution: Albumin rat polyclonal antibody, anti-rat peroxidase conjugated sheep IGG fraction to rat albumin (ICN) was diluted 1:9000 with buffer A.

Substrate solution: 2 tablets of 3,3',5,5' tetramethylbenzidin-dihydrochlorid (Sigma) was dissolved in 10 ml distilled water plus 10 ml buffer A. 4 μ l 30% H₂O₂ was added in the above solution, and mixed.

2.1.4 Solutions and reagents for plasma renin activity (PRA) measurement

Inhibitor cocktail: 1000 mg 1,10-phenanthroline-monohydrate (Merck) was dissolved in 2 ml ethanol (solution 1). 9.28 g Na₂-EDTA (Merck) was dissolved in 160 ml distilled water (solution 2). Solution 1 was added to solution 2 slowly, and mixed. 40 mg neomycin-sulfate (Serva) was added to the above solution, and mixed.

Tris-maleic acid buffer: 9.086 g Tris (hydroxymethyl)-aminomethane (Merck) and 8.705 g maleic acid (Merck) was dissolved in 900 ml distilled water. The PH was adjusted to 6.5 and a final volume of 1000 ml was achieved by adding distilled water.

0.1 M Tris-acetate-buffer (RIA buffer): 60.5 g Tris (hydroxymethyl)-aminomethane (Merck) and 1 g neomycin-sulfate (Serva) was dissolved in 5 L distilled water and the PH was adjusted to 7.4.

2.2 Animals

Male SHRSP bred at the Department of Pharmacology in Kiel and male Wistar rats (Charles River, Germany) weighing 217 ± 15 g (mean \pm SD) were used for the experiments. All rats were housed at constant humidity ($60 \pm 5\%$) and temperature ($25 \pm 1^\circ\text{C}$) and kept on a 12-hour light/dark cycle. They were given free access to a standard chow (Ssniff Spezialdiäten GmbH, Soest, Germany) and were allowed to drink water ad libitum. The study was performed in accordance with the guidelines for animal experiments of the University of Kiel and was approved by the German governmental office dealing with animal protection.

2.3 Stroke prevention in SHRSP

2.3.1 Experimental protocol

At 8 weeks of age, the rats were randomized into six treatment groups based on body weight and blood pressure, and they were housed in individual cages. At the same time the drinking

water was permanently replaced by a 1% NaCl solution. All rats received a subcutaneous injection (0.5 ml) once daily according to the following protocol.

Group 1: Isotonic NaCl (0.9%), n=12

Group 2: LiCl (1 mmol/kg), n=11

Group 3: Captopril (50 mg/kg), n=12

Group 4: Captopril (50 mg/kg) plus LiCl (1 mmol/kg), n=12

Group 5: Telmisartan (0.3 mg/kg), n=14

Group 6: Telmisartan (0.3 mg/kg) plus LiCl (1 mmol/kg), n=14

Treatment with telmisartan was initially started with 1 mg/kg per day. Due to significant blood pressure reductions during the first 4 weeks of treatment, the dose of telmisartan was decreased to 0.3 mg/kg per day.

All animals were inspected daily to detect neurological symptoms such as piloerection, jumping, paralysis of anterior and/or posterior paws, aggression, prostration, loss of body symmetry and convulsions. Body weight and salt water uptake were measured every 2-3 days. After 5 weeks of treatment, 5 rats from each group were deeply anesthetized with chloral hydrate (400 mg/kg) and intracardially perfused with ice cold 0.9% NaCl solution. The brains, kidneys and hearts were removed and quickly frozen in dry ice and stored at -80°C . With the remaining rats drug treatment was continued lifelong. Those rats which were very debilitated (e.g. edema, difficulty in breathing) and expected to die within the next two days were killed, and hearts, kidneys and brains were removed as described above. Blood or 24 h urine samples were collected at different time points for the measurement of the urinary and plasma concentrations of Na^+ , K^+ and Li^+ , urinary albumin excretion and plasma renin activity.

2.3.2 Systolic blood pressure (SBP) measurement

SBP was measured by tail plethysmography with rats under light ether anesthesia.

Measurements were started before the onset of treatment and were continued in 1-4 week intervals during the first 5 months of treatment and in 5-6 week intervals thereafter.

2.3.3 Determination of salt and water intake

Water and salt intake was measured by weighing the drinking solution over a 2-3 day period .

2.3.4 Urine collection

After 11, 19, 27 and 37 weeks of treatment, all rats were housed individually in metabolic cages with free access to rat chow and drinking water (1% NaCl solution) for 1 day (adaptation period). The next day, urine was collected starting immediately after drug treatment, and volume of urine and water intake during a 24 h period was measured. The urine samples were centrifuged at 3000 g for 10 min, and the supernatant was stored at -20°C until the measurement of urinary sodium, potassium, lithium and albumin concentrations.

2.3.5 Blood collection

After 21 and 39 weeks of treatment, blood was collected from the retrobulbar venous plexus after short ether anaesthesia (45-60 s), into an ice-cold 12.5 mM EDTA (Merck) solution (50 μl /ml blood). Blood samples were immediately centrifuged at 10.000 g and 4°C for 10 min, and then the plasma was separated and stored at -20°C until the measurement of plasma sodium, potassium and lithium concentrations, and plasma renin activity.

2.3.6 Determination of urinary and plasma sodium, potassium and lithium concentrations

Sodium and potassium concentrations were measured by a flame photometer (Eppendorf FCM 6341).

Lithium concentration was measured by a flame photometer (Eppendorf EFOX 5053)

2.3.7 Determination of urinary albumin concentration

The 96-well microtiter plates were coated by adding 100 μl /well coating solution. The plates were wrapped in a plastic film and incubated for 3 h at 37°C and, subsequently, for 15 h at 4°C . After removing the coating solution, the microtiter plates were washed 3 times for 4 min by adding 100 μl buffer A/well.

For the standard curve rat serum albumin stock solution (1 mg/ml) was diluted to yield concentrations of: 0.00 - 0.03 - 0.05 - 0.07 - 0.10 - 0.2 - 0.3, 0.4 – 0.6 – 0.8 – 1.00 mg/l. 50 μl buffer A (zero value), 50 μl standard or 50 μl sample (urine diluted with buffer A) were added in each well. Measurements were carried out in a duplicate. After addition of 50 μl of conjugate solution per well, the microtiter plates were incubated for 1 h at 37°C . Thereafter, the plates were washed 4 times for 4 min with 100 μl /well of buffer A. 200 μl /well of the substrate solution were added and incubated for 15 min. The reaction was stopped by adding 50 μl /well H_2SO_4 (Merck) (2 mol/l). The extinctions were measured at 450 nm with a ELISA-

MRX-Plate Reader. The concentrations of albumin in urine samples were calculated with a computer program (Dynex Revelation G 3.04) using an albumin standard curve. The 24 h urinary albumin concentrations were expressed in mg/24 h taking into account the 24 h urine volume.

2.3.8 Determination of plasma renin activity

PRA was measured by determining the level of Ang I generated during a 2h incubation period at 37°C in the presence of an inhibitor cocktail. In brief: plasma (250 µl) was incubated with 50 µl of an inhibitor cocktail and 400 µl Tris-maleic acid buffer (75 mmol/L) in a water bath at 37°C for 2 h. At three different time points - before (blank value), 1h and 2h after the start of the incubation - 150 µl of the incubation mixture was added to ice-cold RIA buffer (150 µl) and transferred into a water bath at 100°C for 5 min. Thereafter, the samples were put on ice and centrifuged (6000 rpm) for 20 min at 4°C. The supernatant (100 µl) was used for the measurement of Ang I by radioimmunoassay. The measurements were performed in duplicate. Renin activity is expressed as ng Ang I/ml per h.

2.3.9 Cresyl violet staining

Coronal sections of 40 µm thickness were cut on a cryostat at – 20°C starting from bregma +3.7 mm according to a rat brain atlas by Paxinos & Watson (1986). Every 20th section (a total of 12 sections) was mounted on a gelatine coated glass slide and stained with cresyl violet for the detection of cell damage by light microscope. The cresyl violet staining was performed according to the protocol described in section 2.4.10.

2.3.10 TUNEL staining

Serial sections of 10 µm thickness from different brain areas (bregma –0.3 mm, -1.8 mm, -3.8 mm and -5.3 mm) were cut on a cryostat at –20 °C. The sections were mounted on gelatine coated glass slides, and stained with TUNEL according to the protocol described in section 2.4.11 after the brain sections were incubated in 4% paraformaldehyde solution for 0.5 h. TUNEL-positive cells were semiquantified in the sections on a scale of 0 to 4: 0, no or few TUNEL-positive cells; 1, random TUNEL positive cells; 2, a discrete region of TUNEL-positive cells; 3, many TUNEL-positive cells; and 4, the entire region is distributed with TUNEL-positive cells.

2.4 Intraluminal thread model of focal cerebral ischemia

The present study employed the intraluminal thread model for middle cerebral artery occlusion (MCAO) with subsequent reperfusion. The intraluminal thread model of MCAO in rats, first introduced by Koizumi et al. (1986) and later modified by Longa et al. (1989), has become the most widely used model to study the pathophysiology and therapy of permanent and transient focal cerebral ischemia. The model is minimally invasive and does not require craniectomy.

2.4.1 Preparation of the occluding thread

The tip of the occluding thread (4/0, 1.5 metric, monofilament, ETHILON, ETHICON GmbH & Co. KG, Germany) was coated with silicon (Provil, Bayer AG, Germany) to achieve a diameter of about 0.25 mm at the distal end (5 mm). The silicon was allowed to harden before use.

2.4.2 Surgery

The rat was anesthetized with an intraperitoneal injection of 4% chloral hydrate at a dose of 400 mg/kg (1ml/100g body weight). The right common carotid artery (CCA) was exposed via a lateral neck incision and separated from the vagus nerve. Then both the external carotid artery (ECA) and the internal carotid artery (ICA) were isolated from the adjacent tissue under the operating microscope. Before inserting the silicone-coated 4-0 nylon monofilament, the right CCA and ECA were ligated with 4/0 suture. The filament was inserted into CCA and gently advanced \approx 17 mm via ICA from the bifurcation of the CCA and ECA, and it was monitored by Laser-Doppler flowmetry (LDF). The filament was secured at the CCA by a tight ligation. Reperfusion was commenced 90 min after MCAO by pulling out the monofilament. Rectal temperature was monitored and maintained between 37.0°C and 37.5°C with a heating pad throughout the surgical procedures.

2.4.3 Regional cerebral blood flow (rCBF) monitored by Laser-Doppler flowmetry

Insufficient MCAO and inadvertent subarachnoid hemorrhage (SAH) are the most common complications of the intraluminal thread model. Continuous bilateral LDF is indispensable to monitor adequate MCAO and is highly sensitive to recognize SAH (Robert et al, 1998). rCBF was monitored in the cerebral cortex of each hemisphere in the supply territory of the middle cerebral artery (MCA) by LDF (Periflux system 5000). The head of the rat was fixed in the stereotaxic apparatus (David Kopf Instruments). The scapula was incised on the midline,

and bilateral 1-mm burr holes were drilled 5.0 mm lateral and 1.0 mm posterior to the bregma. The dura was left intact to prevent cerebrospinal fluid leakage. Tubes with internal diameter 1.0 mm and external diameter 2.0 mm were fixed on the bilateral burr holes by dental cement, and Laser-Doppler flowmeter probes were advanced to gently touch the intact dura mater via the tubes. rCBF was continuously measured during 30 min before ischemia, immediately after the onset of MCA occlusion (0), during 90 min of ischemia, and during 30 min of reperfusion. The rCBF values were recorded every 10 min, and was calculated and expressed as a percentage of the baseline values.

The filament was advanced until ipsilateral flow decreased to about 20% of baseline. If ipsilateral LDF indicated premature reperfusion, the filament was immediately corrected. Contralateral rCBF remained unchanged and fluctuated at about 100% of baseline. After filament withdrawal, blood flow was restored to about 60-70% of baseline.

If ipsilateral LDF could not be reduced to 25% of baseline in rats, the MCA of the rat was not adequately occluded. If contralateral rCBF decrease initially after filament placement, and ipsilateral LDF indicated a lack of reperfusion after filament withdrawal, the rats had suffered SAH. All of these rats were excluded from the experiments.

2.4.4 Experimental design

Rats were divided randomly into six groups and were treated daily by a subcutaneous injection (0.5 ml) according to the following protocol:

Group 1: Isotonic NaCl (0.9%), n=11

Group 2: LiCl (1 mmol/kg), n=10

Group 3: Captopril (25 mg/kg), n=9

Group 4: Captopril (25 mg/kg) plus LiCl (1 mmol/kg), n=8

Group 5: Telmisartan (0.3 mg/kg), n=10

Group 6: Telmisartan (0.3 mg/kg) plus LiCl (1 mmol/kg), n=11

Rats were treated once daily for two weeks. Two hours after the last drug application, rats underwent MCAO for 90 min followed by reperfusion. Drug treatment was continued for another 2 days after MCAO. Neurological evaluations were carried out 2 h after drug treatment at day 1 and day 2 after MCAO. After the final neurological examination, rats were killed by transcardial perfusion with PBS and 4% paraformaldehyde under deep anesthesia. The brains were taken out. Infarct volume measurements and immunohistochemical detections of TUNEL, activated caspase-3 and activated microglia were performed during the

2.4.5 Implantation of the femoral artery catheter

Two days before MCAO, a polyethylene catheter (pp-50) was inserted through the femoral artery into the abdominal aorta under chloral hydrate (400 mg/kg, i.p.) anesthesia. The catheter was filled with heparinized saline, passed through a subcutaneous tunnel, sealed, and secured at the back of the neck. The arterial catheter was used for blood pressure measurement, and blood sample withdrawal.

2.4.6 Measurement of mean arterial blood pressure (MAP)

Measurement of MAP was performed via the arterial catheter with use of a pressure transducer (DTX/Plus, Spectramed) connected to a pressure processor (Gould) coupled to a Gould Brush recorder. The analog output signal of MAP from the pressure processor was digitalized and then processed with a computer program.

2 hours after treatment, the measurement was started when the rat was resting and when basal MAP was stable. After baseline measurement, the rat was injected intraperitoneally chloral hydrate (400mg/kg body weight) and the MAP was recorded after it was stable. Then the MAP was continuously recorded before MCAO, during MCAO and after reperfusion.

2.4.7 Blood collection for the measurement of blood parameters

The blood was withdrawn from the arterial catheter into capillary tubes (Standard heparinized, tube volume 115 μ l) at different time points:

- (1) 2 h after treatment when the rats were conscious;
- (2) 10 min after anesthesia before MCAO;
- (3) 30 min after MCAO;
- (4) 90 min after MCAO;
- (5) 30 min following reperfusion.

At each time point the following physiological parameters in blood samples were measured by RADIOMETER ABL 700 SERIE : pH, pCO₂, pO₂, plasma glucose concentration (cGlu), plasma lactate concentration (cLac), plasma hemoglobin concentration (ctHb) and plasma concentrations of some electrolytes: cK⁺, cNa⁺, cCa²⁺, cCl⁻.

2.4.8 Evaluation of neurological deficits

The neurologic status of each rat was evaluated carefully 24 h and 48 h after MCAO by an observer who had no knowledge of the procedure that the rat had undergone. Two neurological grading systems were used to assess the effects of ischemia.

2.4.8.1 A grading scale of 0-3 developed by Bederson et al. (1986)

The method includes the evaluation of the grade of the forelimb flexion contralateral to the injured hemisphere, resistance to lateral push, and observation for circling behavior (Table 1). These tests were conducted sequentially, if a rat exhibited the appropriate behavior at one step but not at the subsequent step, it was graded as the former. Rats with no observable deficits were graded 0; rats displaying circling behavior together with forelimb flexion and decreased resistance to lateral push were graded 3.

Table 1. The neurological deficit examination system with grading scale of 0-3

Normal	grade 0: no observable deficit
Moderate	grade 1: forelimb flexion
Severe	grade 2: forelimb flexion, decreased resistance to lateral push without circling
	grade 3: the same behavior as grade 2 with circling

2.4.8.2 A grading scale of 3-18 developed by Garcia et al. (1995b)

The neurobehavioral study consisted of the following six tests:

1. Spontaneous activity

The animal was placed in a plastic cage and was observed for 5 minutes. The rat's activity was assessed by its ability to approach all four walls of the cage. Scores indicate the following: 3, rat moved around, explored the environment and approached at least three walls of the cage; 2, slightly affected rat moved about in the cage but did not approach all sides and hesitated to move, although it eventually reached at least one upper rim of the cage; 1, severely affected rat did not rise up at all and barely moved in the cage; and 0, rat did not move at all.

2. Symmetry in the movement of four limbs

The rat was held in the air by the tail to observe symmetry in the movement of the four limbs. Scores indicate the following: 3, all four limbs extended symmetrically; 2, limbs on left side extended less or more slowly than those on the right; 1, limbs on left side showed minimal movement; and 0, forelimb on left side did not move at all.

3. Forepaw outstretching

The rat was brought up to the edge of the table and made to walk on forelimbs while being held by the tail. Symmetry in the outstretching of both forelimbs was observed while the rat

reached the table and the hindlimbs were kept in the air. Scores indicate the following: 3, both forelimbs were outstretched, and the rat walked symmetrically on forepaws; 2, left side outstretched less than the right, and forepaw walking was impaired; 1, left forelimb moved minimally; and 0, left forelimb did not move.

4. Climbing

The rat was placed on the wall of a wire cage. Normally the rat uses all four limbs to climb up the wall. When the rat was removed from the wire cage by pulling it off by the tail, the strength of attachment was noted. Scores indicate the following: 3, rat climbed easily and gripped tightly to the wire; 2, left side was impaired while climbing or did not grip as hard as the right side; and 1, rat failed to climb or tended to circle instead of climbing.

5. Body proprioception

The rat was touched with a blunt stick on each side of the body, and the reaction to the stimulus was observed. Scores indicate the following: 3, rat reacted by turning head and was equally startled by the stimulus on both sides; 2, rat reacted slowly to stimulus on left side; and 1, rat did not respond to the stimulus placed on the left side.

6. Response to vibrissae touch

A blunt stick was brushed against the vibrissae on each side; the stick was moved toward the whiskers from the rear of the animal to avoid entering the visual fields. Scores indicate the following: 3, rat reacted by turning head or was equally startled by the stimulus on both sides; 2, rat reacted slowly to stimulus on left side; and 1, rat did not respond to stimulus on the left side.

The score given to each rat at the completion of the evaluation is the summation of all six individual test scores. The minimum neurological score is 3 and the maximum is 18 (Table 2).

Table 2. The neurological deficit examination system with a scale of 3-18

Test	Score			
	0	1	2	3
Spontaneous activity (in cage for 5 min)	No movement	Barely moves	Moves but does not approach at least 3 sides of cage	Moves and approaches at least 3 sides of cage
Symmetry of movements (four limbs)	Left side: no movement	Left side: slight movement	Left side: moves slowly	Both sides: move symmetrically
Symmetry of forelimbs (outstretching while held by tail)	Left side: no movement, no outreaching	Left side: slight movement to outreach	Left side: moves and outreaches less than right side	Symmetrical outreach
Climbing wall of wire cage		Fails to climb	Left side is weak	Normal climbing
Reaction to touch on either side of trunk		No response on left side	Weak response on left side	Symmetrical response
Response to vibrissae touch		No response on left side	Weak response on left side	Symmetrical response

2.4.9 Tissue processing

Two days after MCAO, rats were deeply anesthetized with chloral hydrate (400 mg/kg) and intracardially perfused with ice cold PBS followed by 4% paraformaldehyde solution. The brains were removed and kept in 4% paraformaldehyde solution overnight for fixation of brain tissue. On the next day the brains were cryoprotected in 30% sucrose for 3-4 days at 4 °C. Coronal sections of 40 µm thickness were cut from bregma +3.7 mm to bregma -6.7 mm according to a rat brain atlas (Paxinos & Watson, 1986) on a cryostat at -20 °C. One of every 20 slices was mounted on a gelatine coated glass slide for the measurement of infarct size. For

immunohistochemical detection, serial slices from different brain areas (bregma -0.3 mm and -1.8 mm) were immersed in 0.1% paraformaldehyde solution as free-floating sections. TUNEL staining, caspase-3 staining and activated microglia staining were performed within 1-2 weeks.

2.4.10 Measurement of the infarct size

Sections (40 μ m) were stained with cresyl violet according to the following protocol:

The brain sections were

1. washed in distilled water for 1 min.
2. incubated in 100% ethanol for 3 min.
3. incubated in 100% xylol for 15 min.
4. incubated in 100% ethanol for 3 min.
5. washed in distilled water for 1 min.
6. stained in 0.1% cresyl violet for 5 min.
7. washed in distilled water for 1 min.
8. washed in acidic alcohol for a few seconds until the staining was optimal.
9. washed in distilled water for 1 min.

The coverslips were mounted using pertex after dehydration.

The stained sections were analyzed at 14 predetermined levels (bregma +3.7, +2.9, +2.1, +1.3, +0.5, -0.3, -1.1, -1.9, -2.7, -3.5, -4.3, -5.1, -5.9 and -6.7 mm). The stained slices were photographed by a digital camera (Victor Company of Japan, Color Video Camera) and the border between infarcted and non-infarcted area was outlined with the Leica image analysis system. The area of infarction was measured on each slice, and the infarct volume was calculated by multiplying the sum of the infarct area with the distance between sections (Zhang et al. 2001).

In addition, contralateral and ipsilateral hemisphere areas were measured, and the difference between ipsilateral and contralateral areas in each section was used to calculate the edema volume (Justicia et al. 1999). There is a possibility that infarct volume is influenced by brain edema, therefore the percentage of hemisphere suffering infarction was calculated using the formula of Swanson et al. (1990), taking cerebral edema into account:

$$\% \text{infarct} = 100 \times (V_C - V_L) / V_C$$

%infarct = the percentage of the hemisphere that had undergone a cerebral infarction

V_C = normal volume of the contralateral hemisphere

V_L = normal volume in the ipsilateral hemisphere

$$V_C \sim d \times \sum_i^n A_C$$

$$V_L \sim d \times \sum_i^n A_L$$

d = distance between sections

A_C = area of normal tissue of the contralateral hemisphere on section i

A_L = area of normal tissue of the ipsilateral hemisphere on section i

2.4.11 Immunohistochemistry

2.4.11.1 TUNEL staining

TUNEL staining was performed according to the following protocol:

The brain sections were

1. incubated in freshly prepared 0.3% H_2O_2 -methanol solution for 1 h at room temperature (RT) to block endogenous peroxide activity.
2. washed in PBS, two times for 5 min each.
3. incubated in permeabilisation solution (0.1% Triton X-100 in 0.1% sodium citrate) for 5 min at RT.
4. washed in PBS, two times for 5 min each.
5. incubated with TUNEL reaction solution for 1 h at 37°C.
6. washed in PBS, three times for 5 min each.
7. incubated with TUNEL POD (Converter-POD: anti-fluorescein antibody, Fab fragment from sheep, conjugated with peroxidase, Roche Diagnostics GmbH) for 30 min at 37°C to detect fluorescein-dUTP.
8. washed in PBS, three times for 5 min each.
9. incubated in DAB solution until staining was optimal as determined by light microscopic examination.
10. washed in PBS, three times for 5 min each.
11. mounted on gelatine coated slides and dried at RT.

Coverslips were mounted using pertex after dehydration.

Negative control staining was performed using distilled water instead of terminal transferase for the preparation of TUNEL reaction solution.

Total of 6 rats were used for TUNEL staining in the each group. TUNEL-labeled cells were counted in the parietal cortex using a computer programm (Leica QWin). Three random and non-overlapping regions (375×500 μ m) were sampled at the cortical border of the TUNEL-

positive area (Figure 2). Only densely labeled cells were considered as positive apoptotic cells, and cells with light diffuse labeling suggesting necrosis were not counted (Figure 3).

2.4.11.2 Activated Caspase-3

Activated caspase-3 was staining according to the following protocol:

The brain sections were

1. washed in PBST, three times for 5 min each.
2. incubated in freshly prepared 0.3% H₂O₂-methanol solution for 30 min at RT.
3. washed in PBST, two times for 5 min each.
4. washed in 5% NGS in PBST for 15 min.
5. incubated with the primary antibody (Cleaved Caspase-3 [17 KDa] antibody, Cell Signaling Technology) diluted in PBST/1% BSA (1:100) overnight at 4°C.
6. washed in PBST, three times for 5 min each.
7. incubated with the secondary antibody (Anti-Rabbit Ig(H+L), biotinylated, Vector) diluted in PBST (5 µg/ml) for 1 h at 37°C.
8. washed in PBST, three times for 5 min each.
9. incubated in ABC solution for 45 min at 37°C.
10. washed in PBS, three times for 5 min each.
11. incubated in DAB solution until staining was optimal.
12. washed in PBS, three times for 5 min each.
13. mounted on gelatine coated slides and dried at RT

Coverslips were mounted using pertex after dehydration.

Negative control staining consisted of omission of the primary antibody in the PBST/1% BSA solution.

Total of 6 rats were used for activated caspase-3 staining in the each group. Caspase-3 labeled cells were counted in the parietal cortex using a computer program (Leica QWin). Three random and nonoverlapping regions (375×500 µm) were sampled at the cortical border of the caspase-3 positive area (Figure 2).

2.4.11.3 Activated microglia

Activated microglia was stained according to the following protocol:

The brain sections were

1. washed in PBST, three times for 5 min each.

2. incubated in freshly prepared 3% H₂O₂-methanol solution for 5 min at RT.
3. washed in PBST, two times for 5 min each.
4. washed in 5% NGS in PBST for 15 min.
5. incubated with the primary antibody (Mouse Anti Rat ED1, Serotec Product Datasheet) diluted in PBS (1:300) for 2 nights at 4°C.
6. washed in PBS, three times for 5 min each.
7. incubated with the secondary antibody (Anti-Mouse Igg (FC), biotin conjugate, developed in goat, adsorbed with human Igg, Sigma) diluted in PBS (1:300) for 1 h at 37°C.
8. washed in PBS, three times for 5 min each.
9. incubated in ABC solution for 45 min at 37°C.
10. washed in PBS, three times for 5 min each.
11. incubated in DAB solution until staining was optimal.
12. washed in PBS, three times for 5 min each.
13. mounted on gelatine coated slides and dried at RT

Coverslips were mounted using pertex after dehydration.

Negative control staining consisted of omission of the primary antibody in the PBS solution.

Total of 6 rats were used for activated microglia staining in each group. Activated microglia were counted in the parietal cortex using a computer program (Leica QWin). Three random and nonoverlapping regions (375×500 μm) were sampled at the cortical border of the activated microglia positive area (Figure 2).

2.5 Statistical analysis

All data are expressed as mean ± S.E.M (standard error of the mean). Comparisons among the vehicle-treated group and drug-treated groups were performed by one-way analysis of variance (ANOVA) followed by a post-hoc test (Bonferroni). Comparisons on physiological parameters between the vehicle-treated group and each drug-treated group were performed by one-way analysis of variance (ANOVA) followed by a post-hoc test (Dunnett). Mortality was compared among the vehicle-treated group and drug-treated groups using the Kaplan-Meier analysis of survival followed by Log-rank Test (Cox-Mantel). Values of $p < 0.05$ were considered to be statistically significant.

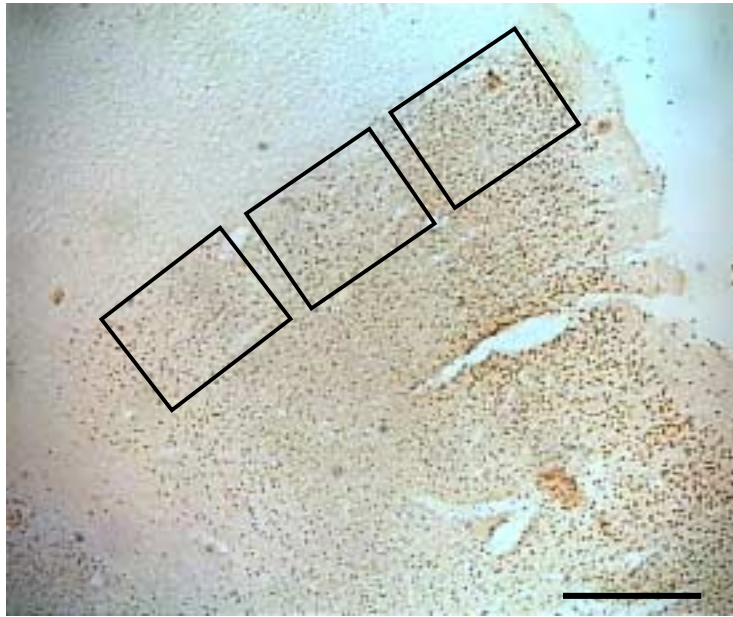


Figure 2. TUNEL (+) cells, activated caspase-3 (+) cells and activated microglia were counted in the parietal cortex using a computer program (Leica QWin). Three random and nonoverlapping regions ($375 \times 500 \mu\text{m}$) were selected in the border of the ischemic cortical area. Scale bar, $500 \mu\text{m}$.

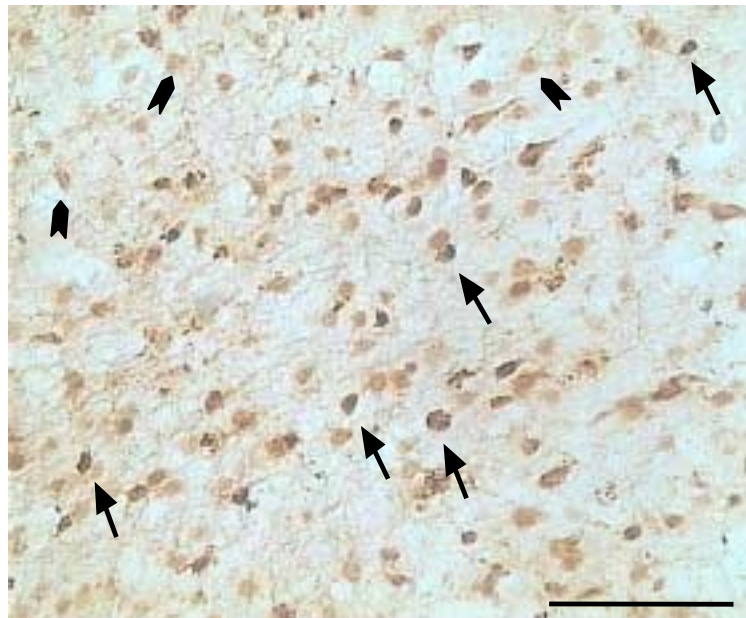


Figure 3. TUNEL staining in the ischemic brain. Only densely labeled cells (arrows) were considered as positive apoptotic cells, and cells with light diffuse labeling indicating necrosis (arrowheads) were not counted. Scale bar, $100 \mu\text{m}$.

3. Results

3.1 Stroke prevention in SHRSP

3.1.1 Survival rate

Average survival was 39 days (range, 31 to 51 days after the start of salt loading) in rats treated with vehicle and 36 days (range, 28 to 56) in rats treated with LiCl. Most rats in both groups died between 4-6 weeks after salt loading and there was no difference in survival rate between these two groups. Captopril (50 mg/kg perday) treatment markedly increased average survival to 247 days (range, 93 to 366). The addition of LiCl to captopril did not further increase the survival rate. The average survival in the captopril plus LiCl treated group was 225 days (range, 117 to 282) (Figure 4, Table 3).

Table 3. The effect of treatment with LiCl, captopril and captopril plus LiCl on survival in SHRSP after the start of salt loading

	n	Average survival, day (ranges)
Vehicle	7	39 (31-51)
LiCl	6	36 (28-56)
Captopril	7	247 (93-366)
Cap.+LiCl	7	225 (117-282)

Telmisartan (initially 1.0 mg/kg per day, finally 0.3 mg/kg per day) treatment markedly increased average survival to 310 days (range, 60 to 405). The addition of LiCl to telmisartan did not further increase survival. The average survival in the combination treated group was 317 days (range, 282 to 366) (Figure 5, Table 4).

Table 4. The effect of treatment with LiCl, telmisartan or telmisartan plus LiCl on survival in SHRSP after the start of salt loading

	n	Average survival, day (ranges)
Vehicle	7	39 (31-51)
LiCl	6	36 (28-56)
Telmisartan	9	310 (60-405)
Telmi.+LiCl	7	317 (282-366)

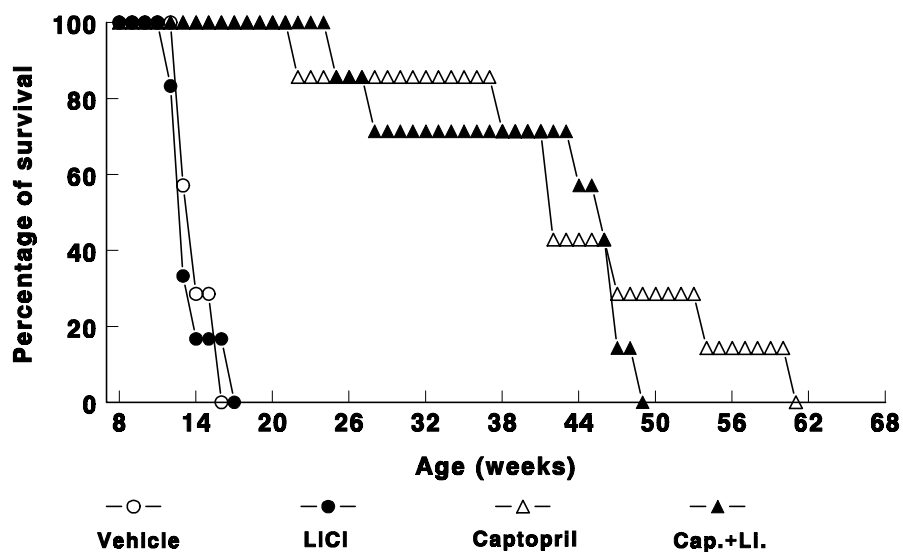


Figure 4. Effect of LiCl, captopril and captopril plus LiCl on survival rate in salt-loaded SHRSP.

From 8 weeks of age, SHRSP were treated subcutaneously with vehicle (0.9% NaCl), LiCl (1.0 mmol/kg/d), captopril (50 mg/kg/d) and captopril plus LiCl lifelong, and at the same time drinking water was permanently replaced with 1% NaCl.

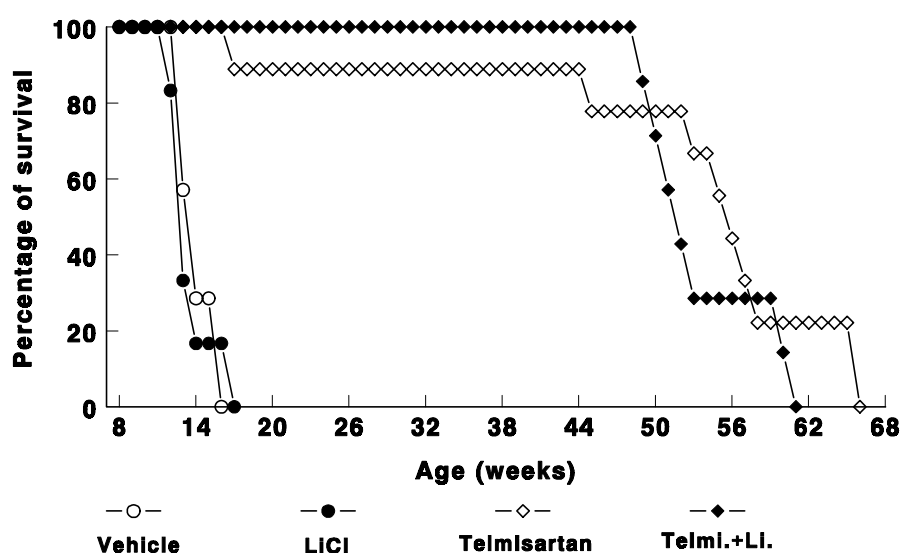


Figure 5. Effect of LiCl, telmisartan and telmisartan plus LiCl on survival rate in salt-loaded SHRSP.

From 8 weeks of age, SHRSP were treated subcutaneously with vehicle (0.9% NaCl), LiCl (1.0 mmol/kg/d), telmisartan (initially 1.0 mg/kg/d, and finally 0.3 mg/kg/d) and telmisartan plus LiCl lifelong, and at the same time drinking water was permanently replaced with 1% NaCl.

3.1.2 Systolic blood pressure

SBP was similar in the rats of all groups at the beginning of the experiment. SBP increased in saline- and captopril-treated rats at 12 weeks of age. Thereafter, SBP levels in rats treated with captopril remained at a level of 180-220 mm Hg. In LiCl- and captopril plus LiCl-treated rats SBP did not increase during the first 4 weeks of treatment. Thereafter, SBP in captopril plus LiCl-treated rats was highly variable during the remaining treatment period and ranged from 150-220 mmHg. The addition of LiCl to captopril reduced blood pressure when compared to captopril alone, with significant differences in SBP levels at 18 weeks ($P<0.01$), 19 weeks ($P<0.01$), 21 weeks ($P<0.05$) and 22 weeks ($P<0.05$) of age (Figure 6).

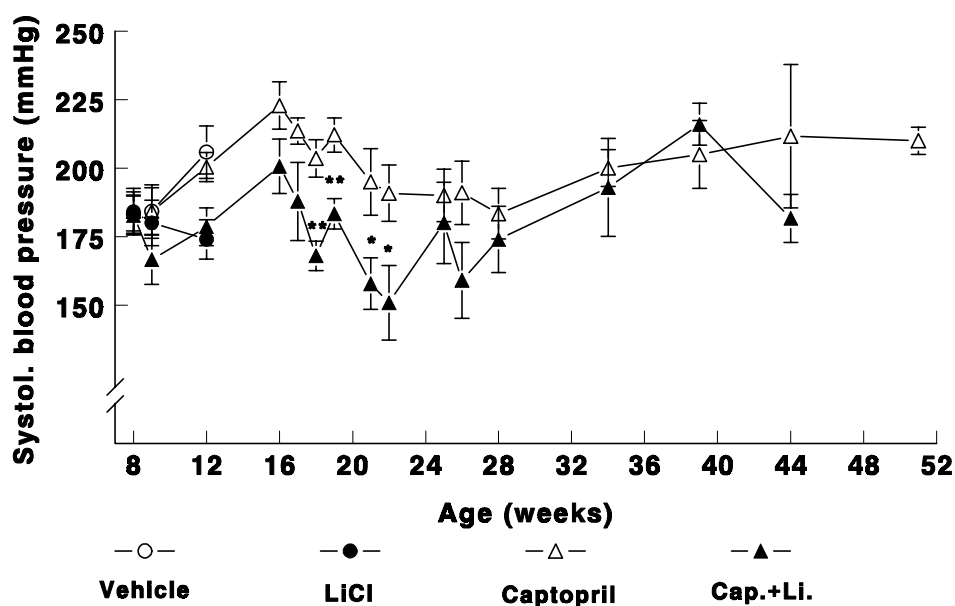


Figure 6. Effect of LiCl, captopril and captopril plus LiCl on systolic blood pressure (SBP) in salt-loaded SHRSP. From 8 weeks of age, SHRSP were treated subcutaneously with vehicle (0.9% NaCl), LiCl (1.0 mmol/kg/d), captopril (50 mg/kg/d) and captopril plus LiCl lifelong. * $P<0.05$, ** $P<0.01$, versus vehicle-treated animals.

Treatment with telmisartan was initially started with 1 mg/kg per day. At 12 weeks of age (4 weeks of treatment) SBP in LiCl-, telmisartan- and telmisartan plus LiCl-treated rats remained below the control level, and telmisartan significantly reduced SBP compared to vehicle ($P<0.01$). Due to significant blood pressure reductions, the dose of telmisartan was decreased to 0.3 mg/kg per day thereafter. The blood pressure increased gradually after dose adjustment, but remained below 220 mm Hg. SBP was comparable in the telmisartan- and telmisartan plus LiCl-group throughout the remaining treatment period (Figure 7).

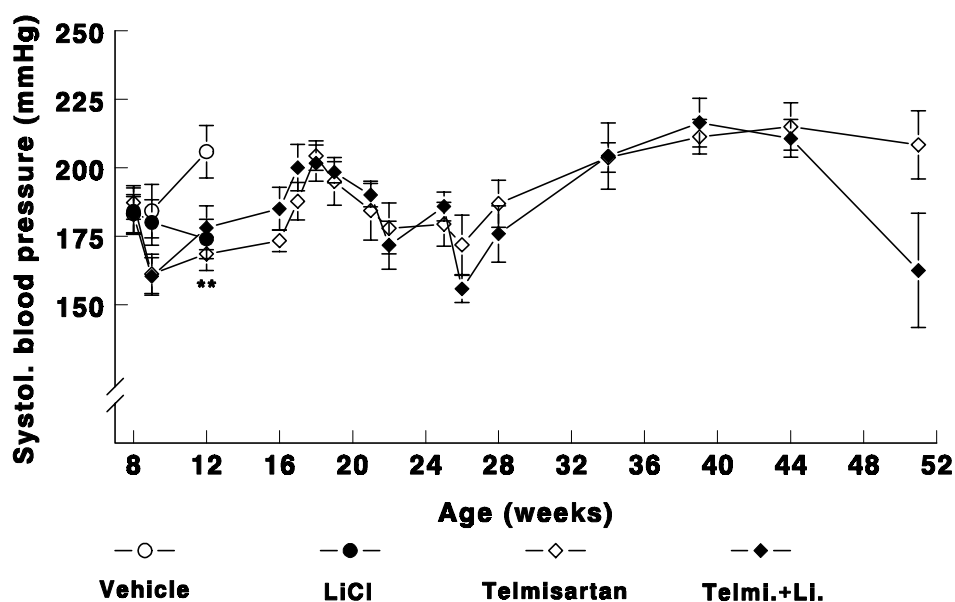


Figure 7. Effect of LiCl, telmisartan and telmisartan plus LiCl on systolic blood pressure (SBP) in salt-loaded SHRSP. From 8 weeks of age, SHRSP were treated subcutaneously with vehicle (0.9% NaCl), LiCl (1.0 mmol/kg/d), telmisartan (initially 1.0 mg/kg/d, and finally 0.3 mg/kg/d) and telmisartan plus LiCl lifelong. ** $P<0.01$ versus vehicle-treated animals.

3.1.3 Body weight

Body weight, as an index of growth, was comparable in all groups until 3 weeks of treatment. Then, the rats in the vehicle- and LiCl-groups failed to increase their body weight and showed a decrease. In contrast, the body weights of rats in the captopril- and captopril plus LiCl-groups continued to exhibit a regular age-related increase. After a long term treatment, large body weight values were observed in some rats with huge edema several days before death, especially in the captopril plus LiCl-group (Figure 8). A similar progress in body weights was observed in rats from the telmisartan – and telmisartan plus LiCl-groups. These rats continued to exhibit a regular age-related increase. Again, large body weight values were observed in some rats with huge edema several days before death (Figure 9).

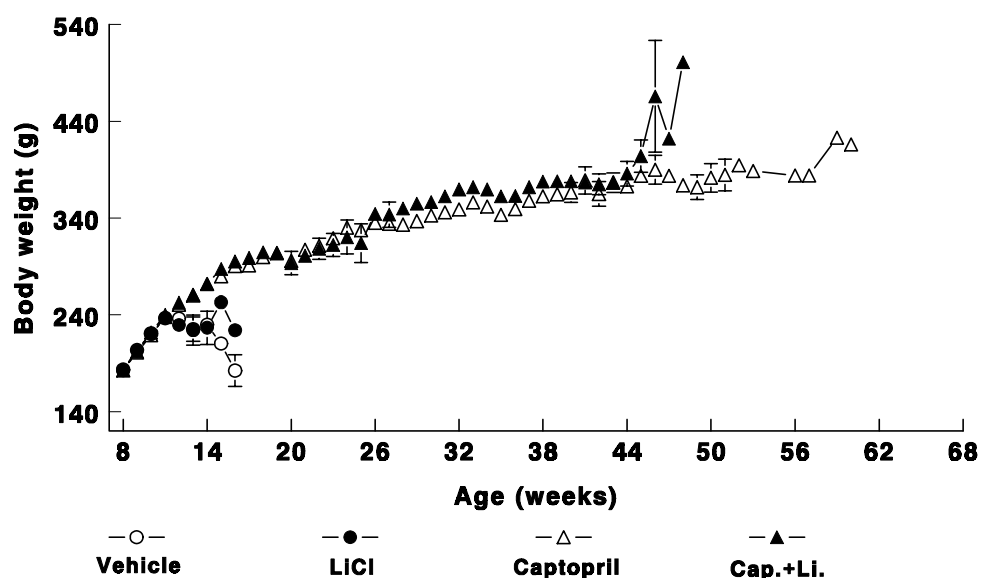


Figure 8. Effect of LiCl, captopril and captopril plus LiCl on body weight in salt-loaded SHRSP.

From 8 weeks of age, SHRSP were treated subcutaneously with vehicle (0.9% NaCl), LiCl (1.0 mmol/kg/d), captopril (50 mg/kg/d) and captopril plus LiCl lifelong.

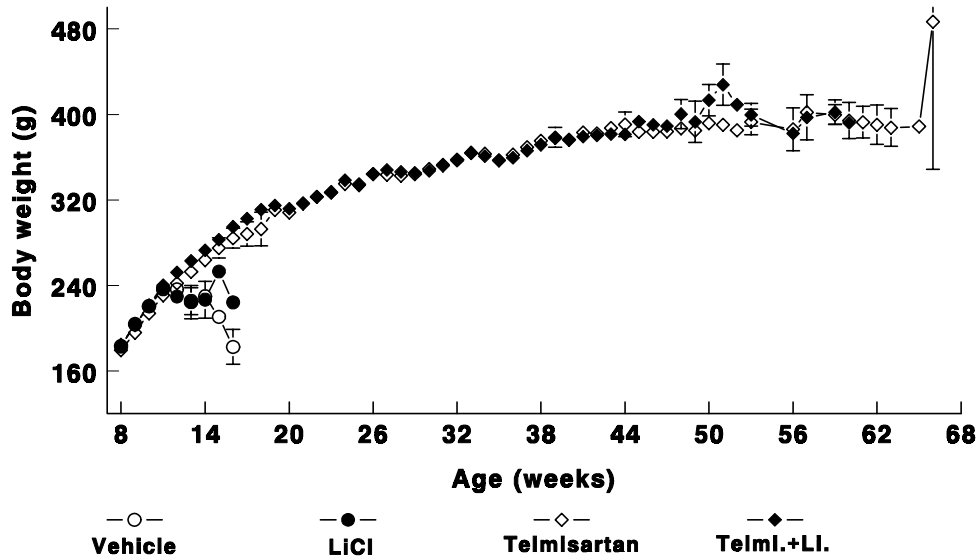


Figure 9. Effect of LiCl, telmisartan and telmisartan plus LiCl on body weight in salt-loaded SHRSP. From 8 weeks of age, SHRSP were treated subcutaneously with vehicle (0.9% NaCl), LiCl (1.0 mmol/kg/d), telmisartan (initially 1.0 mg/kg/d, and finally 0.3 mg/kg/d) and telmisartan plus LiCl lifelong.

3.1.4 Water intake and urinary volume

Water and salt intake were similar in all groups during the first 3 weeks of treatment.

Thereafter, water and salt intake increased in the vehicle- and LiCl-groups, especially in the rats with symptoms of stroke. Water and salt intake was comparable in the rats treated with captopril and captopril plus LiCl during the first 8 weeks of treatment. Thereafter water and salt intake in captopril plus LiCl-treated rats remained at higher levels compared to captopril-treated rats (Figure 10). Measurements of 24 h salt water intake and urinary water excretion at 11, 19, 27, and 37 weeks of treatment from rats in metabolic cages are shown in Figure 11. SHRSP treated with captopril plus LiCl exhibit a higher water intake and urine excretion than rats treated with captopril alone. There was a significant difference in the water intake at 27 weeks of treatment ($P < 0.05$) and in the urine excretion at 11 weeks ($P < 0.05$) and 27 weeks of treatment ($P < 0.01$).

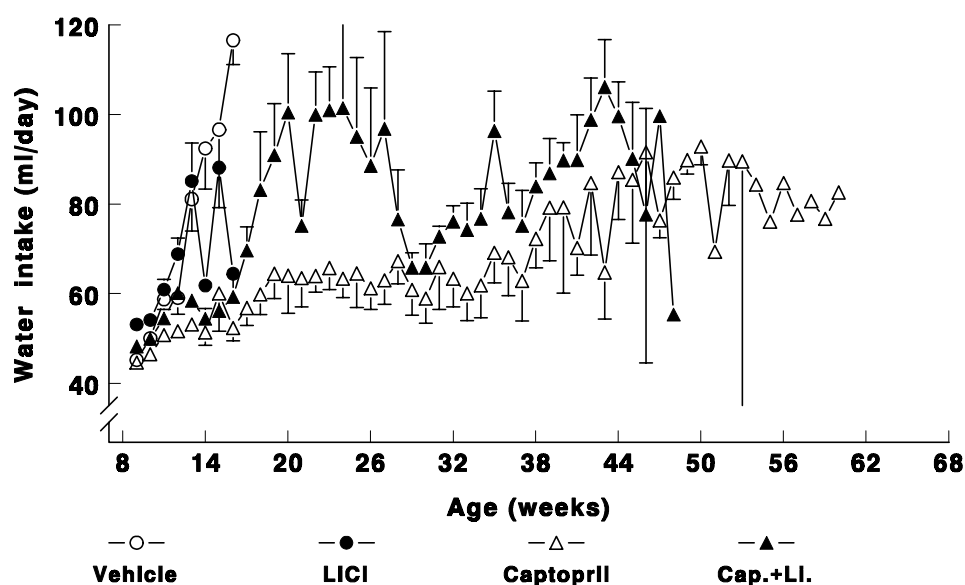


Figure 10. Effect of LiCl, captopril and captopril plus LiCl on salt water intake (1% NaCl) in SHRSP. From 8 weeks of age, SHRSP were treated subcutaneously with vehicle (0.9% NaCl), LiCl (1.0 mmol/kg/d), captopril (50 mg/kg/d) and captopril plus LiCl lifelong.

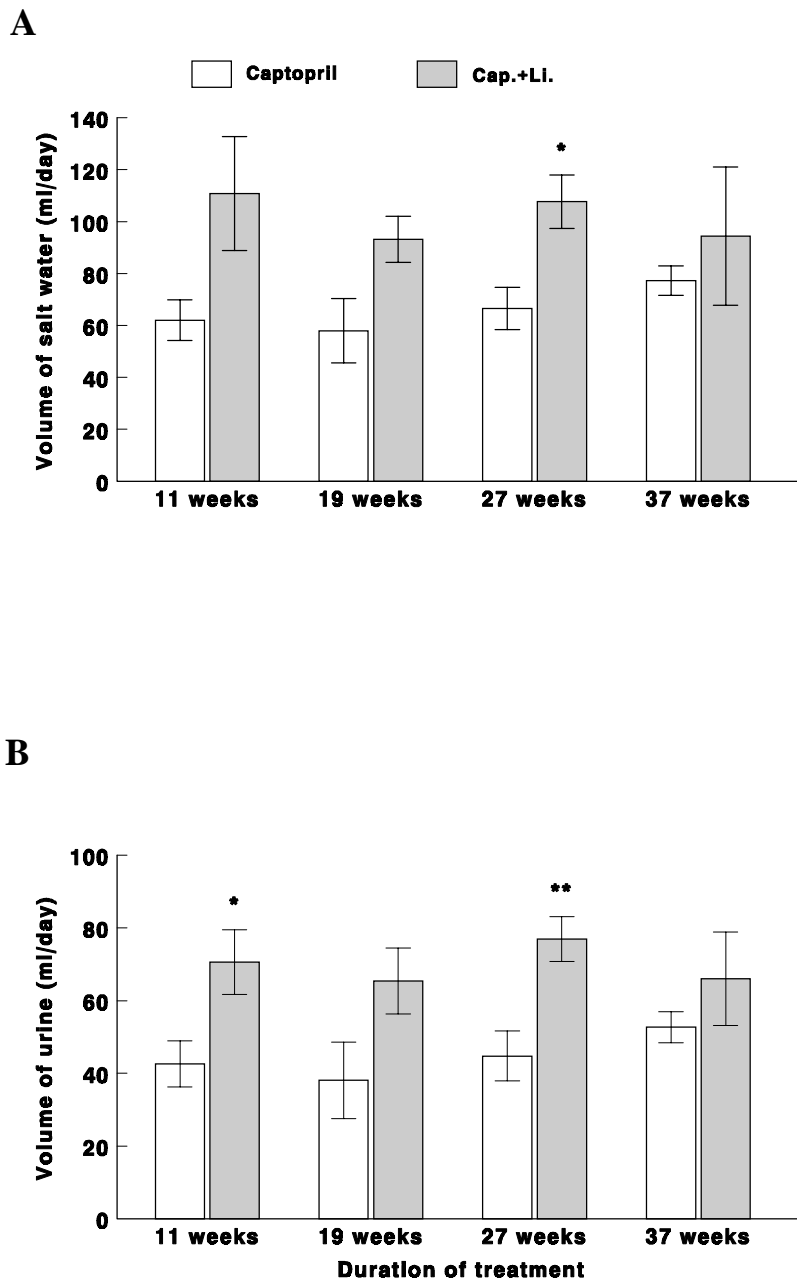


Figure 11. Effect of LiCl, captopril and captopril plus LiCl on salt water intake (A) and urinary excretion (B) in salt-loaded SHRSP. From 8 weeks of age, SHRSP were treated subcutaneously with vehicle (0.9% NaCl), LiCl (1.0 mmol/kg/d), captopril (50 mg/kg/d) and captopril plus LiCl lifelong. At different treatment periods, rats were housed individually in metabolic cages for 1 day (adaptation period). The next day, urine was collected starting immediately after drug treatment, and volume of urine and water intake during a 24 h period were measured. * $P < 0.05$, ** $P < 0.01$ versus vehicle-treated animals.

Water and salt intake were comparable in telmisartan- and telmisartan plus LiCl-treated rats during the first 30 weeks of treatment. Thereafter, water and salt intake increased in animals treated with telmisartan plus LiCl (Figure 12). Measurements of 24 h salt water intake and urinary water excretion from rats in metabolic cages are shown in Figure 13. SHRSP treated with telmisartan plus LiCl exhibited a significantly higher water intake at 27 weeks of treatment and an increased urine excretion at 19 and 27 weeks of treatment compared to rats treated with telmisartan alone ($P < 0.05$).

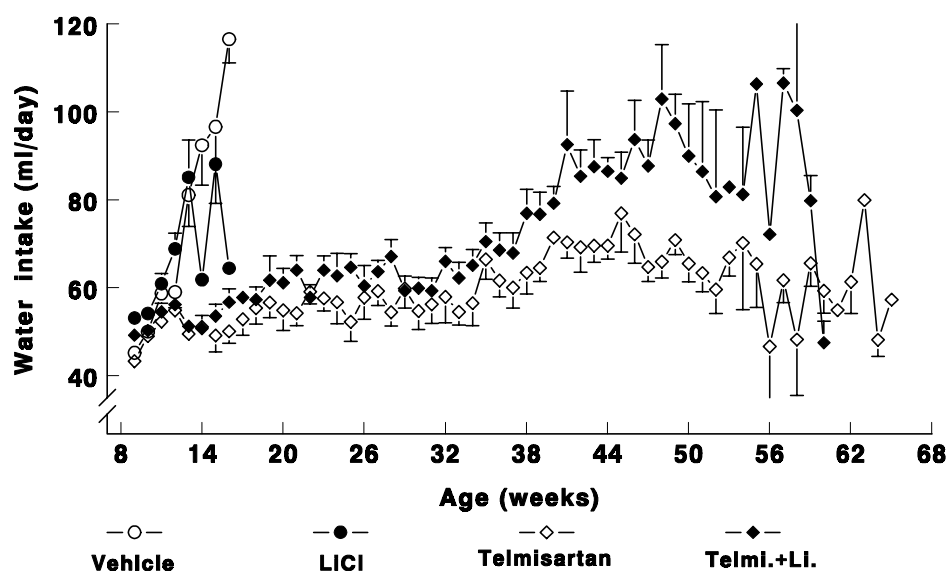
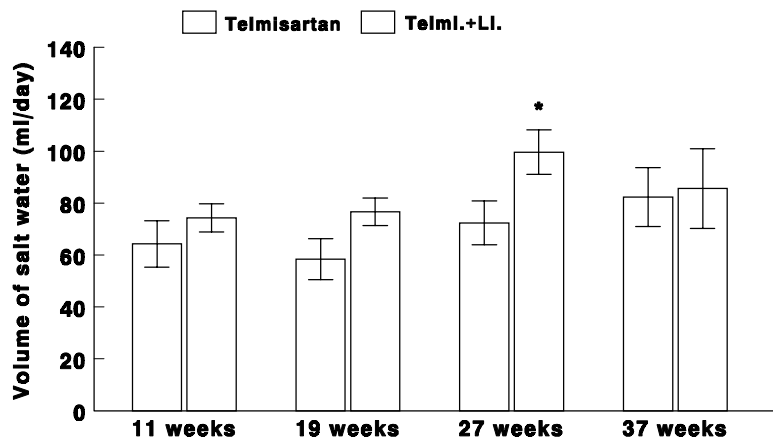


Figure 12. Effect of LiCl, telmisartan and telmisartan plus LiCl on salt water intake (1% NaCl) in SHRSP. From 8 weeks of age, SHRSP were treated subcutaneously with vehicle (0.9% NaCl), LiCl (1.0 mmol/kg/d), telmisartan (initially 1.0 mg/kg/d, and finally 0.3 mg/kg/d) and telmisartan plus LiCl lifelong.

A



B

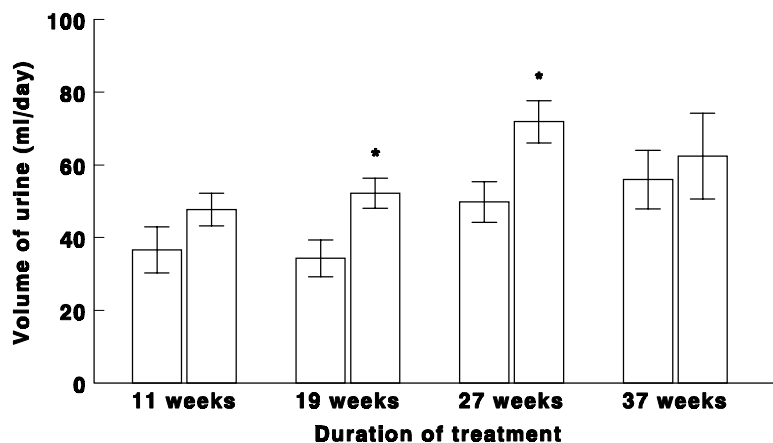


Figure 13. Effect of LiCl, telmisartan and telmisartan plus LiCl on salt water intake (A) and urinary excretion (B) in salt-loaded SHRSP. From 8 weeks of age, SHRSP were treated subcutaneously with vehicle (0.9% NaCl), LiCl (1.0 mmol/kg/d), telmisartan (initially 1.0 mg/kg/d, and finally 0.3 mg/kg/d) and telmisartan plus LiCl lifelong. At different treatment periods, rats were housed individually in metabolic cages for 1 day (adaptation period). The next day, urine was collected starting immediately after drug treatment, and volume of urine and water intake during a 24 h period were measured. * P<0.05 versus vehicle-treated animals.

3.1.5 The concentrations of sodium and potassium in plasma and their urinary excretions

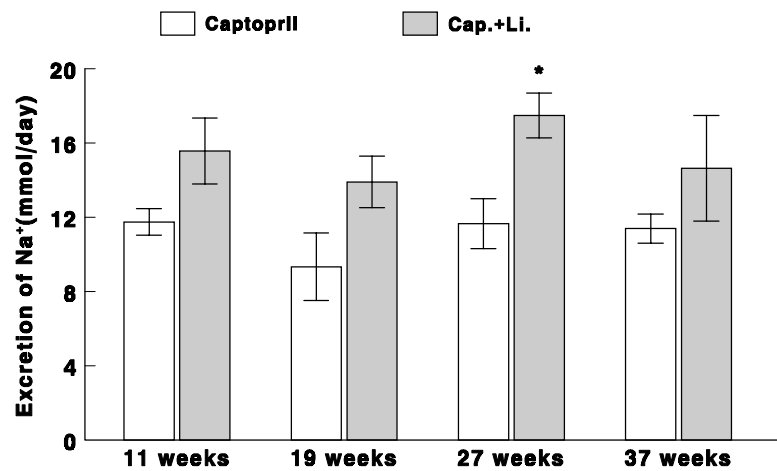
Plasma levels of sodium and potassium were not different between captopril- and captopril plus LiCl-treated rats (Table 5). The urinary excretion of sodium and potassium in these two groups is shown in Figure 14. After 27 weeks of treatment, rats treated with captopril plus LiCl excreted more sodium than rats treated with captopril alone (17.49 ± 1.21 mmol/day versus 11.66 ± 1.35 mmol/day, $P < 0.05$). After 11, 19 and 37 weeks of treatment, the addition of LiCl to captopril slightly increased the excretion of sodium, but there was no significant difference between these two groups. Urinary excretion of potassium was not different between these two groups.

Table 5. The concentration of Na^+ and K^+ in the plasma of SHRSP at 21 weeks of treatment with captopril and captopril plus LiCl

Group	n	Na^+ (mmol/L)	K^+ (mmol/L)
Captopril	6	179.03 ± 2.25	4.98 ± 0.15
Cap.+Li.	5	170.62 ± 6.71	4.95 ± 0.22

Values are mean \pm S.E.M of n rats.

A



B

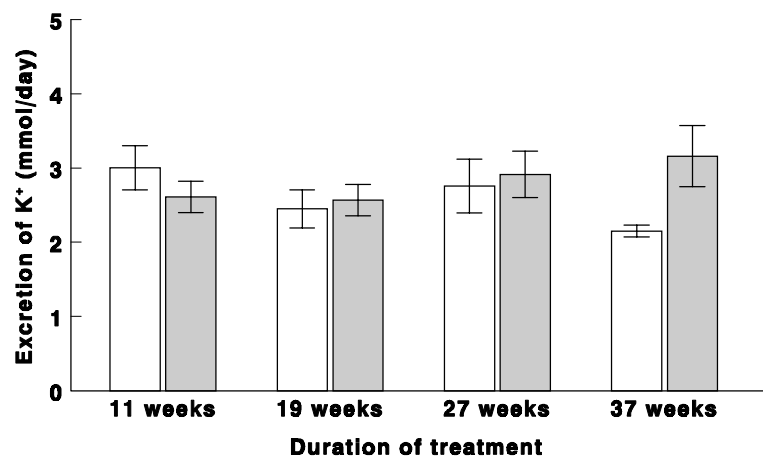


Figure 14. Effect of LiCl, captopril and captopril plus LiCl on urinary excretion of Na⁺ (A) and K⁺ (B) in salt-loaded SHRSP. From 8 weeks of age, SHRSP were treated subcutaneously with vehicle (0.9% NaCl), LiCl (1.0 mmol/kg/d), captopril (50 mg/kg/d) and captopril plus LiCl lifelong. At different treatment periods, rats were housed individually in metabolic cages, and urine was collected during a 24 h period for the measurement of sodium and potassium concentrations. * P<0.05 versus captopril-treated animals.

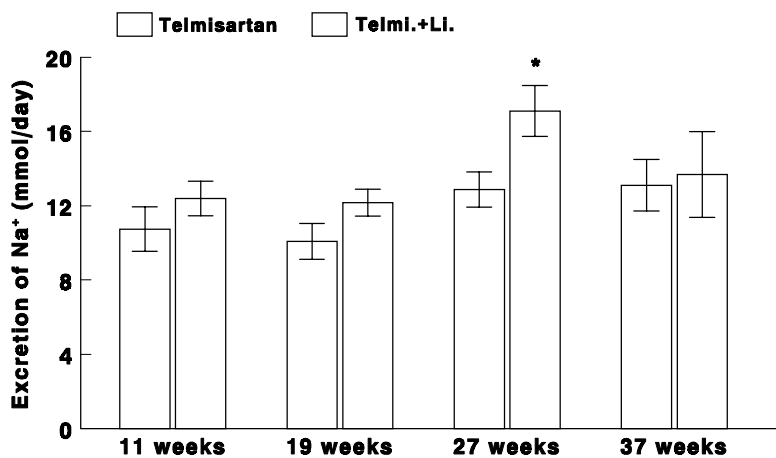
Plasma levels of sodium and potassium were not different between telmisartan- and telmisartan plus LiCl-treated rats (Table 6). The urinary excretion of sodium and potassium in the two groups are shown in Figure 15. At 27 weeks of treatment, rats treated with telmisartan in combination with lithium excreted more sodium than rats treated with telmisartan alone (17.10 ± 1.36 mmol/day versus 12.87 ± 0.95 mmol/day, $P < 0.05$). At 11, 19 and 37 weeks of treatment, the urinary excretions of sodium in the both groups were comparable. Urinary excretion of potassium was not different between these two groups.

Table 6. The concentration of Na^+ and K^+ in the plasma of SHRSP at 21 weeks of treatment with telmisartan and telmisartan plus LiCl

Group	n	Na^+ (mmo/L)	K^+ (mmo/L)
Telmisartan	8	174.01 ± 3.77	4.70 ± 0.13
Telmi.+Li.	7	167.84 ± 4.92	4.68 ± 0.13

Values are mean \pm S.E.M of n rats.

A



B

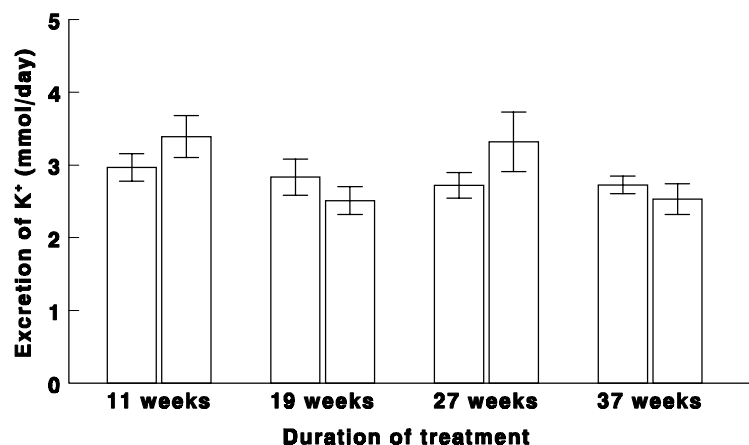


Figure 15. Effect of LiCl, telmisartan and telmisartan plus LiCl on urinary excretion of Na⁺ (A) and K⁺ (B) in salt-loaded SHRSP. From 8 weeks of age, SHRSP were treated subcutaneously with vehicle (0.9% NaCl), LiCl (1.0 mmol/kg/d), telmisartan (initially 1.0 mg/kg/d, and finally 0.3 mg/kg/d) and telmisartan plus LiCl lifelong. At different treatment periods, rats were housed individually in metabolic cages, and urine was collected during a 24 h period for the measurement of sodium and potassium concentrations. * P<0.05 versus telmisartan-treated animals.

3.1.6 Lithium concentration in plasma and urine

Daily subcutaneous injection of LiCl in combination with captopril caused plasma Li⁺-concentrations of 0.66 ± 0.01 mmol/L (n=5) at 21 weeks of treatment. At 39 weeks of treatment the Li⁺-concentration was 0.86 ± 0.21 mmol/L (n=3). In one rat the Li⁺-concentration was 1.28 mmol/L, much higher than in the other two rats (0.63 and 0.66 mmol/L). Li⁺ was below detection limit or 0.02 ± 0.01 mmol/L at 21 and 39 weeks of treatment in captopril-treated rats (Table 7). The urinary excretion of Li⁺ in the two groups is shown in Table 8. Daily lithium excretion in urine had a tendency of increase in the captopril plus LiCl-group, and lithium excretion at 37 weeks of treatment was significantly higher than at 11 weeks of treatment (0.268 ± 0.084 mmol/day versus 0.091 ± 0.010 mmol/day, $P < 0.05$).

Table 7. The concentration of Li⁺ in the plasma of SHRSP at 21 and 39 weeks of treatment with captopril and captopril plus LiCl

Group	Li ⁺ (mmol/L)			
	21 weeks	(n)	39 weeks	(n)
Captopril	–	(6)	0.02 ± 0.01	(3)
Cap.+Li.	0.66 ± 0.01	(5)	0.86 ± 0.21	(3)

Values are mean \pm S.E.M of n rats.

Table 8. Daily Li⁺ excretion in the urine of SHRSP at 11, 19, 27 and 37 weeks of treatment with captopril and captopril plus LiCl

Group	Li ⁺ (mmol/day)			
	11 weeks (n)	19 weeks (n)	27 weeks (n)	37 weeks (n)
Captopril	0.003 ± 0.000 (7)	0.002 ± 0.000 (6)	0.003 ± 0.000 (6)	0.003 ± 0.000 (3)
Cap.+Li.	0.091 ± 0.010 (7)	0.124 ± 0.018 (6)	0.165 ± 0.055 (5)	$0.268 \pm 0.084^*$ (4)

Values are mean \pm S.E.M of n rats. * $P < 0.05$, versus Cap. + Li. group at 11 weeks of treatment.

Daily subcutaneous injection of LiCl in combination with telmisartan caused plasma Li⁺-concentrations of 0.62 ± 0.03 mmol/L (n=7) and 0.56 ± 0.02 mmol/L (n=7) at 21 and 39 weeks of treatment, respectively. Li⁺ was below detection limit or 0.04 ± 0.00 mmol/L at 21 and 39 weeks of treatment in the telmisartan-treated rats (Table 9). The urinary excretion of Li⁺ in the both groups is shown in Table 10. Daily urinary lithium excretions were comparable at the different time points.

Table 9. The concentration of Li⁺ in the plasma of SHRSP at 21 and 39 weeks of treatment with telmisartan and telmisartan plus LiCl

Group	Li ⁺ (mmol/L)			
	21 weeks	(n)	39 weeks	(n)
Telmisartan	–	(8)	0.04 ± 0.00	(7)
Telmi.+Li.	0.62 ± 0.03	(7)	0.56 ± 0.02	(7)

Values are mean \pm S.E.M of n rats.

Table 10. Daily Li⁺ excretion in the urine of SHRSP at 11, 19, 27 and 37 weeks of treatment with telmisartan and telmisartan plus LiCl

Group	Li ⁺ (mmol/day)							
	11 weeks	(n)	19 weeks	(n)	27 weeks	(n)	37 weeks	(n)
Telmisartan	0.014 ± 0.001	(8)	0.013 ± 0.001	(8)	0.013 ± 0.002	(8)	0.010 ± 0.002	(7)
Telmi.+Li	0.149 ± 0.019	(9)	0.125 ± 0.012	(7)	0.134 ± 0.025	(7)	0.158 ± 0.022	(7)

Values are mean \pm S.E.M of n rats.

3.1.7 Daily urinary excretion of albumin

Daily urinary excretion of albumin in the rats treated with captopril plus LiCl remained higher than in the rats treated with captopril alone, but there was no significant difference between the both groups after 11, 19, 27 and 37 weeks of treatment. There was an age-related increase in daily urinary excretion of albumin after long term treatment, but no significant difference among different treatment periods in the each group (Figure 16).

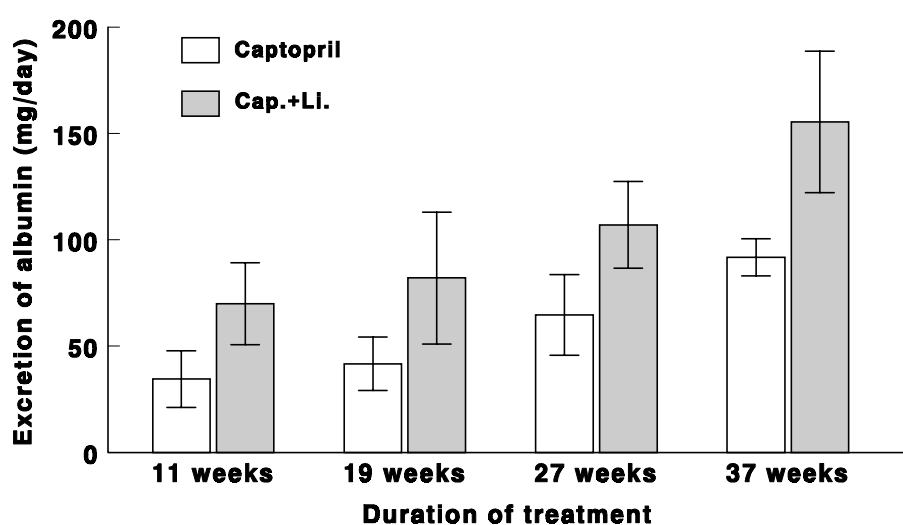


Figure 16. Effect of captopril and captopril plus LiCl on daily urinary excretions of albumin in salt-loaded SHRSP. From 8 weeks of age, SHRSP were treated subcutaneously with vehicle (0.9% NaCl), LiCl (1.0 mmol/kg/d), captopril (50 mg/kg/d) and captopril plus LiCl lifelong. At different treatment periods, rats were housed individually in metabolic cages, and urine was collected during a 24 h period for the measurement of albumin concentration.

At 11, 19 and 27 weeks of treatment, daily urinary excretion of albumin in the rats treated with telmisartan alone or in combination with LiCl remained below 40 mg/day. However, at 37 weeks of treatment, the daily urinary excretion of albumin in both groups significantly increased compared to the corresponding group at 11, 19 and 27 weeks of treatment ($P < 0.01$). There was no significant difference between both groups during the 4 different treatment periods (Figure 17).

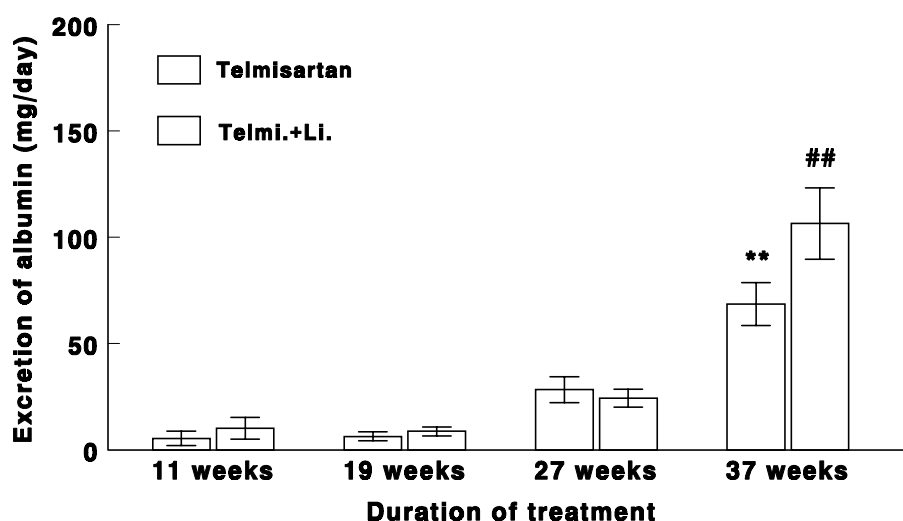


Figure 17. Effect of telmisartan and telmisartan plus LiCl on daily urinary excretions of albumin in salt-loaded SHRSP. From 8 weeks of age, SHRSP were treated subcutaneously with vehicle (0.9% NaCl), LiCl (1.0 mmol/kg/d), telmisartan (initially 1.0 mg/kg/d, and finally 0.3 mg/kg/d) and telmisartan plus LiCl lifelong. At different treatment periods, rats were housed individually in metabolic cages, and urine was collected during a 24 h period for the measurement of albumin concentration. ** P<0.01 versus telmisartan-treated animals and ## P<0.01 versus telmisartan plus LiCl-treated animals at 11, 19 and 27 weeks of treatment.

3.1.8 Plasma renin activity

After 21 weeks of treatment, the PRA in captopril and captopril plus LiCl treated rats was 28.4 ± 1.6 or 25.4 ± 2.7 ng Ang I/ml/h, respectively, and there was no significant difference between the both groups (Table 11).

Table 11. The plasma renin activity in salt-loaded SHRSP at 21 weeks of treatment with captopril and captopril plus LiCl

Group	n	Activity of renin (ng Ang I/ml/h)
Captopril	6	28.4 ± 1.6
Cap.+Li.	5	25.4 ± 2.7

Values are mean \pm S.E.M of n rats.

After 21 weeks of treatment, the PRA in telmisartan and telmisartan plus LiCl treated rats was 22.4 ± 2.7 or 18.0 ± 3.1 ng Ang I/ml/h, respectively, and there was no significant difference between both groups (Table 12).

Table 12. The plasma renin activity in salt-loaded SHRSP at 21 weeks of treatment with telmisartan and telmisartan plus LiCl

Group	n	Activity of renin (ng Ang I/ml/h)
Telmisartan	8	22.4 ± 2.7
Telmi.+ Li.	6	18.0 ± 3.1

Values are mean \pm S.E.M of n rats.

3.1.9 Neurological signs

All animals in the vehicle- and LiCl- groups exhibited at least one of the neurological signs accompanying stroke: piloerection, jumping, paralysis of anterior and/or posterior paws, aggression, prostration, loss of body symmetry and convulsions, a few days before death. Rats treated with captopril, captopril plus LiCl, telmisartan or telmisartan plus LiCl had slight or no neurological signs before death.

3.1.10 Histopathologic studies

Five rats from each group were killed after 5 weeks of treatment. All five of the brains examined from vehicle-treated SHRSP exhibited areas of moderate-to-severe rarefaction, especially in the cerebral cortex. Other lesions observed in vehicle-treated SHRSP included: edema, focal infarction, and one rat had hemorrhage. All five of the brains examined from LiCl-treated SHRSP had the same cerebral lesions as observed in the vehicle group. However, histological analysis of the all five brains from SHRSP treated with captopril alone or in combination with LiCl revealed no evidence of cerebrovascular lesions (Figure 18). After a long term treatment with captopril and captopril plus LiCl, the rats which were very debilitated or exhibited huge edema a few days before death were killed for histological analysis. The brains from these rats in both groups showed rarefaction, and one brain from each group showed infarction and hemorrhage.

Histological analysis of the all five brains from SHRSP treated with telmisartan alone or in combination with LiCl showed no evidence of cerebrovascular lesions (Figure 18).

After a long term treatment with telmisartan and telmisartan plus LiCl, the rats which were very debilitated or exhibited huge edema a few days before death were killed for histological analysis. The brains from four rats treated with telmisartan showed rarefaction, and only one from these four brains exhibited hemorrhage and infarction. The brains from six rats treated with telmisartan plus LiCl showed rarefaction, and only one from these six brains exhibited hemorrhage and infarction.

3.1.11 TUNEL staining

There were many strong TUNEL labeled cells in the brains from the vehicle treated-rats, and some TUNEL positive cells distributed in the corresponding areas with infarction (cresyl violet staining) (Figure 19). LiCl treatment did not significantly change the expression of TUNEL-positive cells in the brains of salt-loaded SHRSP compared to vehicle. However, rats treated with captopril alone or in combination with LiCl for five weeks had significantly less TUNEL positive cells compared to vehicle, in the coronal sections of brains through bregma – 0.3 mm (0.60 ± 0.40 and 0.80 ± 0.58 versus 2.80 ± 0.20 , $P < 0.05$), bregma – 3.8 mm (0.60 ± 0.40 and 1.20 ± 0.37 versus 3.00 ± 0.00 , $P < 0.01$), and bregma – 5.3 mm (1.00 ± 0.55 and 1.20 ± 0.37 versus 3.00 ± 0.45 , $P < 0.05$). No significant difference in the amount of TUNEL positive cells was observed in brain sections through bregma – 1.8 mm. There was no significant difference on the expression of TUNEL-positive cells between the captopril- and captopril plus LiCl-groups (Figure 20). Therefore, captopril alone or in combination with LiCl had anti-apoptotic effect in the brains of salt-loaded SHRSP, but the addition of LiCl to captopril did not offer further anti-apoptotic effect.

After a long term treatment, only two rats in the captopril group and the captopril plus LiCl group could be used for TUNEL staining, with no significant difference between the both groups.

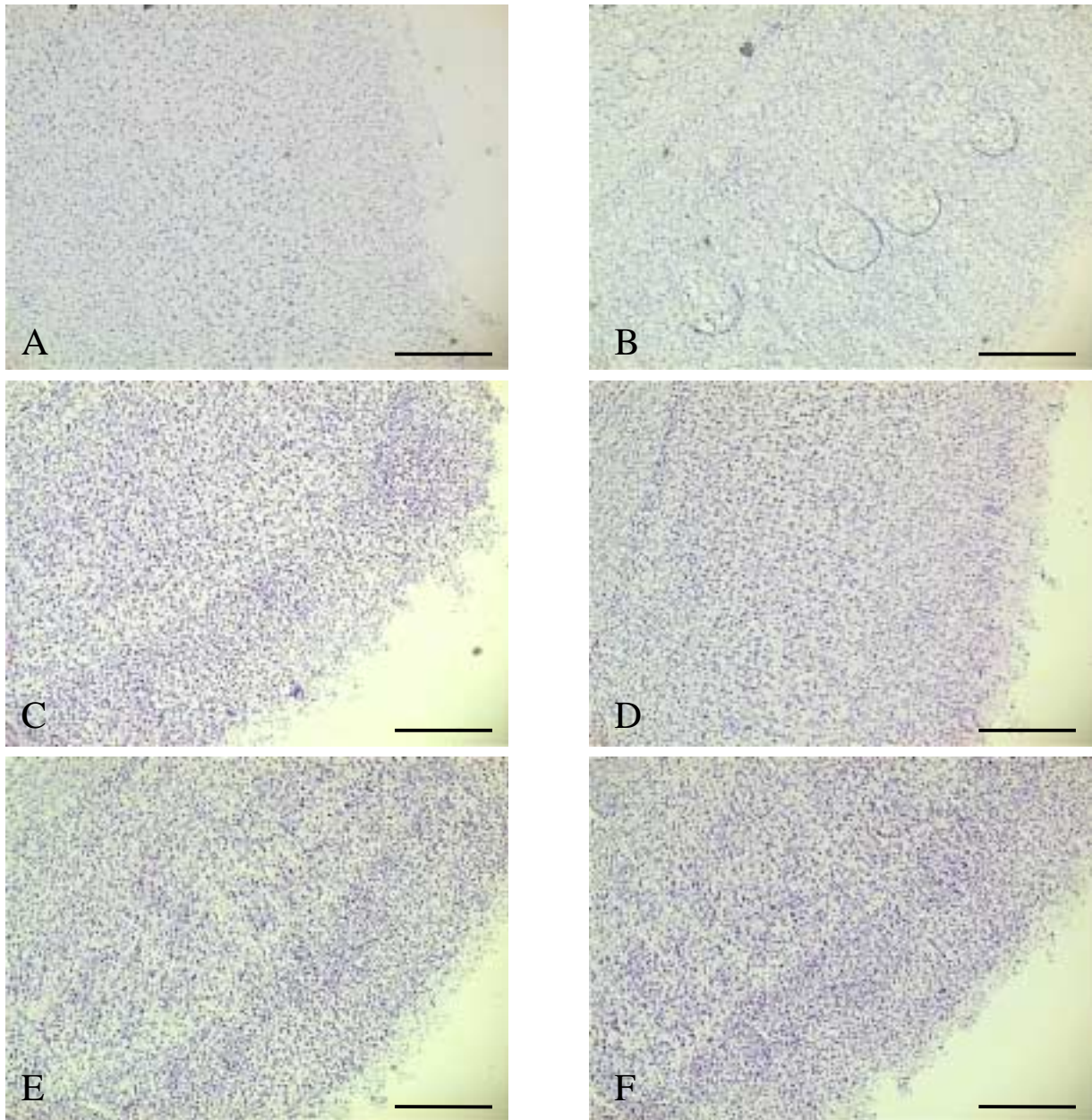


Figure 18. Cresyl violet staining of brain sections through the brain cortex from salt-loaded SHRSP treated for 5 weeks with vehicle (A), LiCl (B), captopril (C), captopril plus LiCl (D), telmisartan (E) and telmisartan plus LiCl (F).

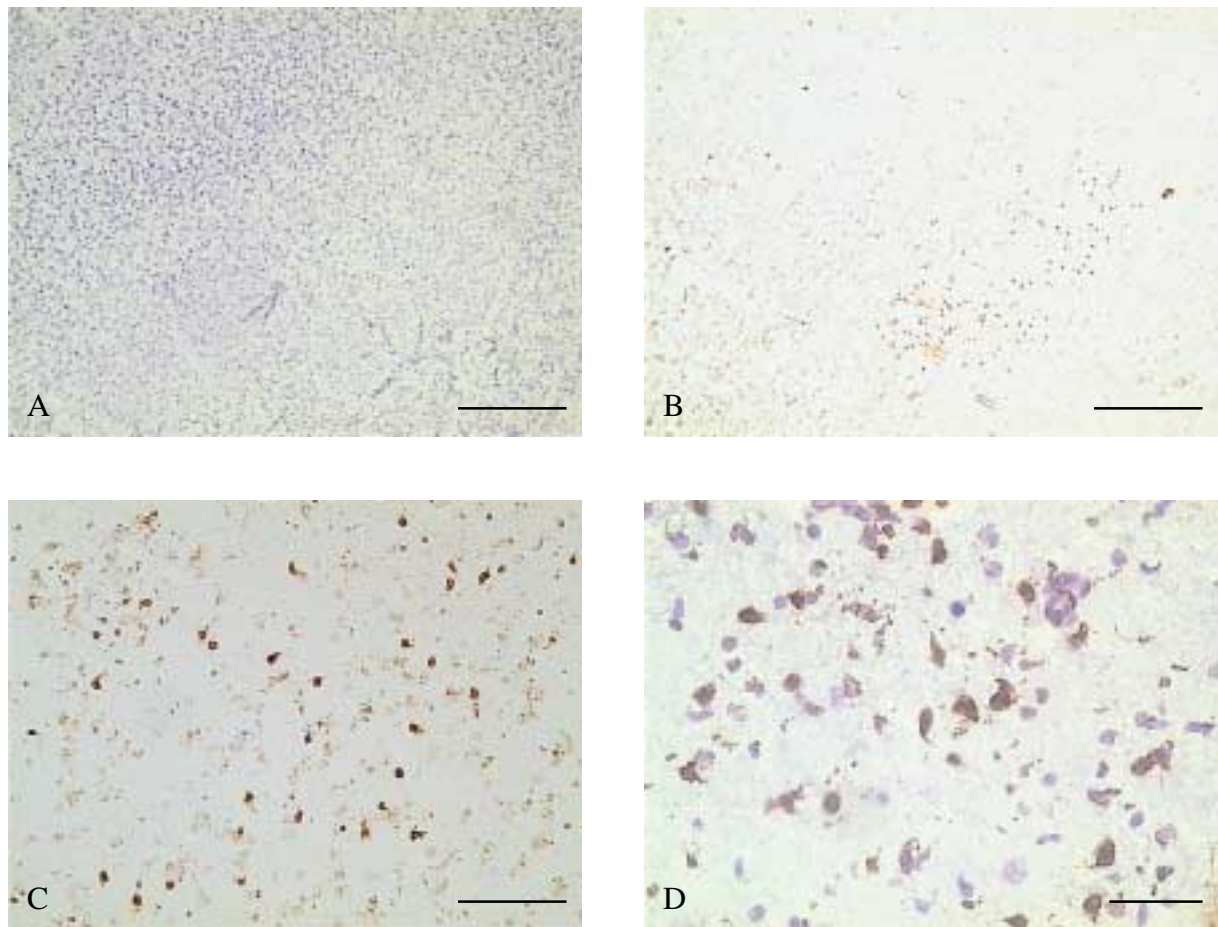


Figure 19. Cresyl violet staining (A), TUNEL staining (B, C), and double staining with cresyl violet and TUNEL (D) in the brain of a vehicle-treated salt-loaded SHRSP. Cresyl violet staining shows an infarct area in the thalamus (A), and with many TUNEL positive strongly labeled cells in the corresponding area of the adjacent section (B). Cells stained with dark brown color are TUNEL labeled cells, and cells stained with blue color show surviving cells. Scale bar: A, B, 500 μm ; C, 125 μm ; D, 50 μm .

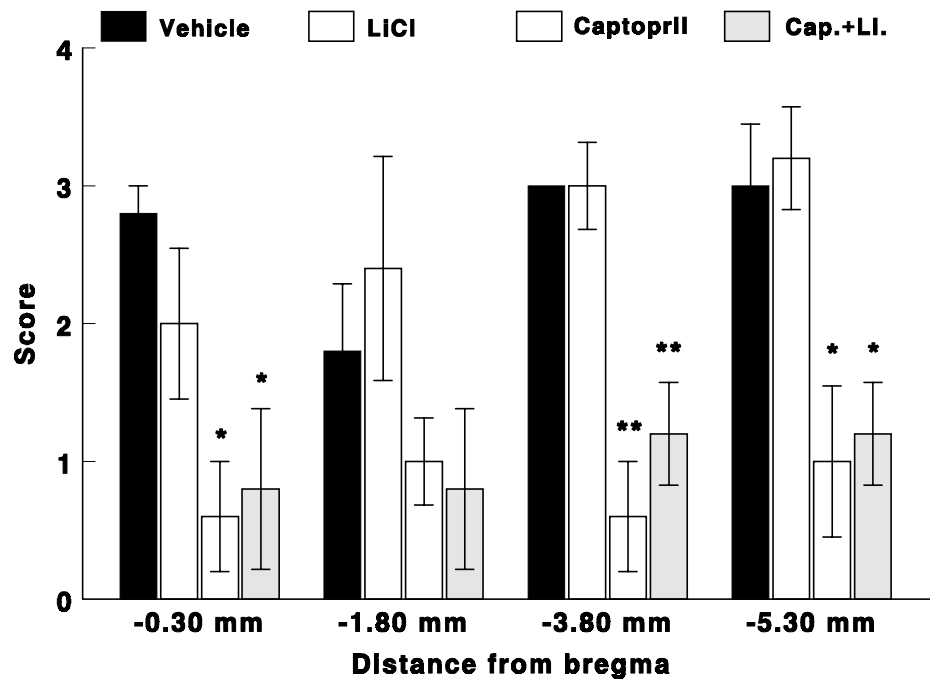


Figure 20. Effect of LiCl, captopril and captopril plus LiCl on apoptotic expression by TUNEL staining in brains from salt-loaded SHRSP. From 8 weeks of age, SHRSP were treated subcutaneously with vehicle (0.9% NaCl), LiCl (1.0 mmol/kg/d), captopril (50 mg/kg/d) and captopril plus LiCl lifelong. After 5 weeks of treatment, 5 rats from each group were killed for TUNEL staining. * $P < 0.05$, ** $P < 0.01$ versus vehicle-treated animals. Scoring system: 0, no or few TUNEL positive cells; 1, random TUNEL positive cells; 2, a discrete region of TUNEL positive cells; 3, many strong TUNEL positive cells; and 4, the entire region is distributed with TUNEL positive cells.

Salt-loaded SHRSP treated with telmisartan for five weeks had significantly less TUNEL-positive cells compared to vehicle, in the coronal sections of brains with bregma – 0.3 mm (0.40 ± 0.40 versus 2.80 ± 0.20 , $P < 0.05$) and bregma – 3.8 mm (0.80 ± 0.37 versus 3.00 ± 0.00 , $P < 0.01$), but no significant difference in bregma – 1.8 mm and – 5.3 mm. The addition of LiCl to telmisartan significantly reduced TUNEL-positive cells compared to vehicle, in the coronal sections of brains with bregma – 3.8 mm (0.20 ± 0.20 versus 3.00 ± 0.00 , $P < 0.01$) and bregma – 5.3 mm (1.00 ± 0.32 versus 3.00 ± 0.45 , $P < 0.05$), but not in the section though bregma – 0.3 mm and bregma – 1.8 mm. There was no significant difference on the expression of TUNEL-positive cells between the telmisartan- and telmisartan plus LiCl-groups (Figure 21). Therefore, telmisartan alone or in combination with LiCl had anti-apoptotic effects in the brains of salt-loaded SHRSP, but the addition of LiCl to telmisartan did not offer further anti-apoptotic effects.

After a long term treatment, four rats from the telmisartan-group and five rats from the telmisartan plus LiCl-group were used for TUNEL staining. There was no significant difference between both groups in the expression of TUNEL-positive cells in the coronal sections of brains with bregma – 0.3 mm, – 1.8 mm, – 3.8 mm and – 5.3 mm (Figure 22). However, after long term treatment, the TUNEL positive cells in the brains of SHRSP in both groups tended to increase compared to five weeks of treatment, and there were significant differences between 5 weeks of treatment and a long-term treatment in the telmisartan plus LiCl-group in bregma – 3.8 mm (0.20 ± 0.20 versus 2.20 ± 0.49 , $P < 0.05$) and bregma – 5.3 mm (1.00 ± 0.32 versus 2.80 ± 0.20 , $P < 0.01$). The increase in TUNEL-positive cells in the brains of SHRSP after a long term treatment may be the age –related increase of apoptosis.

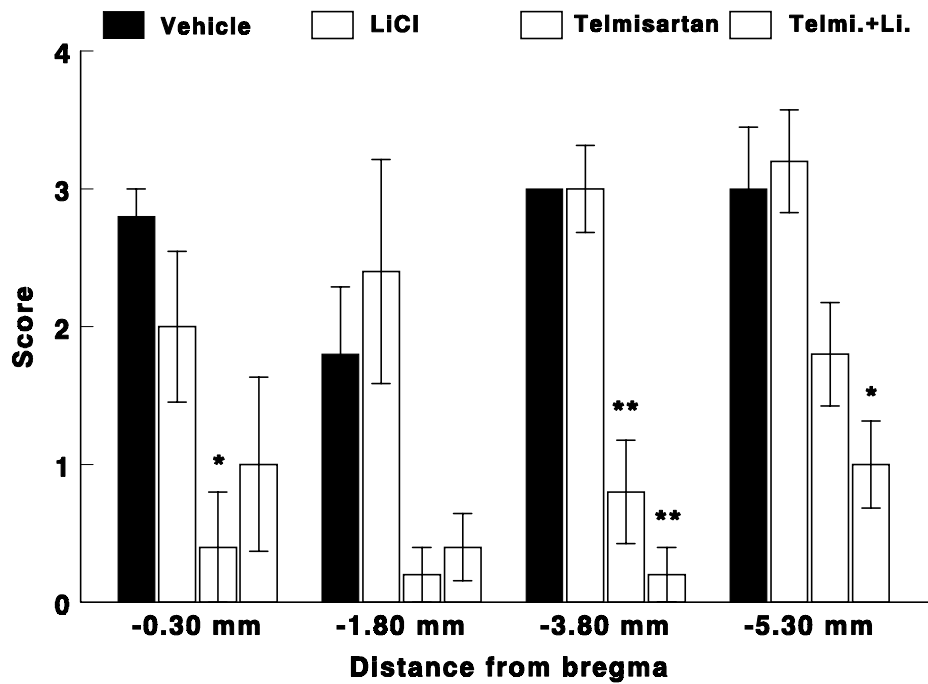


Figure 21. Effect of LiCl, telmisartan and telmisartan plus LiCl on apoptotic expression by TUNEL staining in brains from salt-loaded SHRSP. From 8 weeks of age, SHRSP were treated subcutaneously with vehicle (0.9% NaCl), LiCl (1.0 mmol/kg/d), telmisartan (initially 1.0 mg/kg/d, and finally 0.3 mg/kg/d) and telmisartan plus LiCl lifelong. After 5 weeks of treatment, 5 rats from each group were killed for TUNEL staining. * $P < 0.05$, ** $P < 0.01$ versus vehicle-treated animals. Scoring system: 0, no or few TUNEL positive cells; 1, random TUNEL positive cells; 2, a discrete region of TUNEL positive cells; 3, many strong TUNEL positive cells; and 4, the entire region is distributed with TUNEL positive cells.

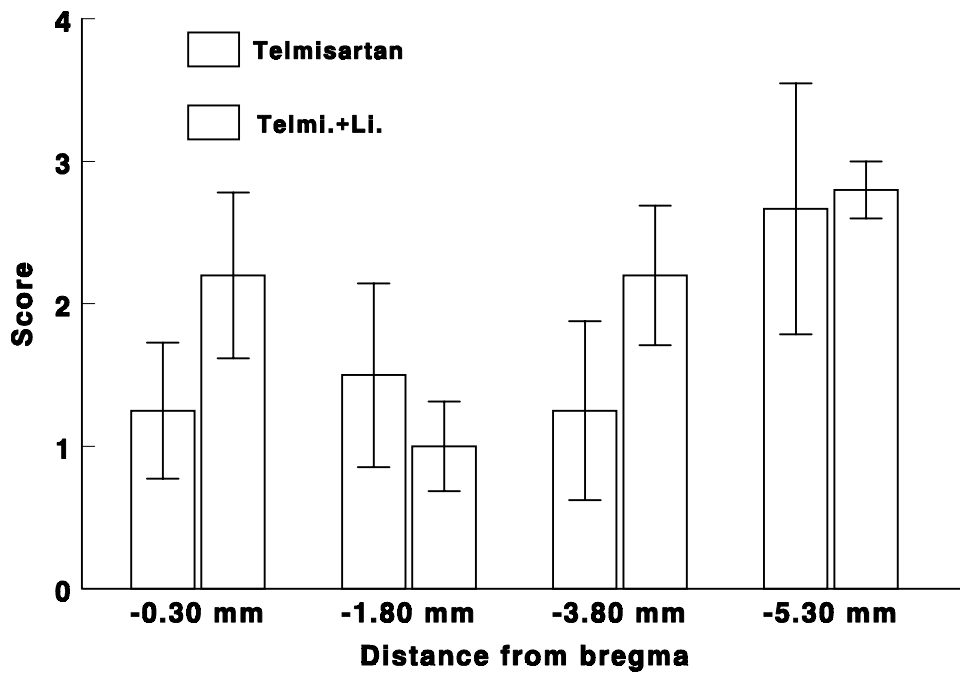


Figure 22. Effect of a long-term treatment with telmisartan and telmisartan plus LiCl on apoptotic expression by TUNEL staining in brains from salt-loaded SHRSP. From 8 weeks of age, SHRSP were treated subcutaneously with vehicle (0.9% NaCl), LiCl (1.0 mmol/kg/d), telmisartan (initially 1.0 mg/kg/d, and finally 0.3 mg/kg/d) and telmisartan plus LiCl lifelong. When the rats were very debilitated they were killed for TUNEL staining. Scoring system: 0, no or few TUNEL positive cells; 1, random TUNEL positive cells; 2, a discrete region of TUNEL positive cells; 3, many strong TUNEL positive cells; and 4, the entire region is distributed with TUNEL positive cells.

3.2 Intraluminal thread model of focal cerebral ischemia

3.2.1 Physiological parameters

3.2.1.1 Mean arterial blood pressure (MAP)

No significant differences in MAP before MCAO, during MCAO and after reperfusion were apparent between LiCl-treated rats and vehicle-treated rats. However, rats treated with captopril alone or in combination with LiCl had significantly lower blood pressure levels during their conscious state and during anesthesia before MCAO, compared to vehicle. Blood pressure in the both groups was significantly lower during the 90-min MCAO period as well as the reperfusion period compared to vehicle (Figure 23).

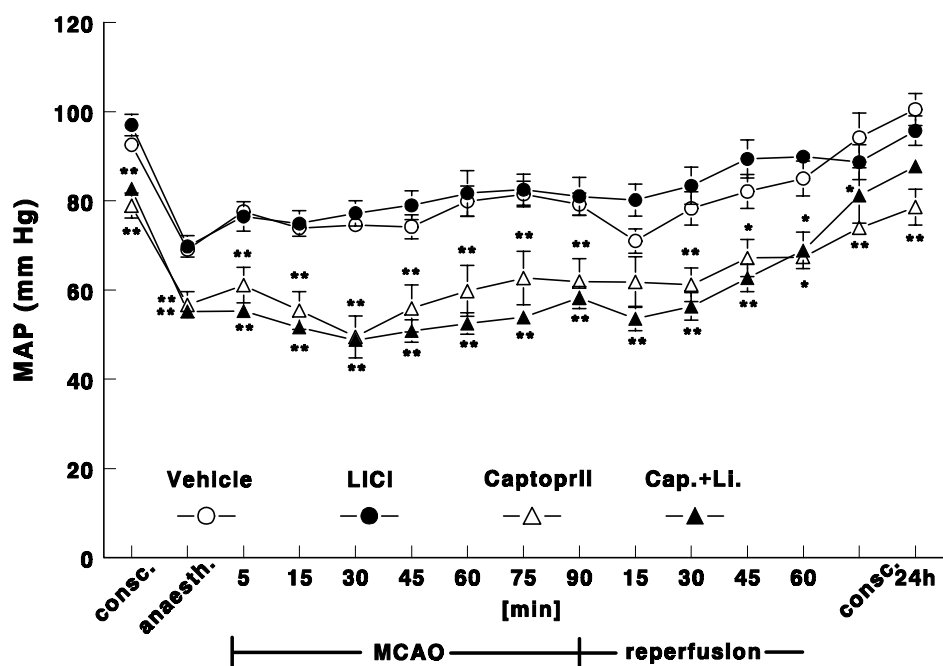


Figure 23. Effect of LiCl, captopril and captopril plus LiCl on mean arterial blood pressure (MAP) in Wistar rats. After 14 days of treatment with LiCl (1 mmol/kg/d), captopril (25 mg/kg/d) and captopril plus LiCl, MAP was measured at different time points before, during and after MCAO.

* P<0.05, ** P<0.01 versus vehicle-treated animals.

Rats treated with telmisartan alone or in combination with LiCl did not significantly change blood pressure level during their conscious state and during anesthesia before MCAO, compared to vehicle. However, blood pressure levels in the telmisartan group were significantly lower at 30, 75 and 90 min after MCAO compared to the vehicle-treated group (Figure 24). In the telmisartan plus LiCl-treated group blood pressure was significantly lower at 30, 45, 60, 75, 90 min after MCAO and at 30, 45, 60 min following reperfusion compared to the vehicle group (Figure 24). The blood pressure levels in telmisartan-, telmisartan plus LiCl-, LiCl- and vehicle-treated rats were similar in the conscious state following reperfusion and 24h after reperfusion (Figure 24).

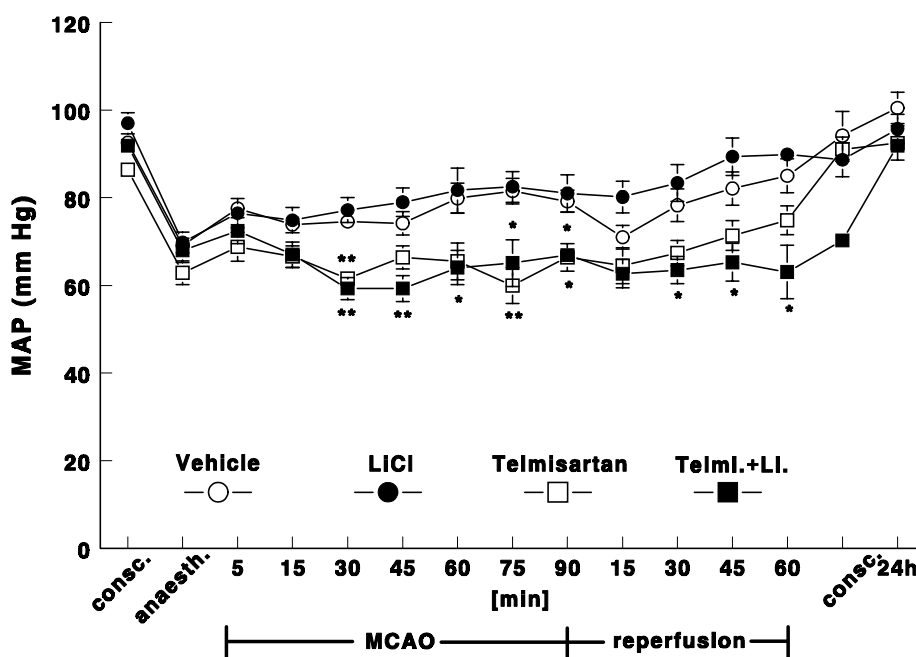


Figure 24. Effect of LiCl, telmisartan and telmisartan plus LiCl on mean arterial blood pressure (MAP) in Wistar rats. After 14 days of treatment with LiCl (1 mmol/kg/d), telmisartan (0.3 mg/kg/d) and telmisartan plus LiCl, MAP was measured at different time points before, during and after MCAO. * $P < 0.05$, ** $P < 0.01$ versus vehicle-treated animals.

3.2.1.2 Blood parameters

The values of pH, pCO₂, and pO₂ in the blood as well as the blood concentrations of hemoglobin, glucose, lactate and the electrolytes Na⁺, K⁺, Ca²⁺, Cl⁻ were normal in the rats treated with LiCl, captopril and captopril plus LiCl before ischemia, during ischemia and after reperfusion, and were not significantly different between the drug-treated groups and the vehicle-group (Table 13 and 14).

The values of pH, pCO₂, and pO₂ in the blood as well as the blood concentrations of hemoglobin, glucose, lactate and the electrolytes Na⁺, K⁺, Ca²⁺, Cl⁻ were normal in the rats treated with telmisartan before ischemia, during ischemia and after reperfusion, and were not significantly different from the vehicle group. However, rats treated with telmisartan plus LiCl had a significantly increased plasma pO₂ in the conscious state before MCAO and at 30 and 90 min after MCAO (P<0.01), and a significantly reduced blood concentration of lactate in the conscious state and during anesthesia just before MCAO (P<0.05), compared to rats treated with vehicle. (Table 15 and 16).

Table 13. Blood parameters before, during and after 90-min MCAO after treatment with LiCl, captopril and captopril plus LiCl

Parameter	Vehicle (n=14)	Treatment		
		LiCl (n= 7)	Captopril (n= 7)	Captopril+LiCl (n= 8)
pH				
Conscious before MCAO	7.430 ± 0.006	7.414 ± 0.013	7.426 ± 0.012	7.419 ± 0.010
Anesthesia before MCAO	7.330 ± 0.010	7.301 ± 0.014	7.337 ± 0.008	7.332 ± 0.014
30 minutes after MCAO	7.363 ± 0.018	7.365 ± 0.023	7.362 ± 0.018	7.341 ± 0.013
90 minutes after MCAO	7.404 ± 0.013	7.395 ± 0.025	7.395 ± 0.023	7.368 ± 0.018
30 minutes after Reperfusion	7.361 ± 0.013	7.357 ± 0.015	7.347 ± 0.009	7.324 ± 0.016
pCO₂ mmHg				
Conscious before MCAO	33.15 ± 1.07	35.59 ± 1.39	33.70 ± 2.65	33.14 ± 1.42
Anesthesia before MCAO	47.37 ± 0.80	50.13 ± 2.76	46.52 ± 0.68	45.73 ± 1.25
30 minutes after MCAO	45.74 ± 1.62	43.39 ± 2.70	40.62 ± 1.51	41.55 ± 1.30
90 minutes after MCAO	38.32 ± 1.11	37.24 ± 2.82	33.95 ± 2.07	35.24 ± 1.10
30 minutes after Reperfusion	41.39 ± 1.13	40.43 ± 2.10	38.65 ± 1.58	37.75 ± 1.58
pO₂ mmHg				
Conscious before MCAO	79.61 ± 1.67	80.06 ± 1.13	85.53 ± 4.33	82.91 ± 1.26
Anesthesia before MCAO	73.35 ± 1.59	71.17 ± 2.71	77.32 ± 2.42	76.06 ± 2.49
30 minutes after MCAO	75.89 ± 1.86	80.46 ± 3.22	87.12 ± 4.40	81.62 ± 3.16
90 minutes after MCAO	81.29 ± 2.35	83.14 ± 1.88	86.88 ± 2.89	88.40 ± 3.26
30 minutes after Reperfusion	83.54 ± 1.66	84.12 ± 2.43	93.32 ± 3.75	86.61 ± 2.56
cGlu mg/dL				
Conscious before MCAO	112.9 ± 7.3	115.0 ± 5.0	118.3 ± 16.4	112.6 ± 9.0
Anesthesia before MCAO	181.1 ± 6.2	171.4 ± 8.1	181.2 ± 12.2	202.1 ± 10.6
30 minutes after	182.4 ± 9.1	169.6 ± 12.5	172.8 ± 10.9	203.5 ± 17.5
90 minutes after MCAO	181.6 ± 9.4	162.4 ± 14.7	158.8 ± 15.4	165.8 ± 12.1
30 minutes after Reperfusion	188.7 ± 10.9	189.8 ± 19.5	178.2 ± 15.7	204.3 ± 15.4
cLac mmol/L				
Conscious before MCAO	1.600 ± 0.909	1.543 ± 0.129	1.550 ± 0.165	1.430 ± 0.143
Anesthesia before MCAO	3.357 ± 0.252	3.271 ± 0.344	2.917 ± 0.379	2.520 ± 0.256
30 minutes after MCAO	2.114 ± 0.116	2.171 ± 0.182	2.317 ± 0.316	2.300 ± 0.188
90 minutes after MCAO	2.029 ± 0.116	2.014 ± 0.160	1.800 ± 0.124	2.280 ± 0.255
30 minutes after Reperfusion	1.736 ± 0.107	1.700 ± 0.124	1.500 ± 0.068	2.320 ± 0.474
ctHb g/dL				
Conscious before MCAO	11.65 ± 0.41	12.90 ± 0.58	12.28 ± 0.42	12.06 ± 0.54
Anesthesia before MCAO	14.31 ± 0.32	14.33 ± 0.93	14.37 ± 1.02	14.68 ± 0.31
30 minutes after MCAO	15.15 ± 0.39	15.01 ± 1.02	13.77 ± 1.19	14.02 ± 0.39
90 minutes after MCAO	15.01 ± 0.33	14.43 ± 0.69	15.20 ± 0.45	14.65 ± 0.52
30 minutes after Reperfusion	14.96 ± 0.35	14.80 ± 0.55	14.48 ± 0.30	13.74 ± 0.59

Data are mean ± SEM of n rats.

cGlu = plasma concentration of glucose; cLac = plasma concentration of lactate; ctHb = plasma concentration of hemoglobin.

Table 14. Blood electrolytes before, during and after 90-min MCAO after treatment with LiCl, captopril and captopril plus LiCl

Parameter	Vehicle (n=14)	Treatment		
		LiCl (n= 7)	Captopril (n= 7)	Captopril+LiCl (n= 8)
cNa⁺ mmol/L				
Conscious before MCAO	143.2 ± 0.6	140.2 ± 0.6	139.7 ± 0.5	139.0 ± 0.6
Anaesthesia before MCAO	137.7 ± 0.5	135.4 ± 0.8	135.0 ± 0.7	133.9 ± 0.8
30 minutes after MCAO	136.1 ± 0.5	133.9 ± 1.0	133.8 ± 0.7	132.9 ± 0.9
90 minutes after MCAO	135.0 ± 0.7	133.8 ± 1.4	133.2 ± 1.1	132.8 ± 1.0
30 minutes after Reperfusion	134.7 ± 0.5	131.9 ± 0.6	133.3 ± 1.1	132.9 ± 1.2
cK⁺ mmol/L				
Conscious before MCAO	3.576 ± 0.114	3.714 ± 0.208	3.832 ± 0.115	3.451 ± 0.129
Anaesthesia before MCAO	4.588 ± 0.074	4.594 ± 0.236	4.702 ± 0.101	4.305 ± 0.101
30 minutes after MCAO	4.361 ± 0.115	4.431 ± 0.232	4.967 ± 0.232	4.670 ± 0.168
90 minutes after MCAO	4.341 ± 0.098	4.361 ± 0.236	4.635 ± 0.172	4.843 ± 0.321
30 minutes after Reperfusion	3.746 ± 0.127	3.955 ± 0.154	4.148 ± 0.168	4.637 ± 0.612
cCa²⁺ mmol/L				
Conscious before MCAO	1.150 ± 0.028	1.191 ± 0.037	1.137 ± 0.031	1.147 ± 0.017
Anaesthesia before MCAO	1.131 ± 0.017	1.127 ± 0.019	1.107 ± 0.015	1.150 ± 0.017
30 minutes after MCAO	1.220 ± 0.014	1.210 ± 0.019	1.138 ± 0.018	1.152 ± 0.015
90 minutes after MCAO	1.175 ± 0.014	1.191 ± 0.029	1.113 ± 0.019	1.194 ± 0.017
30 minutes after Reperfusion	1.184 ± 0.010	1.205 ± 0.024	1.145 ± 0.015	1.182 ± 0.018
cCl⁻ mmol/L				
Conscious before MCAO	112.7 ± 1.3	109.1 ± 1.3	109.8 ± 2.3	109.6 ± 1.5
Anaesthesia before MCAO	106.4 ± 0.6	103.9 ± 1.3	104.0 ± 0.6	104.3 ± 0.7
30 minutes after	105.5 ± 0.6	103.3 ± 1.2	106.8 ± 1.3	104.0 ± 0.9
90 minutes after MCAO	106.1 ± 0.6	104.4 ± 1.1	106.8 ± 1.2	105.6 ± 0.9
30 minutes after Reperfusion	106.7 ± 0.6	103.8 ± 1.1	106.3 ± 1.2	105.8 ± 0.9

Data are mean ± SEM of n rats.

cNa⁺, cK⁺, cCa²⁺ and cCl⁻ indicate plasma concentration of Na⁺, K⁺, Ca²⁺ and Cl⁻.

Table 15. Blood parameters before, during and after 90-min MCAO after treatment with LiCl, telmisartan and telmisartan plus LiCl

Parameter	Vehicle (n=14)	Treatment		
		LiCl (n= 7)	Telmisartan (n= 8)	Telmisartan+LiCl (n= 7)
pH				
Conscious before MCAO	7.430 ± 0.006	7.414 ± 0.013	7.427 ± 0.016	7.410 ± 0.014
Anaesthesia before MCAO	7.330 ± 0.010	7.301 ± 0.014	7.323 ± 0.014	7.357 ± 0.022
30 minutes after MCAO	7.363 ± 0.018	7.365 ± 0.023	7.361 ± 0.017	7.409 ± 0.031
90 minutes after MCAO	7.404 ± 0.013	7.395 ± 0.025	7.372 ± 0.015	7.416 ± 0.028
30 minutes after Reperfusion	7.361 ± 0.013	7.357 ± 0.015	7.325 ± 0.037	7.351 ± 0.020
pCO₂ mmHg				
Conscious before MCAO	33.15 ± 1.07	35.59 ± 1.39	33.99 ± 0.87	35.20 ± 2.22
Anaesthesia before MCAO	47.37 ± 0.80	50.13 ± 2.76	48.08 ± 1.54	46.08 ± 2.20
30 minutes after MCAO	45.74 ± 1.62	43.39 ± 2.70	42.84 ± 2.11	37.29 ± 3.40
90 minutes after MCAO	38.32 ± 1.11	37.24 ± 2.82	37.61 ± 1.21	32.40 ± 2.70
30 minutes after Reperfusion	41.39 ± 1.13	40.43 ± 2.10	42.24 ± 1.62	38.27 ± 1.31
pO₂ mmHg				
Conscious before MCAO	79.61 ± 1.67	80.06 ± 1.13	79.68 ± 2.35	92.24 ± 5.77**
Anaesthesia before MCAO	73.35 ± 1.59	71.17 ± 2.71	78.63 ± 2.57	78.75 ± 3.50
30 minutes after MCAO	75.89 ± 1.86	80.46 ± 3.22	84.56 ± 2.70	93.86 ± 3.36**
90 minutes after MCAO	81.29 ± 2.35	83.14 ± 1.88	86.24 ± 3.67	109.00 ± 8.95**
30 minutes after Reperfusion	83.54 ± 1.66	84.12 ± 2.43	85.45 ± 4.27	87.03 ± 3.87
cGlu mg/dL				
Conscious before MCAO	112.9 ± 7.3	115.0 ± 5.0	105.9 ± 2.7	121.3 ± 10.4
Anaesthesia before MCAO	181.1 ± 6.2	171.4 ± 8.1	207.6 ± 21.2	206.3 ± 3.9
30 minutes after	182.4 ± 9.1	169.6 ± 12.5	172.3 ± 15.9	182.0 ± 16.1
90 minutes after MCAO	181.6 ± 9.4	162.4 ± 14.7	168.0 ± 9.7	170.8 ± 12.8
30 minutes after Reperfusion	188.7 ± 10.9	189.8 ± 19.5	180.7 ± 7.9	194.3 ± 11.3
cLac mmol/L				
Conscious before MCAO	1.600 ± 0.909	1.543 ± 0.129	1.613 ± 0.144	1.143 ± 0.113*
Anaesthesia before MCAO	3.357 ± 0.252	3.271 ± 0.344	3.550 ± 0.408	1.917 ± 0.450*
30 minutes after MCAO	2.114 ± 0.116	2.171 ± 0.182	2.171 ± 0.155	2.067 ± 0.421
90 minutes after MCAO	2.029 ± 0.116	2.014 ± 0.160	2.029 ± 0.087	1.983 ± 0.239
30 minutes after Reperfusion	1.736 ± 0.107	1.700 ± 0.124	1.614 ± 0.067	1.786 ± 0.167
ctHb g/dL				
Conscious before MCAO	11.65 ± 0.41	12.90 ± 0.58	10.99 ± 0.65	12.67 ± 0.97
Anaesthesia before MCAO	14.31 ± 0.32	14.33 ± 0.93	13.73 ± 0.76	14.53 ± 0.44
30 minutes after MCAO	15.15 ± 0.39	15.01 ± 1.02	13.89 ± 0.90	14.46 ± 0.32
90 minutes after MCAO	15.01 ± 0.33	14.43 ± 0.69	13.64 ± 0.93	14.53 ± 0.61
30 minutes after Reperfusion	14.96 ± 0.35	14.80 ± 0.55	13.83 ± 0.66	14.20 ± 0.43

Data are mean±SEM of n rats.

cGlu = plasma concentration of glucose; cLac = plasma concentration of lactate; ctHb = plasma concentration of hemoglobin. * P<0.05, ** P<0.01, statistical comparison to the vehicle-pretreated group.

Table 16. Blood electrolytes before, during and after 90-min MCAO after treatment with LiCl, telmisartan and telmisartan plus LiCl

Parameter	Treatment			
	Vehicle (n=14)	LiCl (n= 7)	Telmisartan (n= 8)	Telmisartan+LiCl (n= 7)
cNa⁺ mmol/L				
Conscious before MCAO	143.2 ± 0.6	140.2 ± 0.6	142.5 ± 0.6	139.2 ± 1.1
Anaesthesia before MCAO	137.7 ± 0.5	135.4 ± 0.8	136.5 ± 0.4	138.7 ± 5.1
30 minutes after MCAO	136.1 ± 0.5	133.9 ± 1.0	134.5 ± 0.7	133.8 ± 1.1
90 minutes after MCAO	135.0 ± 0.7	133.8 ± 1.4	133.6 ± 0.7	132.8 ± 1.7
30 minutes after Reperfusion	134.7 ± 0.5	131.9 ± 0.6	134.2 ± 0.5	134.1 ± 1.1
cK⁺ mmol/L				
Conscious before MCAO	3.576 ± 0.114	3.714 ± 0.208	3.639 ± 0.106	3.693 ± 0.180
Anaesthesia before MCAO	4.588 ± 0.074	4.594 ± 0.236	4.545 ± 0.133	4.667 ± 0.243
30 minutes after MCAO	4.361 ± 0.115	4.431 ± 0.232	5.099 ± 0.305	4.545 ± 0.103
90 minutes after MCAO	4.341 ± 0.098	4.361 ± 0.236	4.795 ± 0.472	4.448 ± 0.137
30 minutes after Reperfusion	3.746 ± 0.127	3.955 ± 0.154	4.723 ± 0.733	4.239 ± 0.122
cCa²⁺ mmol/L				
Conscious before MCAO	1.150 ± 0.028	1.191 ± 0.037	1.141 ± 0.016	1.149 ± 0.032
Anaesthesia before MCAO	1.131 ± 0.017	1.127 ± 0.019	1.148 ± 0.023	1.177 ± 0.035
30 minutes after MCAO	1.220 ± 0.014	1.210 ± 0.019	1.214 ± 0.025	1.170 ± 0.018
90 minutes after MCAO	1.175 ± 0.014	1.191 ± 0.029	1.170 ± 0.017	1.185 ± 0.023
30 minutes after Reperfusion	1.184 ± 0.010	1.205 ± 0.024	1.193 ± 0.023	1.209 ± 0.014
cCl⁻ mmol/L				
Conscious before MCAO	112.7 ± 1.3	109.1 ± 1.3	111.9 ± 1.0	110.0 ± 2.0
Anaesthesia before MCAO	106.4 ± 0.6	103.9 ± 1.3	104.6 ± 0.8	104.7 ± 1.8
30 minutes after	105.5 ± 0.6	103.3 ± 1.2	104.8 ± 0.9	105.3 ± 1.5
90 minutes after MCAO	106.1 ± 0.6	104.4 ± 1.1	105.6 ± 0.8	106.7 ± 0.7
30 minutes after Reperfusion	106.7 ± 0.6	103.8 ± 1.1	105.3 ± 0.5	104.9 ± 0.9

Data are mean±SEM of n rats.

cNa⁺, cK⁺, cCa²⁺ and cCl⁻ indicate plasma concentration of Na⁺, K⁺, Ca²⁺ and Cl⁻.

3.2.2 Measurement of regional cerebral blood flow

To reduce the likelihood that any differences in the neurological or histological outcome were due to alterations in the degree of the ischemic insult, rCBF was monitored before, during and after ischemia. Rats were only included in the study when MCAO caused an immediate and constant reduction of the ipsilateral rCBF in the MCA territory by more than 80% during the 90 min of MCAO. Contralateral rCBF fluctuated at $\approx 100\%$ of baseline in these animals (data not shown). After filament withdrawal, the ipsilateral rCBF restored to 54-76% of baseline. Intraischemic rCBF reductions and postischemic reperfusion levels were comparable between the vehicle- and drug-treated groups, indicating an equivalent relative depth of ischemia (Figure 25).

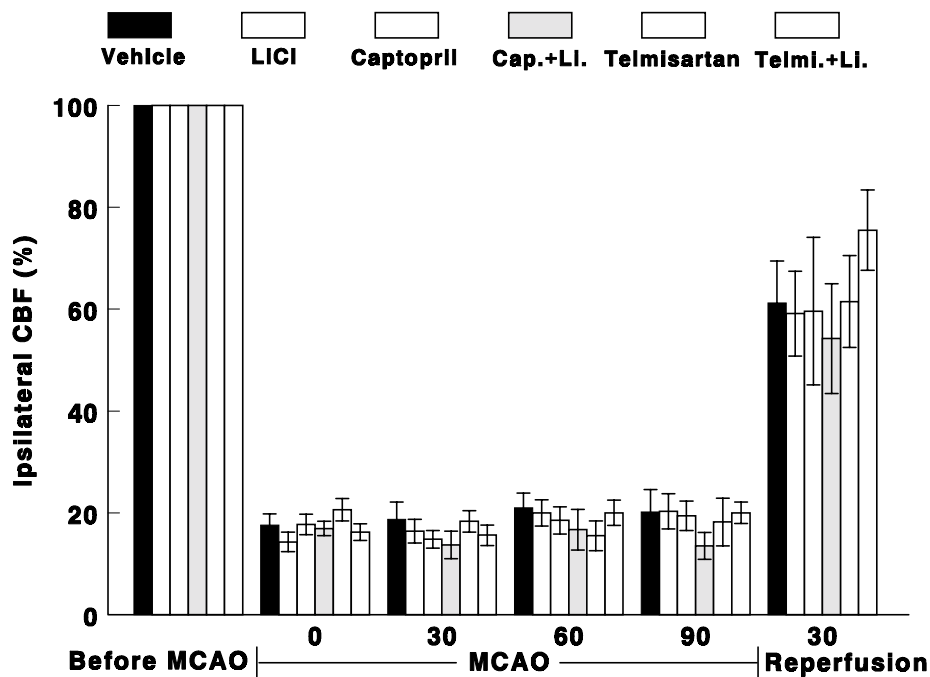


Figure 25. Regional cerebral blood flow (rCBF) before, during and after MCAO in vehicle and drug-treated groups.

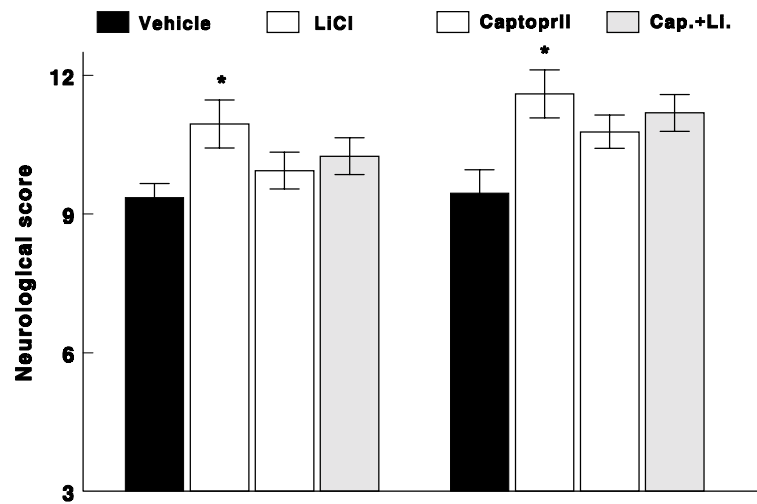
3.2.3 Neurological evaluation

Neurological evaluation was carried out 24 h and 48 h after MCAO by a person who had no knowledge of the treatment that the rats had received. Two kinds of neurological grading systems were used, one was the grading scale of 3-18 developed by Garcia et al. (1995), another one was the grading scale of 0-3 developed by Bederson et al. (1986).

Rats treated with LiCl showed a significantly improved neurological outcome (assessed by the 3-18 grading scale system) compared to rats treated with vehicle 24 h after MCAO (10.95 ± 0.52 versus 9.36 ± 0.30 , $P < 0.05$) and 48 h after MCAO (11.60 ± 0.52 versus 9.45 ± 0.51 , $P < 0.05$). A significant difference in the neurological deficit grade between the LiCl- and vehicle-treated group was also observed 48 h following MCAO using the 0-3 grading scale system (1.70 ± 0.11 versus 2.27 ± 0.17 , $P < 0.05$). Captopril alone or in combination with LiCl had no beneficial effect on neurological outcome at either time point when compared to vehicle (Figure 26).

Rats treated with LiCl plus telmisartan showed a significantly improved neurological outcome (assessed by the 3-18 grading scale system) compared to rats treated with vehicle 24 h after MCAO (11.23 ± 0.54 versus 9.36 ± 0.30 , $P < 0.05$) and 48 h after MCAO (11.73 ± 0.48 versus 9.45 ± 0.51 , $P < 0.01$). A significant difference in the neurological deficit grade between the telmisartan plus LiCl- and the vehicle-treated group was also observed 48 h following MCAO using the 0-3 grading scale system (1.68 ± 0.14 versus 2.27 ± 0.17 , $P < 0.05$). Telmisartan alone had no effect on neurological outcome at 24 h and 48 h after MCAO when compared to vehicle-treated rats. However, the addition of LiCl to telmisartan caused a significantly lower neurological deficit grade compared to rats treated with telmisartan alone 24 h after MCAO (1.77 ± 0.10 versus 2.35 ± 0.17 , $P < 0.05$) as assessed by the 0-3 grading scale system (Figure 27).

A



B

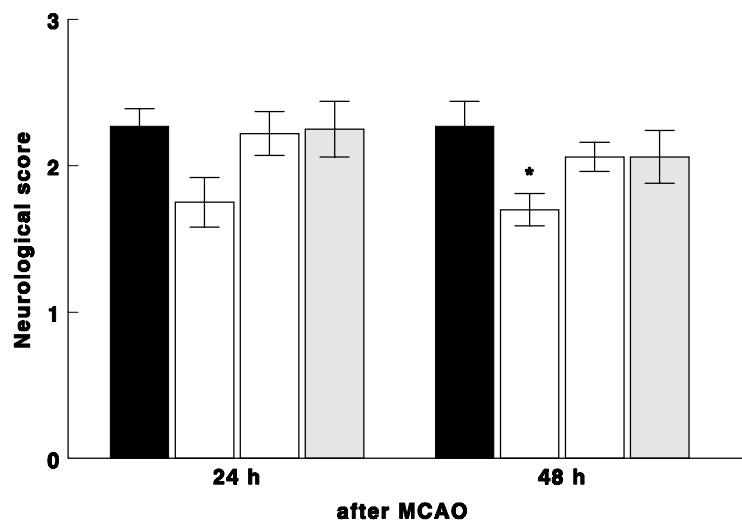
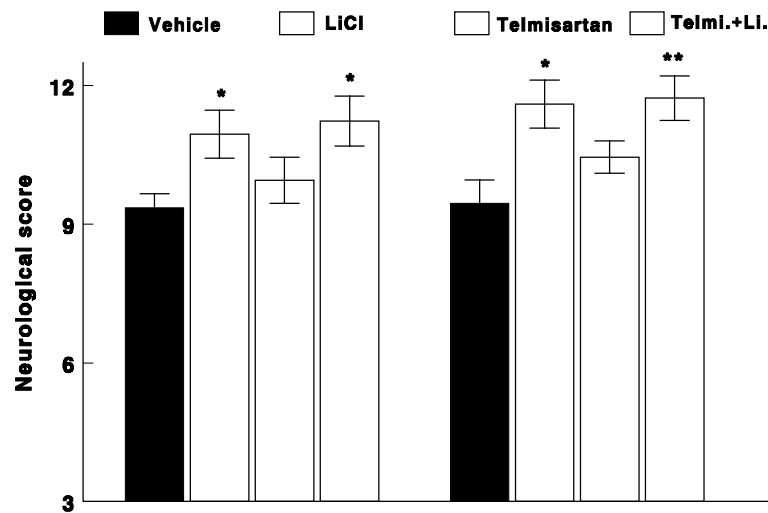


Figure 26. Effect of LiCl, captopril and captopril plus LiCl on neurological outcome in Wistar rats. Rats were treated with LiCl (1 mmol/kg/d), captopril (25 mg/kg/d) and captopril plus LiCl for 14 days before MCAO, and 2 days after MCAO. 24 h and 48 h after MCAO, neurological outcome were assessed by the 3-18 grading scale evaluation system (A) and the 0-3 grading scale evaluation system (B). * P<0.05 versus vehicle-treated animals.

A



B

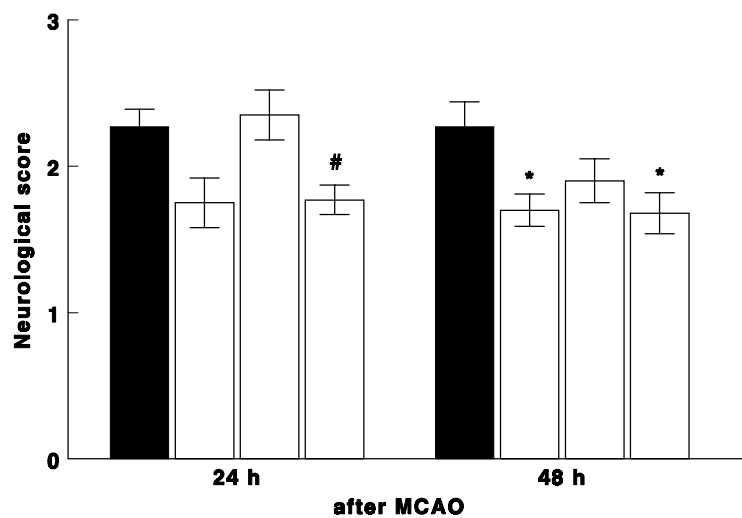


Figure 27. Effect of LiCl, telmisartan and telmisartan plus LiCl on neurological outcome in Wistar rats. Rats were treated with LiCl (1 mmol/kg/d), telmisartan (0.3 mg/kg/d) and telmisartan plus LiCl for 14 days before MCAO, and 2 days after MCAO. 24 h and 48 h after MCAO, neurological outcome were assessed by the 3-18 grading scale evaluation system (A) and the 0-3 grading scale evaluation system (B). * P<0.05, ** P<0.01 versus vehicle-treated animals; # P<0.05 versus telmisartan-treated animals.

3.2.4 Total infarct volume, serial infarct sizes and edema volume

LiCl treatment significantly reduced the total infarct volume by 32.7 % compared to vehicle-treatment (Table 17, Figure 28 and 29). The rats treated with LiCl showed significant reductions in the infarct sizes measured in the cerebrum (+1.3 mm, $p < 0.01$; +0.5 mm, $p < 0.05$; -0.3 mm, $p < 0.05$ and -1.1 mm, $p < 0.01$ from bregma) compared to rats treated with vehicle (Figure 29). Edema may influence total infarct volume. Therefore, the percentage of the hemisphere that had undergone a cerebral infarction (%infarct) was calculated using the equation of Swanson et al. (1990), to correct for cerebral edema. In the LiCl-treated group the %infarct was significantly less than in the vehicle-treated group (Table 17, Figure 29). LiCl treatment slightly reduced edema volume when compared to vehicle treatment. However, this difference did not reach statistical significance (Table 17, Figure 29).

Captopril alone or in combination with LiCl had no effect on total infarct volume, infarct sizes and edema volume (Table 17, Figure 29).

Table 17. The effects of LiCl, captopril and captopril plus LiCl on infarct volume and edema volume in Wistar rats at 48 h after MCAO

Treatment	n	Infarct Volume (mm ³)	%infarct	Edema Volume (mm ³)
Vehicle	11	255.4 ± 26.7	32.8 ± 3.4	73.8 ± 11.8
LiCl	10	171.9 ± 20.8*	20.8 ± 3.0*	55.1 ± 8.7
Captopril	9	268.0 ± 17.5	36.0 ± 2.7	71.3 ± 11.2
Cap.+Li.	8	247.7 ± 20.0	31.7 ± 3.0	73.0 ± 10.7

Data are mean ± SEM of n rats. * $P < 0.05$, statistical comparison to the vehicle-treated animals

Telmisartan plus LiCl treatment significantly reduced infarct size in the cerebrum 0.30 mm posterior to bregma ($p < 0.05$) (Figure 30), but had no effect on total infarct volume compared to vehicle treatment (Table 18, Figure 30). Edema volume was slightly, but not significantly, reduced in rats treated with telmisartan plus LiCl when compared to vehicle treatment (Table 18, Figure 30). Telmisartan alone had no effect on either total infarct volume, infarct sizes or edema volume (Table 18, Figure 30).

Table 18. The effects of LiCl, telmisartan and telmisartan plus LiCl on infarct volume and edema volume in Wistar rats at 48 h after MCAO

Treatment	n	Infarct Volume (mm ³)	%infarct	Edema Volume (mm ³)
Vehicle	11	255.4 ± 26.7	32.8 ± 3.4	73.8 ± 11.8
LiCl	10	171.9 ± 20.8*	20.8 ± 3.0*	55.1 ± 8.7
Telmisartan	10	249.5 ± 16.5	30.2 ± 2.3	81.5 ± 8.6
Telmi.+Li.	11	220.2 ± 13.1	29.6 ± 2.3	53.1 ± 9.4

Data are mean ± SEM of n rats. * P<0.05, statistical comparison to the vehicle-treated animals.

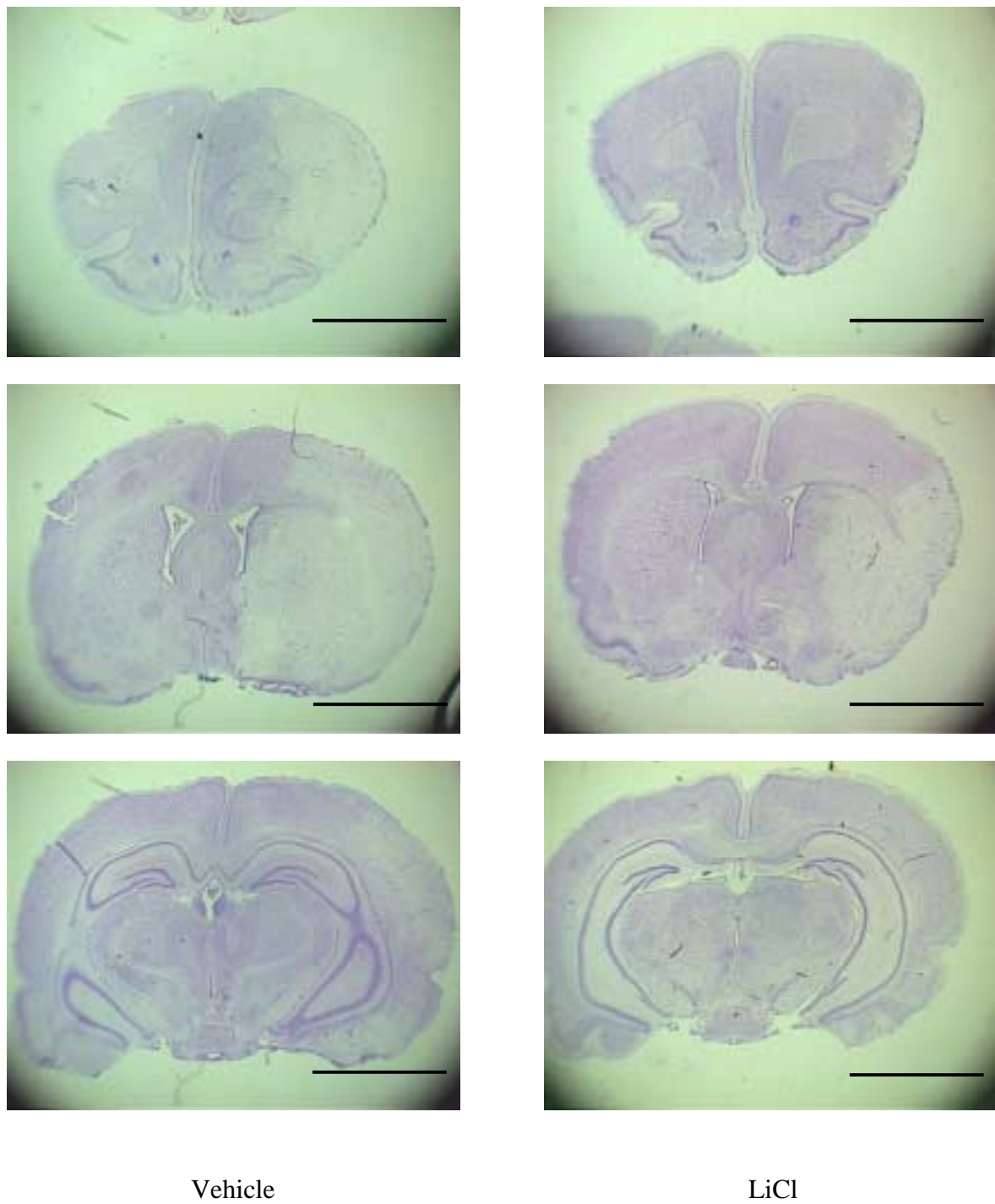


Figure 28. Representative brain slices from a vehicle-treated rat and a LiCl-treated rat 48 h post 90-min MCAO. The brains were sliced coronally and stained with cresyl violet. The blue area is viable tissue, and the pale area is the area damaged by the cerebral infarction. Scale bar, 5 mm.

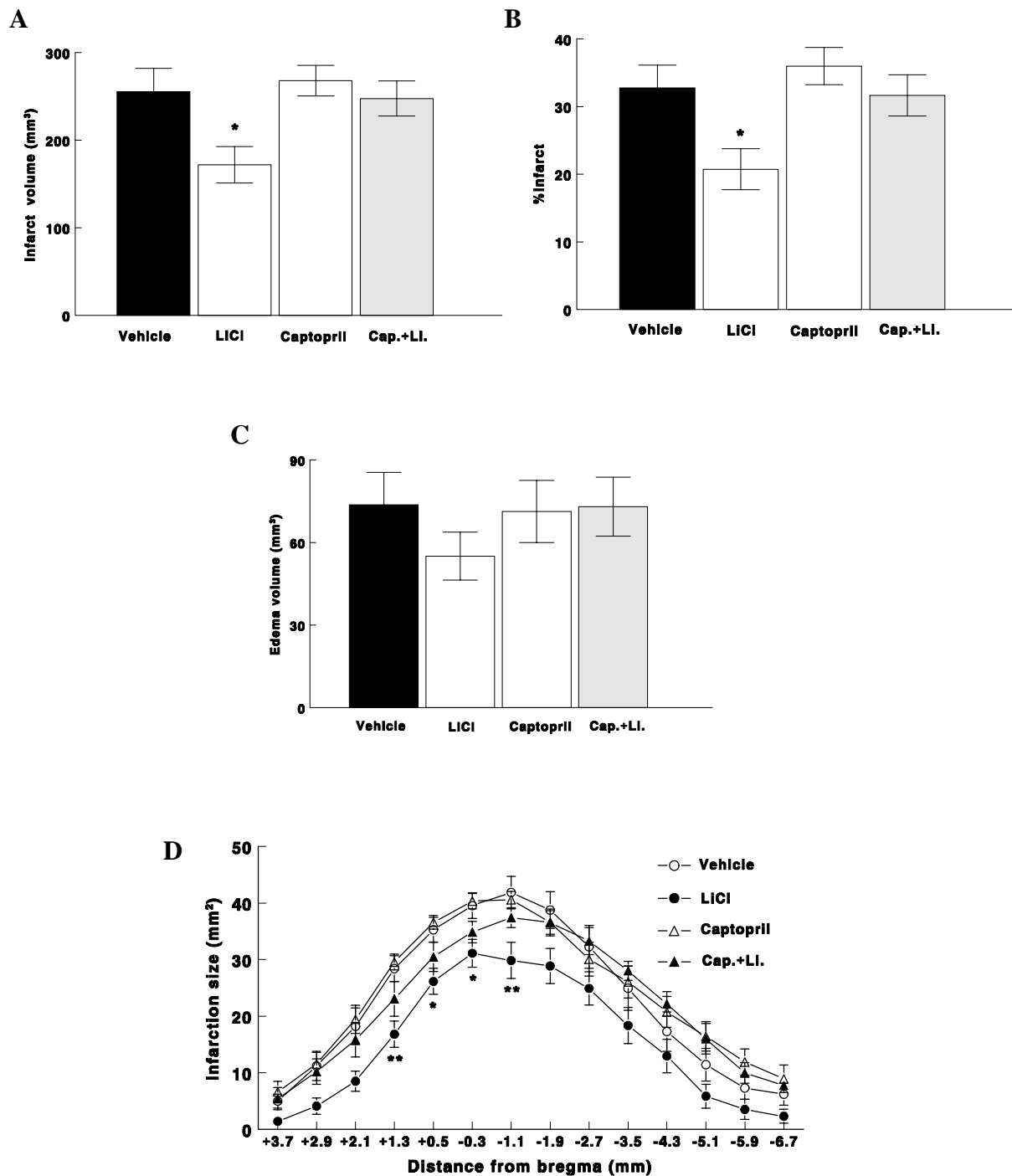


Figure 29. Effect of LiCl, captopril and captopril plus LiCl on infarct volume (A), percentage of infarction (B), edema volume (C) and infarct sizes (D). Percentage of infarction (%infarct) was calculated by the formula of Swanson et al. (1990), and indicate that the damaged volume was expressed as a percentage of the contralateral hemispheric volume with the correction of edema. Rats were treated with LiCl (1 mmol/kg/d), captopril (25 mg/kg/d) and captopril plus LiCl for 14 days before MCAO, and 2 days after MCAO. * $P < 0.05$, ** $P < 0.01$, versus vehicle-treated animals.

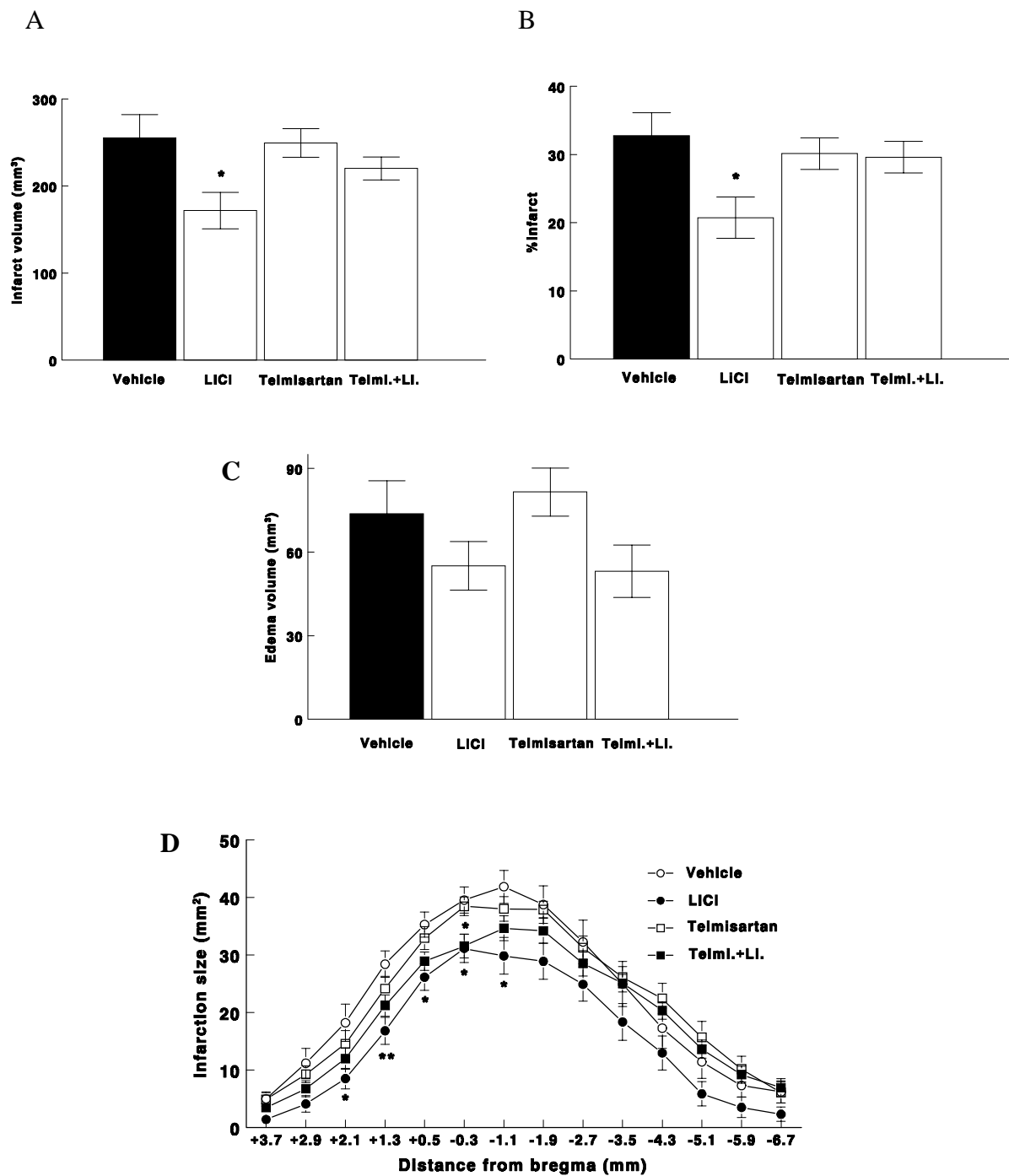


Figure 30. Effect of LiCl, telmisartan and telmisartan plus LiCl on infarct volume (A), percentage of infarction (B), edema volume (C) and infarct sizes (D). Percentage of infarction (% infarct) was calculated by the formula of Swanson et al. (1990), and indicate that the damaged volume was expressed as a percentage of the contralateral hemispheric volume with the correction of edema. Rats were treated with LiCl (1 mmol/kg/d), telmisartan (0.3 mg/kg/d) and telmisartan plus LiCl for 14 days before MCAO, and 2 days after MCAO. * $P < 0.05$, ** $P < 0.01$, versus vehicle-treated animals.

3.2.5 TUNEL staining

TUNEL-positive cells were distributed in the boundary zones (penumbra) and ischemic cores of the cerebral cortex and caudate putamen of the occluded MCA area. Only densely labeled cells were considered as positive apoptotic cells, and cells with light diffuse labeling suggesting necrosis were not counted. We counted the number of TUNEL-positive cells in the penumbra of the parietal cortex on the section through the anterior commissure (0.3 mm posterior to the bregma) and on the section 1.8 mm posterior to the bregma. The section through the anterior commissure revealed significantly less TUNEL-positive cells in rats treated with LiCl than those treated with vehicle ($473 \pm 60.7/\text{mm}^2$ versus $805 \pm 60.5/\text{mm}^2$, $P < 0.01$) (Figure 31 and 32). A 30.3% reduction in the number of TUNEL-positive cells was observed on the section through bregma -1.8 mm, but this difference did not reach statistical significance.

Captopril alone or in combination with LiCl as well as telmisartan alone or in combination with LiCl did not decrease the density of TUNEL-positive cells in the cortical penumbra on either sections (bregma -0.3 mm and -1.8 mm) when compared to vehicle (Figure 32 and 33).

No TUNEL-positive cells were found in the contralateral side.

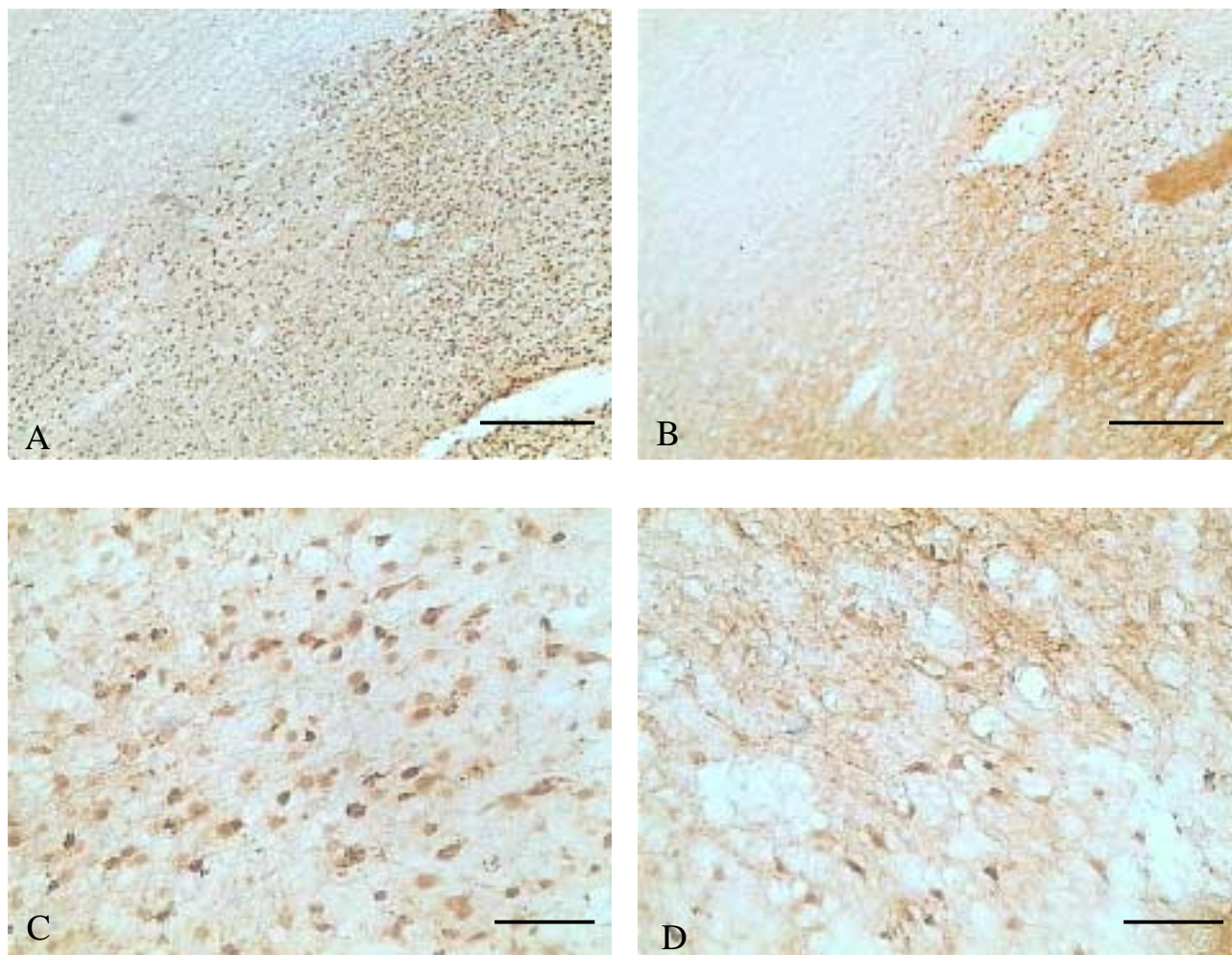


Figure 31. TUNEL staining of brain sections from ischemic parietal cortex in a vehicle-treated rat (A, C) and a LiCl-treated rat (B, D) 48 h after 90-min MCAO. Scale bar: A, B, 250 μm; C, D, 50 μm.

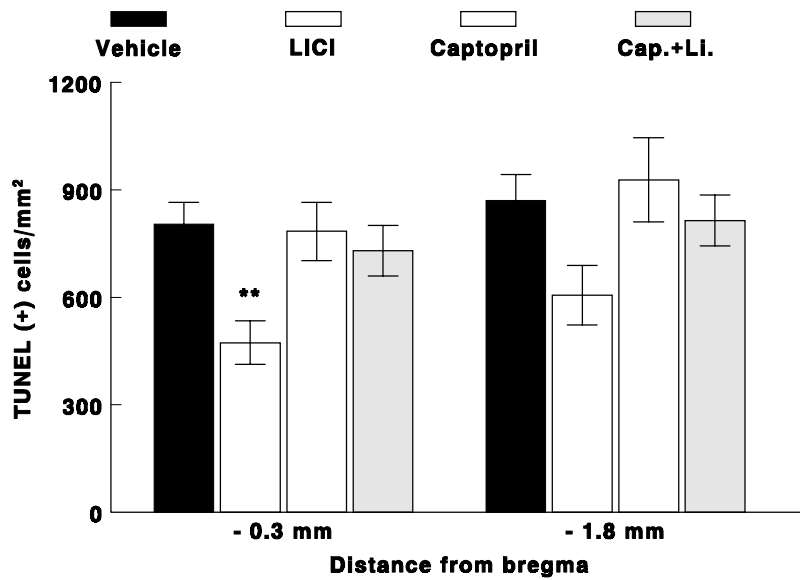


Figure 32. Effect of LiCl, captopril and captopril plus LiCl on the density of TUNEL positive cells in the penumbra of parietal cortex in the rats two days after MCAO. Rats were treated with LiCl (1 mmol/kg/d), captopril (25 mg/kg/d) and captopril plus LiCl for 14 days before MCAO, and 2 days after MCAO. ** P<0.01 versus vehicle-treated animals.

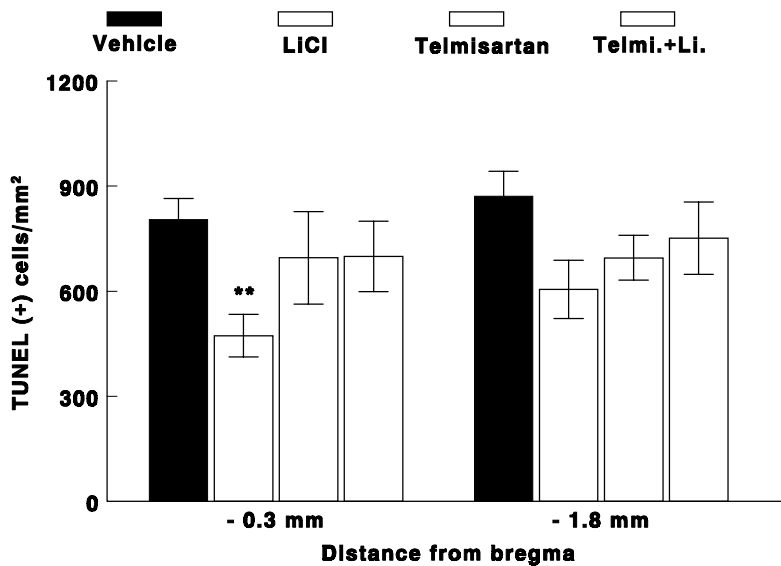


Figure 33. Effect of LiCl, telmisartan and telmisartan plus LiCl on the density of TUNEL positive cells in the penumbra of parietal cortex in the rats two days after MCAO. Rats were treated with LiCl (1 mmol/kg/d), telmisartan (0.3 mg/kg/d) and telmisartan plus LiCl for 14 days before MCAO, and 2 days after MCAO. ** P<0.01 versus vehicle-treated animals.

3.2.6 Activated caspase-3 immunoreactivity

The majority of caspase-3 positive cells were distributed in the inner boundary zones (penumbra) of the cerebral cortex and caudate putamen of the occluded MCA area. On the other hand, only a few stained cells for caspase-3 were found in the ischemic core region. The number of caspase-3 positive cells was counted in the penumbra of the parietal cortex on the section through the anterior commissure (0.3 mm posterior to the bregma) and on the section 1.8 mm posterior to the bregma. Animals treated with LiCl had significantly less caspase-3 positive cells in the penumbral zone on the section through the anterior commissure than those treated with vehicle (215 ± 35.1 versus 386 ± 45.7 , $p < 0.05$) (Figure 34 and 35). On the section 1.8 mm posterior to the bregma, LiCl treatment reduced the number of caspase-3 positive cells by 32.2 % when compared to vehicle, but this difference did not reach statistical significance (Figure 35). The number of caspase-3 positive cells was significantly reduced in brain sections from captopril- and captopril plus LiCl-treated rats compared to those from vehicle-treated rats (224 ± 38.9 and 195 ± 25.2 versus 386 ± 45.7 on the section 0.3 mm posterior to the bregma, $p < 0.05$ and $p < 0.01$; 240 ± 39.5 and 221 ± 25.9 versus 426 ± 45.3 on the section 1.8 mm posterior to the bregma, $p < 0.05$ and $p < 0.01$). Captopril treatment reduced the number of caspase-3 positive cells by 42.0 % and 43.7 % , and captopril plus LiCl treatment reduced the caspase-3 positive cells by 49.5 % and 48.1 % on the sections 0.3 mm and 1.8 mm posterior to the bregma respectively, compared to vehicle (Figure 34 and 35).

The number of caspase-3 positive cells was reduced in the sections which were 0.3 mm and 1.8 mm posterior to the bregma of brains derived from telmisartan plus LiCl-treated rats (217 ± 21.7 versus 386 ± 45.7 in the vehicle-treated group, $P < 0.01$; 253 ± 56.8 versus 426 ± 45.3 in the vehicle-treated group, $P < 0.05$), and the percent of inhibition was 43.8 and 40.6 on the both sections respectively, when compared to vehicle (Figure 34 and 36). Telmisartan-treatment slightly, but not significantly reduced the density of activated caspase-3 positive cells in the cortical penumbra on the both sections (Figure 34 and 36).

A negligible amount of caspase-3 positive cells were found in the cortical area of the contralateral side.

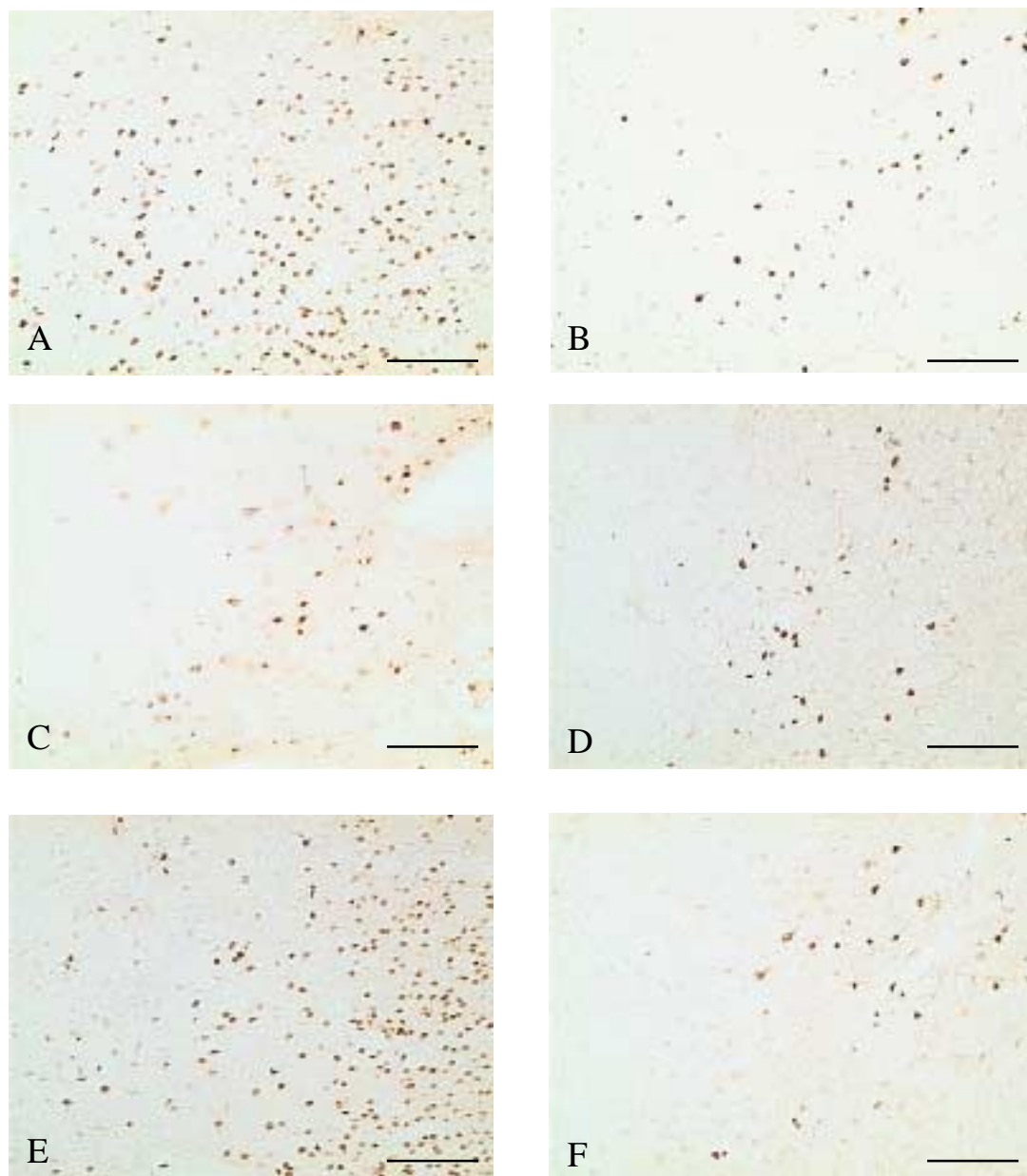


Figure 34. Activated caspase-3 staining on brain sections from ischemic parietal cortex in rats treated with vehicle (A), LiCl (B), captopril (C), captopril plus LiCl (D), telmisartan (E) and telmisartan plus LiCl (F) 48 h after 90-min MCAO. Scale bar, 125 μ m.

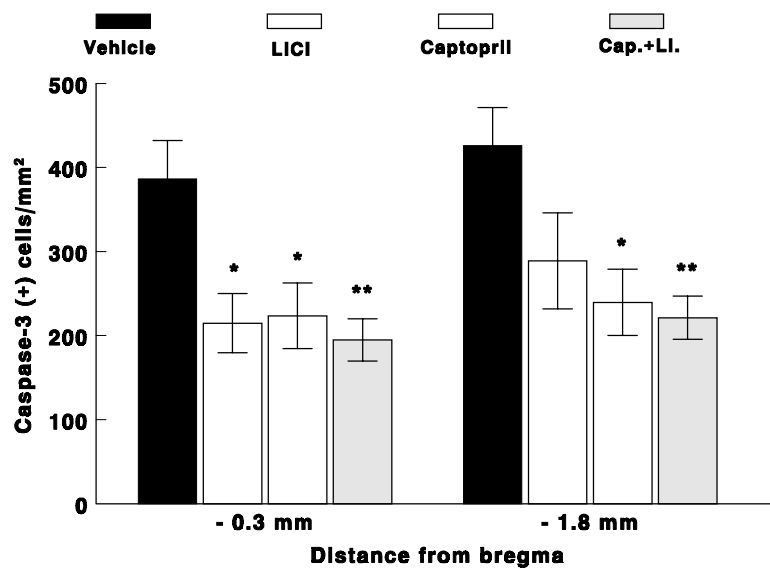


Figure 35. Effect of LiCl, captopril and captopril plus LiCl on the density of activated caspase-3 positive cells in the penumbra of parietal cortex in the rats two days after MCAO. Rats were treated with LiCl (1 mmol/kg/d), captopril (25 mg/kg/d) and captopril plus LiCl for 14 days before MCAO, and 2 days after MCAO. * $P < 0.05$, ** $P < 0.01$ versus vehicle-treated animals.

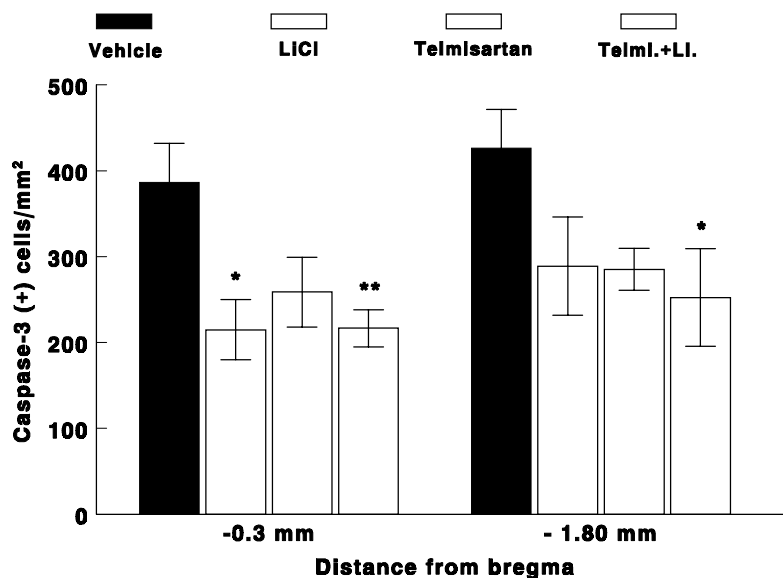


Figure 36. Effect of LiCl, telmisartan and telmisartan plus LiCl on the density of activated caspase-3 positive cells in the penumbra of parietal cortex in the rats two days after MCAO. Rats were treated with LiCl (1 mmol/kg/d), telmisartan (0.3 mg/kg/d) and telmisartan plus LiCl for 14 days before MCAO, and 2 days after MCAO. * $P < 0.05$, ** $P < 0.01$ versus vehicle-treated animals.

3.2.7 Activated Microglia

Inflammatory mediators are involved in the pathogenesis of focal ischemia brain damage. To determine whether LiCl or inhibitors of the RAS inhibit inflammation, we studied microglial activation by using the ED1 antibody, a monoclonal antibody specific for reactive microglia and macrophages.

Activated microglia cells of the amoeboid type (amoeboid microglia), as identified by their enlarged size and stout processes, were most frequently observed in the boundary zone of the infarction and to a minor extent in the infarction core at 2 days after MCAO. We counted the number of activated microglia and macrophages in the penumbra of parietal cortex on the section through the anterior commissure (0.3 mm posterior to the bregma) and on the section 1.8 mm posterior to the bregma. LiCl treatment only slightly decreased the density of activated microglia and macrophages on the sections 0.3 mm and 1.8 mm posterior to bregma (Figure 37 and 38). However, the number of activated microglia and macrophages was significantly reduced in the brain sections from captopril and captopril plus LiCl-treated rats compared to those from vehicle-treated animals (339 ± 36.4 and 256 ± 24.6 versus 617 ± 51.8 on the section 0.3 mm posterior to the bregma, $p < 0.01$; 277 ± 21.9 and 307 ± 48.0 versus 541 ± 33.6 on the section 1.8 mm posterior to the bregma, $p < 0.01$) (Figure 37 and 38). Captopril alone or in combination with LiCl reduced the number of activated microglia by 45.1 % and 58.5 % in the section through the anterior commissure, and by 48.8 % and 43.3 % in the section 1.8 mm posterior to the bregma respectively, compared to vehicle.

The number of activated microglia and macrophages in the penumbra of the brain cortex was significantly reduced in the telmisartan plus LiCl treated tissues on the section through the anterior commissure (397 ± 25.3 versus 617 ± 51.8 in the vehicle-treated group, $p < 0.01$) (Figure 37 and 39). Treatment with telmisartan alone did not significantly decrease the density of activated microglia and macrophages in the penumbra of cortex on both sections (Figure 37 and 39).

No activated microglia and macrophages were found on the contralateral side of the brain sections.

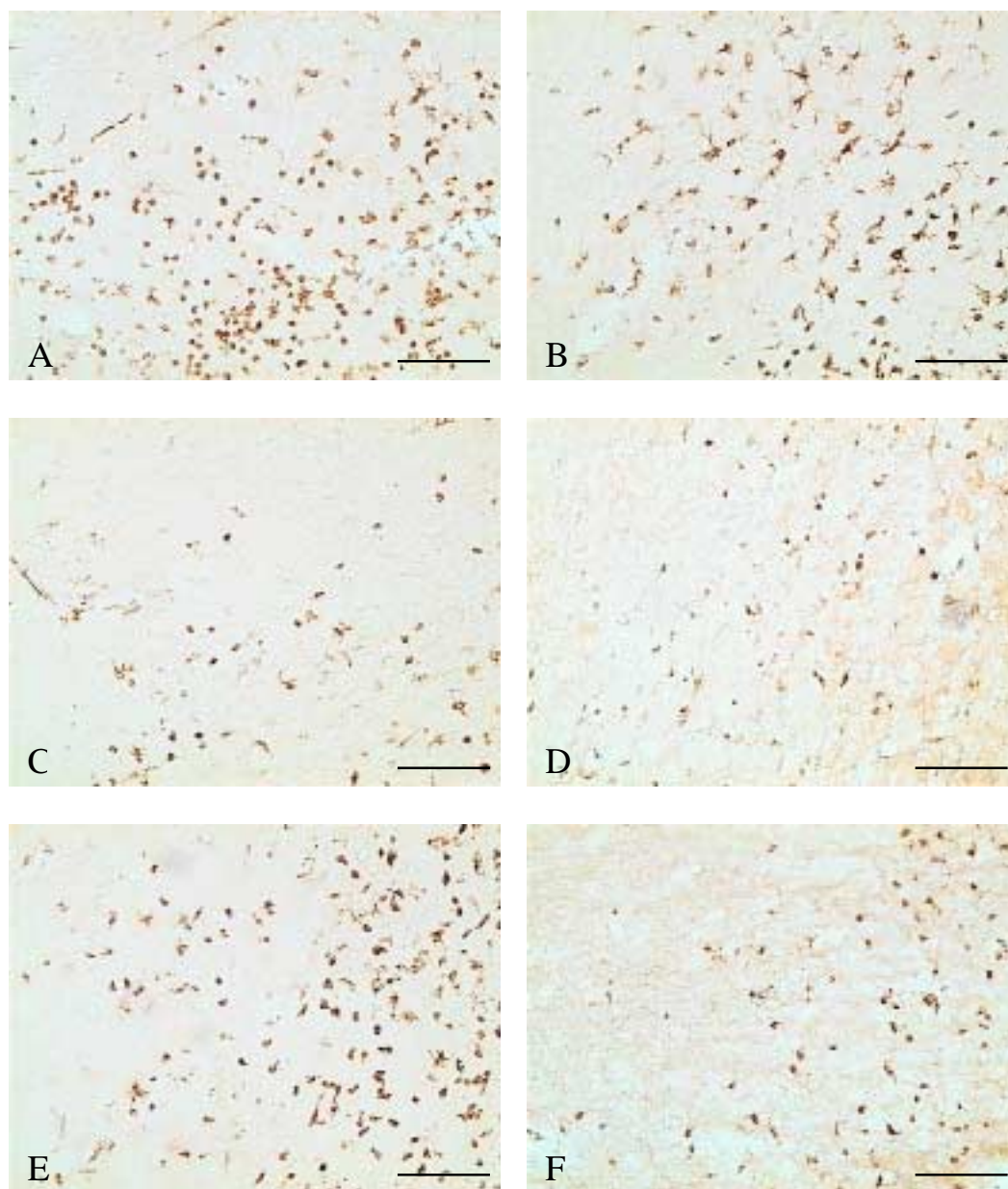


Figure 37. Activated microglia stained by the ED1 antibody on the brain sections from ischemic parietal cortex in rats treated with vehicle (A), LiCl (B), captopril (C), captopril plus LiCl (D), telmisartan (E) and telmisartan plus LiCl (F) 48 h after 90-min MCAO. Scale bar, 125 μ m.

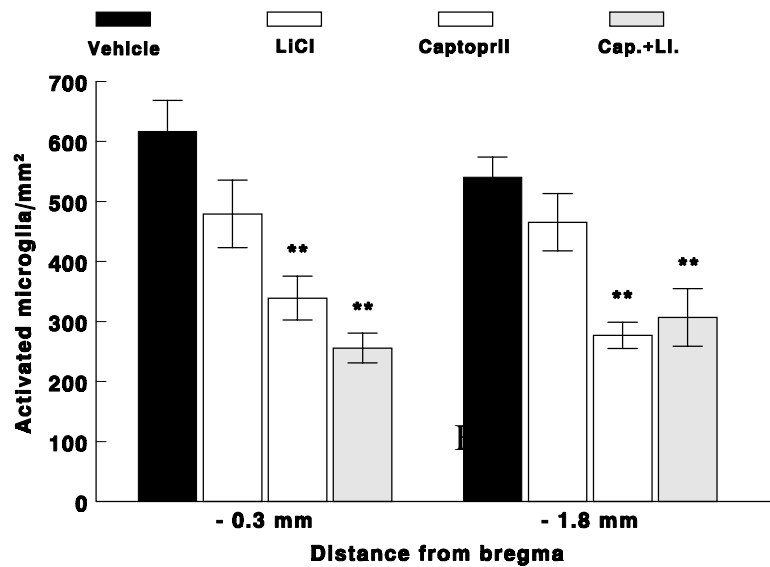


Figure 38. Effect of LiCl, captopril and captopril plus LiCl on the density of activated microglia in the penumbra of parietal cortex in the rats two days after MCAO. Rats were treated with LiCl (1 mmol/kg/d), captopril (25 mg/kg/d) and captopril plus LiCl for 14 days before MCAO, and 2 days after MCAO. ** P<0.01 versus vehicle-treated animals.

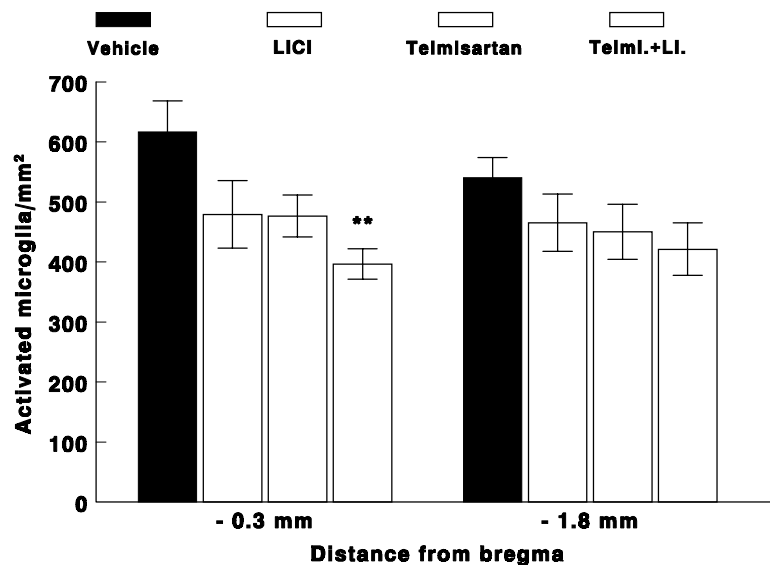


Figure 39. Effect of LiCl, telmisartan and telmisartan plus LiCl on the density of activated microglia in the penumbra of parietal cortex in the rats two days after MCAO. Rats were treated with LiCl (1 mmol/kg/d), telmisartan (0.3 mg/kg/d) and telmisartan plus LiCl for 14 days before MCAO, and 2 days after MCAO. ** P<0.01 versus vehicle-treated animals.

3.2.8 Li⁺-concentration in plasma

Plasma Li⁺-concentration in the drug-treated and vehicle-treated groups is shown in Table 19 and 20. The Li⁺-concentrations in LiCl-, captopril plus LiCl- and telmisartan plus LiCl-treated rats remained below the therapeutic concentration range necessary for the treatment of bipolar disease (0.5-0.9 mmol/L).

Table 19. The concentration of Li⁺ in the plasma of Wistar rats after treatment with LiCl, captopril and captopril plus LiCl for 16 days

Group	n	Li ⁺ (mmol/L)
Vehicle	8	0.01 ± 0.00
LiCl	6	0.40 ± 0.06
Captopril	7	0.02 ± 0.01
Cap.+Li.	6	0.37 ± 0.10

Data are mean ± S.E.M of n rats.

Table 20. The concentration of Li⁺ in the plasma of Wistar rats after treatment with LiCl, telmisartan and telmisartan plus LiCl for 16 days

Group	n	Li ⁺ (mmol/L)
Vehicle	8	0.01 ± 0.00
LiCl	6	0.40 ± 0.06
Telmisartan	5	0.02 ± 0.01
Telmi.+Li.	6	0.29 ± 0.07

Data are mean ± S.E.M of n rats.

4 Discussion

4.1 Stroke development in salt-loaded SHRSP

SHRSP provide an experimental model of hypertensive cerebrovascular and renal disease. The occurrence of stroke in these animals is dramatically increased by replacing the drinking water by a 1% NaCl solution (Nagaoka et al., 1976). In the present study, SHRSP treated with vehicle developed severe hypertension at 12 weeks of age. Death associated with stroke first occurred in 12 week old rats with a 100% mortality at 16 weeks of age. Similar mortality rates in salt-loaded SHRSP have been reported previously (Smeda, 1989). All animals exhibited neurological signs accompanying stroke and drank dramatically more salt water a few days before death. A number of histological changes could be observed in brain sections derived from 13 week old SHRSP including edema, brain cell rarefaction, focal infarctions and hemorrhages. Furthermore, a high number of apoptotic cells in these brains could be detected by TUNEL staining, and TUNEL stained apoptotic cells were frequently located to the areas with focal infarction (cresyl violet staining). To our best knowledge it is the first time to detect apoptotic cells by TUNEL staining in brains from salt-loaded SHRSP. The mechanisms by which SHRSP develop stroke rapidly after salt-loading are not quite clear. The present results suggest a possible contribution of an enhanced apoptosis rate in brains derived from SHRSP to the pathogenesis of stroke.

Other factors have been postulated to contribute to stroke development in salt-loaded SHRSP. The participation of the RAS in the development of hypertensive vascular injury has been widely demonstrated. Numerous studies with ACE inhibitors and Ang II receptor antagonists have clearly identified Ang II as a major factor responsible for the development of end-organ damage in hypertensive vascular disease (Laragh and Sealey, 1990). Physiologically, the RAS is suppressed by a high salt diet and activated by salt-depletion. However, in SHRSP, paradoxically, the RAS is, after a transient inhibition, strongly activated in the malignant phase of hypertension despite salt loading. Morbidity and mortality in salt-loaded SHRSP are associated with a rise in the activity of the RAS (Volpe et al., 1990; Shibota et al., 1979). Recently Kyselovic et al. (2001) revealed that the paradoxical plasma renin activity (PRA) increase in salt-loaded SHRSP is accompanied by elevated renal levels of renin mRNA, confirming that the physiological downregulation by salt of renin production by the kidney is lost in those hypertensive rats. Activation of renin production is probably secondary to renal damage that is accelerated by the high dietary salt intake in this strain, as previously suggested by others (Matsunaga et al., 1975; Shibota et al., 1979).

In the present study, in untreated SHRSP the salt water intake was constant during the first 4 weeks of treatment and tended to increase thereafter. The thirst and salt-appetite-promoting properties induced by Ang II are responsible for the increase in salt water intake observed during the days preceding death (Phillips, 1987). Ang II, the most important peptide of the RAS, exerts a number of actions such as vasoconstriction, renal salt and water retention, aldosterone and vasopressin release, and sympathetic facilitation, all of which may play a detrimental role in the hypertensive state (Edling et al. 1995, Griendling et al. 1996). Additionally, the vascular detrimental influence of the RAS may not be limited to its effects on vascular resistance and salt and water excretion. Neutrophil adhesion to endothelium is the first step of leukocyte-mediated vascular injury. An increased adherence of granulocytes to the luminal surface of aortic and cerebral vascular endothelium and subendothelial space from SHRSP has been observed. Ang II may influence neutrophil accumulation via production of neutrophil chemoattractant activity in vascular endothelial cells (Stier et al., 1989). Moreover, Ang II stimulates the synthesis and release of aldosterone, and it is suggested that the elevations in plasma aldosterone of salt-loaded SHRSP before stroke may play an important role in initiation of stroke in SHRSP (Smeda et al., 1999). Recently a growing body of evidence suggests that the RAS functions as a regulator of apoptosis in a variety of cell types (Filippatos et al., 2001). The increased apoptosis in the brain of salt-loaded SHRSP may be associated with the increased activity of RAS.

4.2 Effects of captopril and captopril plus lithium on stroke prevention in salt-loaded SHRSP

The results of the present study revealed that captopril at a dose of 50 mg/kg per day by a long-term subcutaneous injection markedly prolonged survival in salt-loaded SHRSP, and significantly increased average survival days from 39 days in untreated group to 247 days. The addition of LiCl (1 mmol/kg per day) to captopril (50 mg/kg per day) did not offer further beneficial effects, and the average survival days in the combination treated group was 225 days. The average survival days in lithium treated group was 36 days, comparable to the control group. However, our previous results showed that a lower dose of captopril (25 mg/kg per day) and LiCl (1 mmol/kg per day) act synergistically to prolong survival in salt-loaded SHRSP. In this study, the addition of LiCl to captopril increased the average survival from 147 days to more than 237 days, which is similar to the average survival days in rats treated with captopril at 50 mg/kg per day. Taken together, these results show that the effects of captopril on survival and stroke prevention in salt-loaded SHRSP were dose dependent, and

lithium acts synergistically with the low dose of captopril (25 mg/kg per day) but not with the high dose of captopril (50 mg/kg per day) on survival and stroke prevention in salt-loaded SHRSP.

In the present study, we detected apoptosis by TUNEL staining in the brains from rats after 5 weeks of treatment, and it is interesting to note that the rats treated with captopril had significantly less apoptotic events than the rats treated with vehicle. Recently several lines of evidences showed that captopril may have anti-apoptotic effects. Captopril has been shown to inhibit Fas-induced apoptosis in human activated peripheral T cells and human lung epithelial cells, and prevent activation-induced apoptosis in T cell hybridomas by interfering with T cell activation signals (Odaka and Mizuochi, 2000). It is suggested that the efficacy of captopril to inhibit experimental lung fibrogenesis is related to inhibition of apoptosis (Wang et al., 2000). In our present study, we showed for the first time that captopril had anti-apoptotic effects in the brain of salt-loaded SHRSP, and this effect may be associated with the mechanisms by which captopril markedly increased survival and prevent stroke in these rats. Histological results showed that no cerebrovascular lesions existed in the brains from rats treated with captopril (50 mg/kg per day) for five weeks. However, five weeks after salt-loading, all five brains from untreated rats exhibited severe cerebrovascular lesions: rarefaction, focal infarction and edema, and some areas with rarefaction and infarction in these brains were corresponding to the areas with strong TUNEL-positive cells. These results demonstrate that apoptosis is related to stroke occurrence in salt-loaded SHRSP, and the effect of captopril on stroke prevention in these rats may be partly due to the anti-apoptotic effect of captopril.

The addition of lithium to captopril (50 mg/kg per day) did not offer further beneficial effects on survival and stroke prevention in salt-loaded SHRSP. However, in our previous study lithium and captopril at a low dose (25mg/kg per day) act synergistically on survival in the same model. The mechanisms involved in this synergistic interactions remain unclear. Many studies in salt-loaded SHRSP have shown that long-term administration of ACE inhibitors prevents the development of renal and cerebral damage and reduces mortality in this model (Stier et al., 1989; Stier et al., 1991; Vacher et al., 1993; MacLeod et al., 1997). No information is available on the effects of a combination treatment with lithium and an ACE inhibitor in this model. Our previous study has shown that the systolic blood pressure in the rats treated with captopril alone or in combination with lithium remained below control levels at 12-16 weeks of age. Thereafter, both groups developed severe hypertension, and the blood pressure in both groups was comparable. These results would suggest that the synergistic

effects between captopril and lithium on survival and stroke prevention via mechanisms beyond the reduction of blood pressure.

In contrast, in our present study, the addition of lithium to captopril (50mg/kg perday) further reduced blood pressure in salt-loaded SHRSP, compared to the rats treated with captopril (50mg/kg per day) alone. However, despite the more pronounced antihypertensive action of the combination therapy, there was no further beneficial effect on survival in these rats.

It has been shown that long term lithium treatment protects cultured neurons from different brain regions against glutamate-induced apoptosis (Nonaka et al., 1998a). Moreover, Chen and Chuang (1999) reported that long-term, but not acute, lithium treatment protects against glutamate excitotoxicity by suppressing p53 and Bax expression and increasing Bcl-2 expression in cerebellar granule cells. In addition to the protective effects in vitro, a growing body of evidence is demonstrating that lithium exert neuroprotective effects in vivo. Inouye et al. (1995) found that lithium pretreatment delayed radiation-induced apoptosis in the cells of the external granular layer after newborn mice were exposed to gamma irradiation. In our present study, 5 weeks of treatment with captopril (50 mg/kg per day) alone or in combination with lithium significantly reduced the apoptotic expression in the brains of salt-loaded SHRSP when compared with vehicle, but the addition of lithium to captopril did not offer further anti-apoptotic effect. The reason may be because both treatments completely prevent salt-loaded SHRSP from stroke. However, we can not rule out the possibility that the synergistic effects of lithium and captopril at a low dose (25 mg/kg/day) on stroke prevention in salt-loaded SHRSP in our previous study may be related to their synergistic anti-apoptotic effect.

In our present study, the plasma lithium concentrations of salt-loaded SHRSP in the captopril plus lithium group were 0.66 ± 0.01 (n=5) and 0.86 ± 0.21 (n=3) mmol/L at 21 and 39 weeks of treatment, respectively. Lithium has a narrow therapeutic range, with effective plasma concentrations ranging from 0.5 to 0.9 mmol/L being close to the toxic concentration of 2.0 to 3.0 mmol/L (Silverstone and Romans, 1996). Therefore, the average plasma lithium concentrations in the rats after a long term treatment were in the therapeutic range. However, the plasma lithium concentration of one rats at 39 weeks of treatment was 1.28 mmol/L, which is beyond the range of the therapeutic concentrations. It is possible that lithium exerts a toxic effect on kidney after a long-term treatment. As lithium excretion is achieved almost exclusively via renal means, its pharmacokinetic fate is highly influenced by age, fluid status and various haemodynamic factors. Age-related changes in glomerular filtration rates may result in a prolonged plasma half-life in the elderly population (Finley et al., 1995).

Interference of the RAS by ACE inhibition may have potentiated lithium toxicity in several ways. First, it aggravated the hypotension, which in itself impairs glomerular filtration. Second, it interfered with the normal autoregulatory response to hypotension, thus worsening renal failure, and further impairing lithium excretion. Finally, ACE inhibition has also been associated with varying degrees of renal insufficiency that may reduce lithium clearance rates (Finley et al., 1995). In our present study, daily urinary albumin excretion remained higher in rats treated with captopril plus lithium than in rats treated with captopril alone during the whole treatment period. In contrast, in our previous study, urinary albumin excretion was lower in captopril (25 mg/kg) plus lithium-treated rats compared to rats treated with captopril (25 mg/kg per day) alone (Gohlke et al., 1999). These contradictory results may be explained by toxic interactions between lithium and captopril at a high dose (50 mg/kg per day) on kidney function, whereas no such adverse interaction may occur between lithium and the low dose of captopril.

Clinical observations reveal a reduction in lithium clearance in patients stabilized on lithium after the introduction of an ACE inhibitor, leading to an increase in serum lithium concentration. This phenomenon can be explained in part by the ACE inhibitor-induced decrease in aldosterone levels that may lead to sodium depletion and subsequent lithium retention (Finley et al., 1996). In contrast, in our present study the lithium excretion in the urine of salt-loaded SHRSP treated with captopril plus lithium tended to gradually increase. In the present study, salt water intake and urinary sodium excretion was higher in rats treated with captopril (50 mg/kg per day) plus lithium than rats treated with captopril alone. The plasma sodium and potassium concentrations, and the urinary potassium excretion were comparable between the both groups. Therefore, the fluid and electrolyte status in rats from both groups seem to remain in balance, which may be one of the reasons why lithium clearance was not impaired in the present study.

PRA was comparably high (>20 ng Ang I/ml/h) in captopril- and captopril plus lithium treated rats after 21 weeks of treatment. This finding may be explained by the ACE inhibitor – induced reduction in circulating Ang II levels, thus impairing the Ang II-mediated feedback inhibition of renin secretion by the kidney. However, high PRA values are also consistent with the paradoxical PRA increase in SHRSP after salt-loading.

The body weight in rats treated with captopril alone or in combination with lithium increased with age, and remained comparable between both groups up to 45 weeks of treatment. Thereafter, most rats from both groups developed huge edema a few days before death. No neurological signs or slight neurological signs were seen in rats from both groups a few days

before their death. Brain hemorrhage was only detectable in one rat from the each treated group, while all rats showed a marked hypertrophy of their hearts and kidneys. In contrast, as mentioned above, all rats treated with vehicle or lithium exhibited severe cerebrovascular lesions and had symptoms of stroke a few days before death. These results suggest that rats treated with captopril died mainly because of heart and kidney failure as a result of long term hypertension and salt-loading, but did not develop stroke. Under these conditions, the addition of lithium does not produce any further beneficial effects but appear to exert nephrotoxic effects in combination with a high dose of the ACE inhibitor as indicated by an increased urinary albumin excretion. In contrast, when combined with a low dose of captopril (25 mg/kg per day), lithium prevented the occurrence of stroke in ACE inhibitor treated rats and further increased survival but did not produce nephrotoxicity after long-term treatment. In summary, the effects of captopril on survival and stroke prevention in salt-loaded SHRSP are dose dependent, and the addition of lithium further increased survival when combined with a low dose of captopril, but not with the higher dose of the ACE inhibitor. The effects of captopril alone or in combination with lithium on stroke prevention may be associated with their anti-apoptotic effects.

4.3 Effects of telmisartan and telmisartan plus lithium on stroke prevention in salt-loaded SHRSP

Our results demonstrated that telmisartan at a dose of 1 mg/kg per day initially and 0.3 mg/kg per day lifelong by subcutaneous injection markedly prolonged survival in salt-loaded SHRSP, and significantly increased average survival from 39 days in untreated group to 310 days. Two rats treated with telmisartan survived up to 15 months, which was comparable to the normal lifespan of SHRSP without salt loading. The addition of lithium to telmisartan did not offer further beneficial effects, and the average survival in the combination treated-rats was 317 days. The average survival in lithium treated rats was 36 days, comparable to the vehicle group. When comparing the survival rate of rats treated with captopril (50 mg/kg/day) alone or in combination with lithium, treatment with telmisartan alone or in combination with lithium further increased survival in these rats by 2-3 months.

Telmisartan is a potent, long-lasting, nonpeptide antagonist of the AT1 receptor with very high lipophilicity (Wienen et al., 2000). It has been shown that, following peripheral administration, telmisartan can penetrate the blood-brain barrier in a dose- and time-dependent manner to inhibit centrally mediated effects of Ang II (Gohlke et al., 2001). An inhibition of centrally mediated effects of Ang II was achieved with doses of 0.3-10 mg/kg

i.v. and 1-30 mg/kg p.o.. Furthermore, a dose-dependent increase in the CSF concentration of telmisartan could be measured after one week oral treatment with the AT₁ receptor antagonist (Gohlke et al. 2001). Wagner et al. (1998) revealed that 10 mg /kg of body weight of telmisartan p.o. reduced blood pressure in SHRSP to a similar extent as 50 mg/kg of body weight captopril. Therefore, for the purpose of the present study, it was reasonable to start treatment with telmisartan at a dose of 1 mg/kg per day. However, due to a significant reduction of blood pressure compared to captopril (50 mg/kg per day) during the first 4 weeks of treatment, the dose of telmisartan was reduced to 0.3 mg/kg per day. The blood pressure increased gradually after dose adjustment, but remained below 220 mm Hg. The addition of lithium to telmisartan did not further reduce blood pressure, and the blood pressure was comparable between the both groups during the whole treatment period.

We examined histological lesions and detected apoptosis by TUNEL staining in the brains of salt-loaded SHRSP after 5 weeks of treatment. The results showed that none of the rats treated with telmisartan alone or in combination with lithium developed stroke. The apoptotic expression in the brains from the both groups were comparable, all markedly less than in the vehicle-treated group. It is well established that Ang II may induce apoptosis in various cell types (Dimmeler et al., 1997; Kajstura et al., 1997; Shenoy et al., 1999; Tanaka et al., 1995). A recent *in vivo* study demonstrated that Ang II induces apoptosis in a dose-dependent manner in proximal tubular cells in adult rats (Cao et al., 2000). It was initially considered that Ang II induces cell proliferation via the AT₁ receptor and influences apoptosis via AT₂ receptor (Stoll et al., 1995; Yamada et al., 1996). However, more recent *in vitro* and *in vivo* studies (Leri et al., 1998; Cao et al., 2000) have also suggested that both AT₁ and AT₂ receptors are involved in both proliferation and apoptosis. Ang II may induce apoptosis via different receptor signaling pathways, depending on the cell type, the age of the animal, and local environmental factors (Bonnet et al., 2001). In salt-loaded SHRSP, the RAS is paradoxically very strongly activated in the malignant phase of hypertension, which is associated with increased morbidity and mortality due to cerebrovascular and renal lesions in these rats (Volpe et al., 1990). The results of our present study showed that the AT₁ receptor antagonist telmisartan exhibited anti-apoptotic effects in brains from salt-loaded SHRSP, and the effects of telmisartan on survival and stroke prevention in these rats may be related to its anti-apoptotic effect. The addition of lithium to telmisartan did not offer further anti-apoptotic effects after 5 weeks of treatment, which may be because telmisartan alone at this regimen completely prevent salt-loaded SHRSP from stroke. After a long term treatment, the amount of TUNEL positive cells in the brains of SHRSP in both groups tended to increase when

compared to brains after five weeks of treatment, which may be related to an age-dependent increase in apoptotic events.

The plasma Li^+ -concentration in salt-loaded SHRSP treated with telmisartan plus lithium for 21 and 39 weeks were 0.62 ± 0.03 and 0.56 ± 0.02 mmol/L, respectively. They were all in the therapeutic range, and lithium clearance during different periods of treatment were consistent. Lithium-induced polydipsia in these rats was observed after 30 weeks of treatment, and therefore occurred much later than in the rats treated with lithium plus captopril in which the polydipsia was induced as early as after 8 weeks of treatment. After a long-term treatment with telmisartan or in combination with lithium, the PRA and urinary albumin excretion were comparable, and fluid and electrolytes remained in balance in both groups.

The body weight in both groups were comparable with an age-related increase. However, after a long-term treatment, most rats in both groups developed huge edema a few days before death, and these rats showed severe heart and kidney lesions. Comparable to these symptoms, the daily urinary albumin excretion markedly increased at the late stage in these two groups. In contrast, the brain lesions from these rats were not severe, only one rat treated with telmisartan or telmisartan plus lithium showed brain hemorrhages. Moreover, similar to rats treated with captopril, no neurological signs or slight neurological signs were seen in the rats from both groups a few days before their death.

In summary, our results demonstrated that telmisartan at initially 1 mg/kg per day and finally 0.3 mg/kg per day by subcutaneous injection markedly prolonged survival in salt-loaded SHRSP, and the effect of telmisartan on stroke prevention may be associated with its anti-apoptotic effect. The addition of lithium to telmisartan did not offer further beneficial effect on survival.

4.4 Effects of lithium on focal cerebral ischemia in normotensive rats

The first important finding of the present study is that chronic treatment with a low dose of lithium decreased infarct volume and improved neurological outcome. Similar findings were obtained by Nonaka and Chuang (1998) in rats with permanent MCAO after chronic treatment with lithium. In their study, rats were treated with lithium (initially 1.5 mmol/kg, then 2.3 mmol/kg and finally 3 mmol/kg) for 16 days, and neurological evaluations or quantification of infarct volume were carried out at 24 h after MCAO. Both studies differ with respect to the model used (transient versus permanent MCAO), the dose of lithium (1 mmol/kg versus 3 mmol/kg) and the time point (48 h versus 24 h after MCAO). Furthermore, in the study by Nonaka & Chuang (1998) no attempt was made to examine the possible

mechanisms that may be responsible for the lithium-induced neuroprotection. In the present study, the neuroprotective effects of lithium were associated with a reduction of apoptotic events in the brain cortex assessed by two different methods. The results clearly demonstrate that chronic treatment with lithium (1 mmol/kg) inhibits activated caspase-3 expression and decreases DNA fragmentation in the brain after transient focal cerebral ischemia. The apoptotic parameters were evaluated two days after MCAO, since i) pannecrosis is visible 24-48 h after MCAO (Garcia et al., 1993) and ii) the number of apoptotic cells, mostly neurons, increases as early as 0.5 h, peaks at 24-48 h and persists for 4 weeks after the onset of reperfusion. Furthermore, apoptotic cells were located primarily in the inner boundary zone of the infarct of rats subjected to transient (2 h) focal ischemia. (Li et al., 1995a, b).

Ischemia is known to produce reactive oxygen and nitrogen species, to induce cleavage of poly(ADP-ribose) polymerase, caspase activation and DNA fragmentation in neuronal cells. In particular, recent biochemical and immunohistochemical studies have demonstrated enhanced expression and activation of intracellular proteases, notably caspase-3, which act as initiators and executors of the apoptotic process (Velier et al., 1999). The involvement of caspases in apoptotic processes following ischemia is supported by the observation that treatment with caspase inhibitors reduces ischemia-induced brain damage (Cheng et al., 1998; Endres et al., 1998). This data suggests that apoptotic mechanisms are activated during ischemia and that inhibition of apoptosis reduces ischemic brain damage.

The gradual expansion of the ischemic lesion after MCAO has been visualized in the parietal cortex by microtubule-associated protein 2 immunostaining (Mabuchi et al., 2000). Therefore, we used the penumbra of the parietal cortex to measure the density of apoptotic and inflammatory cells to assess the possible therapeutic effects of lithium on apoptotic and inflammatory processes. Our results demonstrate that lithium significantly inhibited activated caspase-3 immunoreactivity and decreased DNA fragmentation in the ischemic penumbra of the brain cortex 48 h after MCAO. Several studies have demonstrated anti-apoptotic effects of lithium. Chronic treatment with lithium increased the expression of Bcl-2, an anti-apoptotic protein, both, *in vitro* and *in vivo*, and reduced the levels of the pro-apoptotic proteins, p53 and Bax (Manji et al., 1999). This data supports the hypothesis that the lithium-mediated protection from cerebral ischemia involves anti-apoptotic mechanisms. Cerebral ischemia induces an exaggerated inflammatory response in the surroundings of the cerebral infarct that might contribute to neuronal necrosis and apoptosis due to the release of cytokines and other neurotoxic factors (Stoll et al., 1998). A significant number of reactive mononuclear phagocytes, both, microglia and invading macrophages, appears within the infarct area and

along neighboring marginal areas 2 days after ischemia (Giulian et al., 1993). In the present study, activated microglia as a parameter for ongoing inflammatory processes, was investigated 48 h after MCAO. Lithium did not inhibit activated microglia in the ischemic penumbra of the brain cortex. Therefore, it seems likely that anti-apoptotic, rather than anti-inflammatory effects of lithium had contributed to its neuroprotective effects.

Numerous studies (Nonaka et al., 1998; Nonaka and Chuang, 1998; Yuan et al., 1999) have shown that lithium must be chronically administered to reach therapeutic effects.

Furthermore, it has been postulated that lithium may exert major effects at the genomic level. Recently lithium has been demonstrated to inhibit glycogen synthase kinase-3 β (GSK-3 β), an enzyme which is involved in proapoptotic-signaling. Therefore, the neuroprotective actions of lithium may be partly due to inhibition of GSK-3 β (Bijur et al., 2000). Moreover, lithium has been reported to modulate the activator protein 1 (AP-1) DNA binding activity and the expression of genes regulated by AP-1. However, the mechanisms underlying these effects have not been fully elucidated (Yuan et al., 1999).

Our results clearly indicate that the effects of lithium in rats with focal ischemia cannot be simply explained by indirect effects of the drug on e.g. changes in blood pressure or blood parameters such as pO₂, pCO₂, hemoglobin and electrolytes (Na⁺, K⁺).

In the present study, the plasma Li⁺-concentration in Wistar rats after 16 days treatment reached values of 0.40 ± 0.06 mmol/L. This concentration is below the therapeutic concentrations of lithium (0.5-0.9 mmol/L) required in man for the treatment of manic depression (Silverstone and Romans, 1996). In vitro study showed that pre-treatment of cortical neurons with LiCl suppressed glutamate-induced excitotoxicity at the therapeutic and sub-therapeutic concentration of 0.2-1.6 mmol/L with almost complete protection at 1 mmol/L (Hashimoto et al., 2002). In the present study, a low dose of lithium reduced the infarct volume by 32.7%. A more pronounced effect of lithium can be expected at higher doses as demonstrated by Nonaka & Chuang (1998) who used a 3-fold higher dose of lithium compared to our study.

In conclusion, we demonstrated that a low-dose treatment with lithium (1 mmol/kg) reduced infarct volume and improved neurological outcome in rats with transient focal cerebral ischemia. Lithium showed a significant inhibition of caspase-3 and DNA fragmentation in the ischemic penumbra of the brain cortex, indicating that a reduction of apoptotic processes is responsible for the neuroprotective effects of lithium against ischemic brain injury.

4.5 Effects of captopril and captopril plus lithium on focal cerebral ischemia in normotensive rats

In the present study, pretreatment of rats with captopril (25 mg/kg/day, sc.) did not exhibit beneficial effects on infarct volume and neurological outcome following focal brain ischemia. In contrast, in a previous study, captopril (10 mg/kg) by acute i.v. injection improved neurological outcome from incomplete cerebral ischemia in rats (Werner C, et al., 1991). The reason for these discrepancies may be due to differences in the animal model used, the dose and the duration of captopril administration. In the present study, captopril at a dose of 25 mg/kg by daily subcutaneous injection for 2 weeks significantly decreased blood pressure in normotensive rats. MAP was reduced in the conscious state and during anesthesia before the onset of MCAO. Moreover, MAP was consistently lower in the captopril-treated group compared to the vehicle-treated group during the MCAO and reperfusion period. Therefore, it can not be excluded that MAP partly remained under the lower limit of the cerebral blood flow (CBF) autoregulation during the period of MCAO and reperfusion in rats treated with captopril. Such an effect would have masked a possible neuroprotective effect of captopril in the ischemic brain. However, it has been demonstrated that the lower and upper limits of the CBF autoregulation curve were shifted to lower pressures following treatment with ACE inhibitors (Barry et al., 1984; Paulson et al., 1985). Therefore brains may be protected against a decrease of the blood pressure induced by ACE inhibition by a shift of the lower limit of CBF autoregulation. In the present study, blood pressure in captopril-treated rats remained below 60 mmHg during 5 to 60 minutes of MCAO, and was about 20 mm Hg lower than the blood pressure in vehicle-treated rats. Blood pressure was further decreased during the whole MCAO period by the addition of lithium to captopril. Again, this reduction in blood pressure may have prevented possible beneficial effects of the combination therapy with captopril and lithium on infarct volume and neurological outcome. However, the reduction in blood pressure induced by captopril alone or captopril in combination with lithium did not further aggravate the ischemic damage compared with vehicle-treated animals.

The results of the present study suggest an anti-apoptotic effect of captopril in the ischemic brain. Captopril reduced activated caspase-3 immunoreactivity in the ischemic penumbra of the brain cortex on the sections 0.3 mm and 1.8 mm posterior to the bregma. However, we were unable to see any significant difference in apoptosis between captopril-treated and vehicle-treated animals by using the TUNEL technique in the ischemic penumbra of cortex. One explanation for these discrepancies may be the lack of specificity of the TUNEL technique in *in vivo* models, in which both apoptotic and necrotic cells have been shown to be

labeled with this method (de Torres et al., 1997). An inhibitory effect of captopril on apoptosis has also been demonstrated in human lung epithelial cells in culture (inhibition of the Fas-induced apoptosis) and in epithelial cells (inhibition of the bleomycin-induced apoptosis) (Uhal et al., 1998, Wang et al., 2000).

The addition of lithium to captopril led to more pronounced inhibition of activated caspase-3 positive cells in the ischemic penumbra of brain cortex when compared to captopril alone. Again, the combination therapy did not decrease the number of TUNEL-positive cells.

Cellular inflammation, triggered by ischemia, is a significant contributor to the final pathology of ischemic stroke. Microglia is activated after ischemic injury and can exert multiple functions by transforming into phagocytes, or by production of neurotoxic factors (Banati et al., 1993; Lees, 1993). It has been shown that microglial cells or macrophages both contribute to the gradual expansion of cerebral infarction through the production of interleukin-1 β (IL-1 β) (Mabuchi et al., 2000). Ang II may be involved in pro-inflammatory processes. Ang II dose-dependently increased the release of interleukin-6 (IL-6) by vascular smooth muscle cells (VSMC) via stimulation of AT1 receptors. In the ischemic penumbra of the brain, the expression of IL-6 appeared at day 1, increased at day 3, and remained elevated up to 14 days after transient (3 hours) MCAO in rats (Block et al., 2000). Ang II has also been shown to activate nuclear factor κ B (NF- κ B) and to increase the expression of monocyte chemoattractant protein-1 (MCP-1) in VSMC and monocytes (Kranzhofer et al. 1999, Hernandez-Presa et al., 1997). NF- κ B is a common transcription factor involved in the regulation of many pro-inflammatory genes (Barnes and Karin, 1997). NF- κ B activation is greatly increased in brain tissue in rodent models of stroke. For example, NF- κ B is activated in CA1 hippocampal neurons of rats following transient global forebrain ischemia. A delayed increase in NF- κ B activation occurred several days after focal ischemia/reperfusion and was associated with the activation of glial cells (Mattson and Camandola, 2001). Furthermore, inhibitors of NF- κ B exert protective effects against cell damage in certain experimental paradigms that involve inflammatory responses possibly by the inhibition of the cytokine-mediated activation of microglial cells (Qin et al., 1998).

In the present study, we detected the density of activated microglia or macrophages in the ischemic penumbra of the brain cortex, and found that captopril markedly reduced the number of activated microglia and macrophages. It has been reported that long-term treatment with captopril exerts an effective anti-inflammatory activity against arthritis in rats. This effect was mediated via the reduction of leukotriene B(4) and IL-6 (Agha and Mansour, 2000). ACE inhibitor treatment attenuated several parameters associated with inflammation that are

controlled by NF- κ B in a rabbit model of atherosclerosis and decreased the activation of NF- κ B in the kidney (Hernandez-Presa et al., 1998, Morrissey and Klahr, 1997). Therefore, a decrease in Ang II generation by ACE inhibition could account for the reduced activation of NF- κ B. Moreover, it can be speculated that the anti-inflammatory effect of captopril in the ischemic penumbra of the brain cortex observed in the present study may be related to its inhibitory effect on the Ang II-mediated IL-6 release as well as to the suppression of the Ang II-mediated activation of NF- κ B. However, further studies are necessary to elucidate the anti-inflammatory effect of ACE inhibitor in the ischemic brain. No additional inhibitory effects on activated microglia or macrophages were observed following the addition of lithium to captopril suggesting that the anti-inflammatory effect was related to the action of captopril. In the brain, the existence of an active RAS is well documented (Ganten et al., 1984). Recently Walther et al. (2002) demonstrated a direct correlation between brain angiotensin II and the severity of ischemic injury in either transgenic mice after focal cerebral ischemia and in vitro experiments using primary neuronal cultures. Ang II exhibited deleterious effects in ischemic injury, and neuroprotection against ischemia/hypoxia can be achieved by a drug- as well as a transgene-induced suppression of AT1 receptor function in vivo and in vitro. It has been showed that ACE inhibitors decrease ACE in the cerebrospinal fluid (CSF) of rats after systemic administration, and the ability of the drugs to penetrate from the blood into the CSF paralleled their lipophilicity (Gohlke et al. 1989). Geppetti et al. (1987) demonstrated a substantial inhibition of ACE in the human CSF following acute oral treatment of patients with captopril (75 mg). Moreover, indirect evidence for an inhibition of ACE in CSF after systemic ACE inhibitor administration stems from *in vivo* studies demonstrating that the dipsogenic and pressor effects of i.c.v. injected renin or Ang I were decreased after a single p.o. dose of captopril (Evered et al., 1980; Unger et al., 1983). Therefore, captopril decreased Ang II in brain tissue and antagonized the deleterious effect of Ang II in ischemic injury, and the inhibitory effect of captopril on apoptosis or inflammation in the ischemic penumbra of brain cortex may be related to its preinhibition of Ang II in the brains of rat before ischemia. After ischemia, the blood brain barrier was destroyed and more captopril penetrates into brain tissue to further inhibit ACE and to reduce Ang II production.

In summary, treatment of rats with the ACE inhibitor captopril (25 mg/kg per day s.c.) for 2 weeks before transient focal ischemia and for 2 days postischemia did not improve neurological deficits and reduce infarction volume. The addition of lithium to captopril did not provide neuroprotection possibly as a result of excessive blood pressure reduction during the period of MCAO and reperfusion. However, captopril alone as well as in combination

with lithium markedly reduced the activity of caspase-3, and decreased the number activated microglia or macrophages in the ischemic penumbra of the brain cortex. Therefore, captopril may exert beneficial effects on the delayed neuronal death following brain ischemia.

4.6 Effects of telmisartan and telmisartan plus lithium on focal cerebral ischemia in normotensive rats

In the present study, telmisartan at a dose of 0.3 mg/kg per day did not improve neurological deficits and did not decrease infarct volume in normotensive rats with focal ischemia. In a recent study, it has been demonstrated in normotensive rats that blockade of central AT₁ receptors induced by intracerebroventricular infusion of the AT₁ receptor antagonist irbesartan for 5 days prior to the MCAO exerted neuroprotective effects in ischemic neuronal tissue and improved recovery from brain ischemia (Dai et al., 1999). In addition, the overexpression of the AP-1 transcription factors, c-Fos and c-Jun, which have been associated with the induction of apoptosis in neurons and positively correlated with the degree of neurological deficits following focal brain ischemia, was markedly reduced by central pretreatment with the AT₁ receptor antagonist. Central AT₂ receptors contribute to the beneficial effects of AT₁ receptor antagonists on neurological outcome following cerebral ischemia (J. Culman, WJ Dai, P. Gohlke, A. Blume, and T. Unger, submitted). However, systemic (i.v.) treatment with irbesartan (30 mg/kg per day) for 5 consecutive days before MCAO did not improve neurological deficits. One reason for this lack of effect of systemically administered irbesartan may be the incomplete and only short-lasting blockade of brain AT₁ receptors (Polidori et al., 1998; Culman et al., 1999; Funk et al., 2000). In contrast to irbesartan, telmisartan exerts a complete blockade of centrally-mediated effects of Ang II which – at higher doses – lasted for 24 h. Compared to irbesartan (30-100 mg/kg, i.v.) much lower doses of telmisartan (0.3-10 mg/kg, i.v.) were necessary to achieve central effects. However, the dose of subcutaneously applied telmisartan used in the present study (0.3 mg/kg) may still be not sufficient to adequately block brain AT₁ receptors. This would explain the failure of telmisartan to exhibit beneficial effect in rats with focal cerebral ischemia.. Therefore, an effective blockade of brain AT₁ receptors appears to be crucial for the neuroprotective effects of AT₁ receptor antagonists in ischemic neuronal tissue. Recently Nishimura et al. (2000) reported that selective antagonism of AT₁ receptors by chronic peripheral administration of the AT₁ antagonist candesartan normalized cerebrovascular autoregulation and protected against brain ischemia in genetically hypertensive rats. In their study, candesartan at a dose of 0.5 mg/kg per day by subcutaneous

injection for 2 weeks significantly reduced infarct volume in SHR with focal ischemia. The reasons for the discrepancies between the both studies may involve (1) the use of different AT₁ antagonists (telmisartan versus candesartan) and (2) the use of normotensive versus hypertensive rats. Candesartan has a higher affinity to the AT₁ receptor when compared to telmisartan. Furthermore, the blockade of AT₁ receptors by candesartan is insurmountable as a result of its tight binding to and slow dissociation from the receptor. Both drugs also differ with respect to their ability to penetrate the blood brain barrier. Two recent studies have compared the ability of both drugs to inhibit centrally mediated effects of Ang II following peripheral application (Gohlke et al., 2001, Gohlke et al., 2002). The results revealed that much lower doses of candesartan compared to telmisartan were sufficient to effectively block central effects of Ang II over a 24 h period despite the fact that telmisartan is the more lipophilic compound (log D at pH 7.4=+3.2 for telmisartan versus -1.7 for candesartan). Therefore, candesartan at a dose of 0.5 mg/kg per day appear to be more effective in blocking brain AT₁ receptors when compared to telmisartan (0.3 mg/kg per day). However, in the present study, the major aim was not to study the effect of an AT₁ receptor antagonist on brain ischemia but to investigate possible synergistic interactions between the AT₁ receptor antagonist and lithium. Therefore, sub-maximal doses of both drugs were included in the study.

The addition of lithium to telmisartan improved neurological deficits in the rats one day or two days after MCAO, but did not offer further beneficial effects compared to rats treated with lithium alone. Lithium treatment significantly decreased infarct volume and reduced infarct sizes in the sections which were +2.1, +1.3, +0.5, -0.3 and -1.1 mm from bregma. However, the combination therapy with telmisartan and lithium did not significantly reduce infarct volume, and only significantly decreased the infarct size in the section with greatest damage which was 0.3 mm posterior to the bregma. Therefore, it appears that under the present experimental conditions telmisartan partly abolishes the neuroprotective effects of lithium. Treatment with telmisartan alone significantly reduced blood pressure at 30, 75 and 90 minutes of MCAO only, while the addition of lithium to telmisartan led to blood pressure reduction at 30, 45, 60, 75, 90 minutes of MCAO, and 30, 45, 60 minutes following reperfusion. It has been reported that AT₁ receptor antagonists or ACE inhibitors can shift the upper and lower limits of CBF autoregulation to the left, in the direction of lower blood pressure, in both normotensive or hypertensive rats (Nishimura et al., 2000; Barry et al., 1984; Paulson et al., 1985). However, it is not known whether telmisartan at the low dose used in the present study can exert a similar effect. Therefore, it is possible that the combination

therapy with telmisartan and lithium abolished the beneficial effect of lithium on infarct volume because of blood pressure reduction. In contrast, the beneficial effects of the combination therapy with telmisartan and lithium on neurological outcome still remained. Although some studies of cerebral ischemia have revealed a close correlation between histology and behavior (Bederson et al., 1986; Aronowski et al., 1996), other studies have shown a dissociation between histology and sensorimotor behavior or cognitive function (van der Staay et al., 1996; Wahl et al., 1992). Several factors could account for the lack of consistent correlation between histology and behavior. It is possible for the recovery of some sensorimotor functions to occur spontaneously several days after MCAO in the absence of accompanying histology improvement (van der Staay et al., 1996). Presumably, these behavioral improvement are due to compensatory changes that occur elsewhere in the brain. The most frequently used methods to quantify infarct volume after MCAO are not capable of measuring diffuse morphological changes, which could affect behavior. Clearly, until there is a better understanding of how histological changes affect behavior, it will be necessary to continue assessment of both histological and functional outcomes of potential treatments of stroke.

It is well established that Ang II induces apoptosis in various cell type via AT1 or AT2 receptor (Bonnet et al., 2001). Therefore, it can be speculated that telmisartan protects neurons against Ang II which may cause neuronal damage after brain ischemia. In the present study, treatment with telmisartan at a low dose (0.3 mg/kg) slightly (but not significantly) reduced activated caspase-3 positive cells in the ischemic penumbra of cortex in the brain sections which were 0.3 mm and 1.8 mm posterior to the bregma. The addition of lithium to telmisartan led to a significant decrease in the density of activated caspase-3 positive cells in the brain sections that were 0.3 mm and 1.8 mm posterior to the bregma, which is consistent with the anti-apoptotic effect of lithium. Moreover, the combination therapy with lithium and telmisartan significantly reduced activated microglia or macrophages on sections through the ischemic penumbra of the brain cortex 0.3 mm posterior to bregma. In contrast, treatment with telmisartan or lithium alone both failed to significantly inhibit activated microglia in the ischemic penumbra.

It is interesting to note that the combination therapy with lithium and telmisartan for two weeks significantly increased pO_2 in the plasma of rats before MCAO, and at 30 and 90 minutes of MCAO. Consistent with the increase in the plasma pO_2 , the plasma concentration of lactate was significantly reduced before MCAO in the telmisartan plus LiCl-treated group. Disruption of cerebral energy metabolism is the hallmark of disorders of stroke. Such a

disruption is due mainly to insufficient supplies of either one or both of the substrates of aerobic energy metabolism, oxygen and glucose (Schurr and Rigor, 1998).

In summary, telmisartan at a dose of 0.3 mg/kg per day did not exhibit beneficial effects on neurological deficits and infarct volume in normotensive rats with focal cerebral ischemia.

The combination therapy with telmisartan and lithium improved neurological outcome and metabolism in the same model, and inhibited both activated caspase-3 and activated microglia and macrophages in the ischemic penumbra of cortex.

5. Summary

In the present study, the effect of lithium alone or in combination with the ACE inhibitor, captopril or the AT1 receptor antagonist, telmisartan, were investigated in two animal models of stroke: First, the stroke-prone spontaneously hypertensive rat (SHRSP), an animal model of severe hypertension associated with the development of cerebral, renal and cardiac dysfunction. In these animals, the onset of stroke is accelerated by salt-loading. Second, a model of focal cerebral ischemia with 90 min occlusion of the middle cerebral artery (MCAO) followed by reperfusion.

Stroke-Prone Spontaneously Hypertensive Rats

In a previous study we demonstrated synergistic interactions between captopril (25 mg/kg per day) and LiCl (1 mmol/kg per day) on survival rate and stroke prevention in salt-loaded SHRSP. The present study was designed to investigate whether a higher dose of captopril (50 mg/kg per day) could further increase survival in salt-loaded SHRSP and whether the synergistic effect between lithium and captopril was preserved under these conditions.

Furthermore, we studied the effect of the AT1 receptor antagonist, telmisartan (0.3 mg/kg per day) alone or in combination with LiCl on the survival rate in these animals.

8 week-old SHRSP were salt-loaded (1% NaCl as drinking solution) and treated subcutaneously with LiCl alone or in combination with captopril or telmisartan. After 5 weeks of treatment, brains from 5 rats per group were used for cresyl violet staining (for determination of infarction volume) and TUNEL staining (for determination of apoptosis). With the remaining rats drug treatment was continued lifelong. Blood or 24 h urine samples were collected at different time points. Our results demonstrated that captopril markedly prolonged average survival time from 39 days in vehicle-treated rats to 247 days. Lithium alone did not increase survival compared to vehicle (average survival 36 days). The addition of lithium to captopril caused significant blood pressure reductions compared to captopril treatment alone, but did not further increase survival (average survival 225 days). Both treatment regimes completely prevented the occurrence of stroke and significantly reduced apoptosis 5 weeks after initiation of treatment. The daily urinary excretion of albumin in both groups increased with age indicating the onset of renal failure. Similar beneficial effects were also seen after treatment with the AT1 receptor antagonist telmisartan. The average survival time in telmisartan-treated rats was 310 days. The addition of lithium to telmisartan did not further increase survival (average survival 317 days). Blood pressure in both groups was comparable during the whole treatment period.

Middle Cerebral Artery Occlusion

Normotensive Wistar rats were treated subcutaneously with LiCl (1 mmol/kg per day), captopril (25 mg/kg per day) and captopril plus LiCl as well as with telmisartan (0.3 mg/kg per day) and telmisartan plus LiCl. Drug treatment was started 2 weeks before MCAO and was continued for another 2 days after MCAO. Neurological evaluations were carried out 24 h and 48 h after MCAO. Then, the rats were killed and the brains were used for the measurement of infarct volume and the immunohistochemical detection of TUNEL, activated caspase-3 and activated microglia. In separate experiments, blood pressure and other blood parameters such as pCO₂, pO₂, electrolytes and blood sugar were measured at different time points before, during and after MCAO. The results demonstrated that chronic treatment with lithium decreased the infarct volume and improved the neurological outcome. The neuroprotective effects of lithium were associated with a reduction of activated caspase-3 expression and inhibition of DNA fragmentation in the ischemic penumbra of the brain cortex. In contrast, neurological deficits and infarct volume were not affected by captopril treatment. The addition of lithium to captopril did not provide additional neuroprotection, possibly due to an excessive blood pressure reduction during the period of MCAO and reperfusion. However, captopril alone as well as in combination with lithium markedly reduced the number of cells positively stained for activated caspase-3 and activated microglia and macrophages in the ischemic penumbra of the brain cortex. Therefore, captopril may exert beneficial effects on the delayed neuronal death following brain ischemia. Telmisartan did not exhibit beneficial effects on neurological deficits and infarct volume. The combination therapy with telmisartan and lithium improved neurological outcome and metabolism and inhibited both activated caspase-3 and activated microglia or macrophages in the ischemic penumbra of brain cortex. However, the addition of telmisartan to lithium did not offer further beneficial effects when compared to lithium alone.

In summary, both inhibitors of the renin-angiotensin system completely prevented the occurrence of stroke in salt-loaded SHRSP and markedly increased survival in these rats. The rats survived for about 7-10 months and most of the animals died due to heart and renal failure. Under these conditions, lithium did not exert further beneficial effects.

In the model of transient focal cerebral ischemia, lithium exhibited neuroprotective effects. However, there were no synergistic interactions between lithium and captopril or lithium and telmisartan.

6. Zusammenfassung

In der vorliegenden Studie wurden die Effekte einer Behandlung mit Lithium alleine oder in Kombination mit 1. dem ACE Hemmmer Captopril oder 2. dem AT₁ Rezeptorantagonisten Telmisartan in zwei Tiermodellen für den Schlaganfall untersucht: der Schlaganfall-gefährdeten spontan hypertensiven Ratte (SHRSP), ein Tiermodell der schweren Hypertonie verbunden mit der Entwicklung zerebraler, renaler und kardialer Dysfunktionen. Bei diesen Tieren wird das Einsetzen einen Schlaganfalls durch Salzbelastung beschleunigt. Das zweite Tiermodell war das Setzen einer der fokalen Gehirnschämie mit 90-minütiger Okklusion der mittleren Zerebralarterie (MCAO) gefolgt von einer Reperfusion bei normotensiven Tieren.

Schlaganfall-gefährdete spontan hypertensive Ratten

In einer früheren Studie konnten wir synergistische Interaktionen zwischen Captopril (25 mg/kg pro Tag) und LiCl (1 mmol/kg pro Tag) hinsichtlich der Überlebensrate und der Schlaganfallprävention in salzbelasteten SHRSP beobachten. In der vorliegenden Studie sollte untersucht werden, ob eine höhere Dosis von Captopril (50 mg/kg pro Tag) zu einer weiteren Steigerung der Überlebensrate führt, und ob der synergistische Effekt zwischen Lithium und Captopril unter diesen Bedingungen erhalten bleibt. Weiterhin untersuchten wir den Effekt des AT₁ Rezeptorantagonisten, Telmisartan (0.3 mg/kg pro Tag) allein oder in Kombination mit LiCl auf die Überlebensrate dieser Tiere. Acht Wochen alte SHRSP wurden salzbelastet (1% NaCl als Trinkflüssigkeit) und subkutan mit LiCl allein oder in Kombination mit Captopril oder Telmisartan behandelt. Nach 5 Wochen Behandlung wurden die Gehirne von je 5 Ratten pro Behandlungsgruppe für die Cresylviolett-Färbung (zur Bestimmung des Infarkt volumens) und die TUNEL-Färbung (zum Nachweis der Apoptose) verwendet. Mit den verbleibenden Ratten wurde die Behandlung lebenslang fortgesetzt. Blut und 24-Stunden Urin wurden zu verschiedenen Zeitpunkten gewonnen. Unsere Ergebnisse zeigen, dass Captopril die mittlere Überlebensrate deutlich von 39 Tagen bei Vehikel-behandelten Ratten auf 247 Tage verlängerte. Lithium alleine führte zu keiner Verlängerung der Überlebensrate im Vergleich zu Vehikel (mittlere Überlebensrate 36 Tage). Die Zugabe von Lithium zu Captopril bewirkte eine signifikante Blutdrucksenkung im Vergleich zur alleinigen Captopril-Behandlung, führte aber zu keiner weiteren Erhöhung der Überlebensrate (mittlere Überlebensrate 225 Tage). Beide Behandlungsarten verhinderten vollständig das Auftreten eines Schlaganfalls und zeigten 5 Wochen nach Beginn der Behandlung eine signifikante

Verminderung der Apoptose. Die tägliche Albuminexkretion in den Urin steigerte sich mit zunehmendem Alter, ein Zeichen für ein einsetzendes Nierenversagen. Vergleichbare benefizielle Effekte wurde auch nach Behandlung mit Telmisartan beobachtet. Die mittlere Überlebenszeit bei Telmisartan-behandelten Ratten betrug 310 Tage. Die Zugabe von Lithium zu Telmisartan führte zu keiner weiteren Erhöhung der Überlebensrate (mittlere Überlebensrate 317 Tage). Der Blutdruck in beiden Behandlungsgruppen war während des gesamten Behandlungszeitraumes vergleichbar hoch.

Okklusion der mittleren Zerebralarterie

Normotensive Wistar Ratten wurden subkutan mit LiCl (1 mmol/kg pro Tag), Captopril (25 mg/kg pro Tag) und Captopril plus LiCl sowie mit Telmisartan (0.3 mg/kg pro Tag) und Telmisartan plus LiCl behandelt. Die Behandlung wurde 2 Wochen vor der MCAO begonnen und für weitere 2 Tage nach der MCAO fortgeführt. Neurologische Untersuchungen wurden 24h und 48h nach der MCAO durchgeführt. Danach wurden die Tiere getötet und die Gehirne für die Messung des Infarktolumens und den immunohistochemischen Nachweis von TUNEL, aktivierter Caspase-3 und aktivierten Mikroglia verwendet. In getrennten Experimenten wurde der Blutdruck und weitere Blutparameter wie pCO₂, pO₂, Elektrolyte und Blutzucker zu verschiedenen Zeitpunkten vor, während und nach der MCAO gemessen. Die Ergebnisse zeigten, dass eine chronische Behandlung mit Lithium das Infarktvolumen senkte und den neurologischen „Outcome“ verbesserte. Die neuroprotektiven Effekte von Lithium waren begleitet von einer Reduktion der Expression der aktivierten Caspase-3 und einer Hemmung der DNA Fragmentierung in der ischämischen Penumbra des Gehirncortex. Im Gegensatz hierzu blieben das neurologische Defizit und das Infarktvolumen nach einer Behandlung mit Captopril unverändert. Die Zugabe von Lithium zu Captopril brachte keine zusätzliche Neuroprotektion, möglicherweise aufgrund einer zu starken Blutdrucksenkung während der Phase der MCAO und der Reperfusion. Eine Behandlung mit Captopril allein sowie in Kombination mit Lithium verminderte jedoch die Anzahl an Zellen mit positiver Immunreaktivität für aktivierte Caspase-3 und aktivierte Mikroglia und Makrophagen in der ischämischen Penumbra des Gehirncortex. Captopril könnte daher vorteilhafte Effekte auf den verzögerten neuronalen Zelltod nach einer Gehirnschämie haben. Telmisartan zeigte keine benefiziellen Wirkungen auf das neurologische Defizit und das Infarktvolumen. Die Kombinationstherapie mit Telmisartan und Lithium verbesserte das neurologische „Outcome“ und den Metabolismus und hemmte sowohl die aktivierte Caspase-3 wie auch die aktivierte

Mikroglia und Makrophagen in der ischämischen Penumbra des Gehirncortex. Die Zugabe von Telmisartan zu Lithium brachte jedoch keine zusätzlichen Vorteile im Vergleich zur alleinigen Lithiumbehandlung.

Zusammenfassend verhinderten beide Hemmstoffe des Renin-Angiotensin Systems vollständig das Auftreten eines Schlaganfalls bei salzbelasteten SHRSP und verlängerten deutlich das Überleben dieser Ratten. Die Ratten überlebten etwa 7 – 10 Monate und der Großteil der Tiere starb an Herz- und Nierenversagen. Unter diesen Bedingungen erbrachte eine zusätzliche Behandlung mit Lithium keine weiteren Vorteile. Im Modell der transienten, fokalen Gehirnschämie war Lithium neuroprotektiv wirksam. Es konnten jedoch keine synergistischen Interaktionen zwischen Lithium und Captopril oder Lithium und Telmisartan beobachtet werden.

References

Agha AM, Mansour M (2000) Effects of captopril on interleukin-6, leukotriene B(4), and oxidative stress markers in serum and inflammatory exudate of arthritic rats: evidence of antiinflammatory activity. *Toxicol Appl Pharmacol* 168:123-130

Ardailou R (1999) Angiotensin II receptors. *J Am Soc Nephrol* 10:S30-S39

Armstrong RC, Aja TJ, Hoang KD, Litwack G, Fritz LC, Tomaselli KJ (1997) Activation of the ced3/ICE-related protease CPP32 in cerebellar granule neurons undergoing apoptosis but not necrosis. *J Neurosci* 17:553-562

Aronowski J, Samways E, Strong R, Rhoades HM, Grotta JC (1996) An alternative method for the quantitation of neuronal damage after experimental middle cerebral artery occlusion in rats: analysis of behavioral deficit. *J Cereb Blood Flow Metab* 16:705-713

Banati RB, Gehrman J, Schubert P, Kreutzberg GW (1993) Cytotoxicity of microglia. *Glia* 7:111-118

Barnes PJ, Karin M (1997) Nuclear factor- κ B: a pivotal transcription factor in chronic inflammatory diseases. *N Engl J Med* 336:1066-1071

Barry DI, Paulson OB, Jarden JO, Juhler M, Graham DI, Strandgaard S (1984) Effects of captopril on cerebral blood flow in normotensive and hypertensive rats. *Am J Med* 76:79-85

Bederson JB, Pitts LH, Tsuji M, Nishimura MC, Davis RL, Bartkowski H (1986) Rat middle cerebral artery occlusion: evaluation of the model and development of a neurologic examination. *Stroke* 17:472-476

Bijur GN, De Sarno P, Jope RS (2000) Glycogen synthase kinase-3 β facilitates staurosporine- and heat shock-induced apoptosis. Protection by lithium. *J Biol Chem* 275:7583-7590

Birch NJ (1991) Lithium and the Cell: Pharmacology and Biochemistry. Academic, San Diego

Block F, Peters M, Nolden-Koch M (2000) Expression of IL-6 in the ischemic penumbra. Neuroreport 11:963-967

Bonfoco E, Krainc D, Ancarcrona M, Nicotera P, Lipton SA (1995) Apoptosis and necrosis: Two distinct events induced respectively by mild and intense insult with NMDA or nitric oxide/superoxide in cortical cell cultures. Proc. Natl. Acad. Sci. USA 91:7162-7166

Bonnet F, Cao Z, Cooper ME (2001) Apoptosis and angiotensin II: yet another renal regulatory system? Exp Nephrol 9:295-300

Braun JS, Jander S, Schroeter M, Witte OW, Stoll G (1996) Spatiotemporal relationship of apoptotic cell death to lymphomonocytic infiltration in photochemically induced focal ischemia of the rat cerebral cortex. Acta Neuropathol (Berl) 92:255-263

Bredesen DE (1995) Neural apoptosis. Ann Neurol 38:839-851

Camargo MJF, von Lutterotti N, Campbell WG, Pecker MS, James GD, Timmermans PB, Laragh JH (1993) Control of blood pressure and end-organ damage in maturing salt-loaded stroke-prone spontaneously hypertensive rats by oral angiotensin II receptor blockade. J Hypertens 11:31-40

Camargo MJF, von Lutterotti N, Pecker MS, James GD, Timmermans PBMWM, Laragh JH (1991) DuP 753 increases survival in spontaneously hypertensive stroke-prone rats fed a high sodium diet. Am J Hypertens 4:S341-S345

Cao Z, Kelly DJ, Cox A, Casley D, Forbes JM, Martinello P, Dean R, Gilbert RE, Cooper ME (2000) Angiotensin type 2 receptor is expressed in the adult rat kidney and promotes cellular proliferation and apoptosis. Kidney Int 58:2437-2451

Catto A, Carter AM, Barrett JH, Stickland M, Bamford J, Davies JA, Grant PJ (1996)

Angiotensin-converting enzyme insertion/deletion polymorphism and cerebrovascular disease. *Stroke* 27:435-440

Charriaut-Marlangue C, Aggoun-Zouaoui D, Represa A, Ben-Ari Y (1996)

Apoptotic features of selective neuronal death in ischemia, epilepsy and gp 120 toxicity. *Trends Neurosci* 19:109-114

Charriaut-Marlangue C, Margail I, Represa A, Popovici T, Plotkine M, Ben-Ari Y

(1996) Apoptosis and necrosis after reversible focal ischemia: an in situ DNA fragmentation analysis. *J cereb Blood Flow Metab* 16:186-194

Chen J, Jin K, Chen M, Pei W, Kawagechi K, Greenberg DA, Simon RP (1997)

Early detection of DNA strand breaks in the brain after transient focal ischemia: implications for the role of DNA damage in apoptosis and neuronal cell death. *J Neurochem* 69:232-245

Chen RW, Chuang DM (1999)

Long term lithium treatment suppresses p53 and Bax expression but increases Bcl-2 expression. A prominent role in neuroprotection against excitotoxicity. *J Biol Chem* 274:6039-6042

Cheng Y, Deshmukh M, D'Costa A, Demaro JA, Gidday JM, Shah A, Sun Y, Jacquin

MF, Johnson EM, and Holtzman DM (1998) Caspase inhibitor affords neuroprotection with delayed administration in a rat model of neonatal hypoxic-ischemic brain injury. *J Clin Invest* 101:1992-1999

Choi DW (1990) Cerebral hypoxia: some new approaches and unanswered questions. *J*

Neurosci 10:2493-2501

Choi DW (1992) Excitotoxic cell death. *J. Neurobiol* 23:1261-1276

Cohen JJ (1993) Overview: Mechanisms of apoptosis. *Immunol Today* 14:126-130

Cohen GM (1997) Caspases: the executioners of apoptosis. *Biochem J* 326:1-16

Coyle p (1982) Middle cerebral artery occlusion in the young rat. *Stroke* 13:855-859

Culman J, Baulmann J, Blume A, Unger T (2001) The renin-angiotensin system in the brain: an update. *J Renin Angiotensin Aldosterone Syst* 2:96-102

Culman J, von Heyer C, Piepenburg B, Rascher W, Unger T (1999) Effects of systemic treatment with irbesartan and losartan on central responses to angiotensin II in conscious, normotensive rats. *Eur J Pharmacol* 367:255-265

Dai W-J, Funk A, Herdegen T, Unger T, Culman J (1999) Blockade of central angiotensin AT1 receptors improves neurological outcome and reduces expression of AP-1 transcription factors after focal brain ischemia in rats. *Stroke* 30:2391-2399

Das S, Bhargava HN (1985) Effect of lithium treatment on blood pressure and angiotensin-converting enzyme activity in normotensive Wistar-Kyoto and spontaneously hypertensive rats. *Arch Int Pharmacodyn Ther* 276:82-91

de Gasparo M, Catt KJ, Inagami T, Wright JW, Unger Th (2000) International union of Pharmacology. XXIII. The angiotensin II receptors. *Pharmacol Rev* 52:415-472

de Torres C, Munell F, Ferrer I, Reventos J, Macaya A (1997) Identification of necrotic cell death by the TUNEL assay in the hypoxic-ischemic neonatal rat brain. *Neurosci Lett* 230:1-4

del Rio-Hortega P (1932) Microglia. In "Cytology and Cellular Pathology of the Nervous System" (Penfield W. ed.). pp. 481-584. Paul P. Hocker, Inc New York

Diep QN, Li JS, Schiffrin EL (1999) In vivo study of AT(1) and AT(2) angiotensin receptors in apoptosis in rat blood vessels. *Hypertension* 34:617-624

Diez J, Panizo A, Hernandez M, Vega F, Sola I, Fortuno MA, Pardo J (1997) Cardiomyocyte apoptosis and cardiac angiotensin-converting enzyme in spontaneously hypertensive rats. *Hypertension* 30:1029-1034

Dimmeler S, Rippmann V, Weiland U, Haendeler J, Zeiher AM (1997) Angiotensin II induces apoptosis of human endothelial cells. Protective effect of nitric oxide. *Circ Res* 81:970-976

D'Mello SR, Anelli R, Calissano P (1994) Lithium induces apoptosis in immature cerebellar granule cells but promotes survival of mature neurons. *Exp Cell Res* 211:332-338

Doi Y, Yoshinari M, Yoshizumi H, Ibayashi S, Wakisaka M, Fujishima M (1997) Polymorphism of the angiotensin-converting enzyme (ACE) gene in patients with thrombotic brain infarction. *Atherosclerosis* 132:145-150

Dybpunkt JM, Ankarcróna M, Burkitt M, Sjöholm A, Ström K, Orrenius S and Nicotera P (1995) Different prooxidant levels stimulate growth, trigger apoptosis, or produce necrosis of insulin-secreting RINm5F cells. *J Biol Chem* 269:30553-30560

Edling O, Bao G, Feelisch M, Unger T, Gohlke P (1995) Moexipril, a new angiotensin-converting enzyme (ACE) inhibitor: pharmacological characterization and comparison with enalapril. *J Pharmacol Exp Ther* 275:854-863

Ellis ML, Patterson JH (1996) A new class of antihypertensive therapy: angiotensin II receptor antagonists. *Pharmacotherapy* 16:849-860

Endres M, Namura S, Shimizu-Sasamata M, Waeber C, Zhang L, Gomez-Isla T, Hyman BT, Moskowitz MA (1998) Attenuation of delayed neuronal death after mild focal ischemia in mice by inhibition of the caspase family. *J Cereb Blood Flow Metab* 18:238-247

Evered MD, Robinson MM, Richardson MA (1980) Captopril given intracerebroventricularly, subcutaneously or by gavage inhibits angiotensin-converting enzyme activity in the rat brain. *Eur J Pharmacol* 68(4):443-449

Fernandez LA, Caride VJ, Stromberg C, Naveri L, Wicke JD (1994) Angiotensin AT₂ receptor stimulation increases survival in gerbils with abrupt unilateral carotid ligation. *J Cardiovasc Pharmacol* 24:937-940

Fernandez LA, Spencer DD, Kaczmar T Jr (1986) Angiotensin II decreases mortality rate in gerbils with unilateral carotid ligation. *Stroke* 17:82-85

Ferrer I, Tortosa A, Macaya A, Sierra A, Moreno D, Munell F, Blanco R, Squier W (1994) Evidence of nuclear DNA fragmentation following hypoxia-ischemia in the infant rat brain and transient forebrain ischemia in the adult gerbil. *Brain Pathol* 4:115-122

Filippatos G, Tilak M, Pinillos H, Uhal BD (2001) Regulation of apoptosis by angiotensin II in the heart and lungs (Review). *Int J Mol Med* 7:273-280

Fink K, Linmin Z, Namura S, Shimizu-Sasamata M, Endres M, Ma J, Dalkara T, Yuan J, Moskowitz M (1998) Prolonged therapeutic window for ischemic brain damage caused by delayed caspase activation. *J Cereb Blood Flow Metab* 18:1071-1076

Finley PR, O'Brien JG, Coleman RW (1996) Lithium and angiotensin-converting enzyme inhibitors: evaluation of a potential interaction. *J Clin Psychopharmacol* 16:68-71

Finley PR, Warner MD, Peabody CA (1995) Clinical relevance of drug interactions with lithium. *Clin Pharmacokinet* 29:172-191

Flaris NA, Densmore TL, Molleston MC, Hickey WF (1993) Characterization of microglia and macrophages in the central nervous system of rats: definition of the differential expression of molecules using standard and novel monoclonal antibodies in normal CNS and in four models of parenchymal reaction. *Glia* 7:34-40

Fornes P, Richer C, Vacher E, Bruneval P, Giudicelli JF (1993) Losartan's protective effects in stroke-prone spontaneously hypertensive rats persist durably after treatment withdrawal. *J Cardiovasc Pharmacol* 22:305-313

Fournier SA, Pruna A, El Esper N, Makdassi R, Oprisiu R, Westeel PF, Mazouz H, Achad J-M (2000) Captopril prevention project-what shall we do about captopril and the risk of stroke? *Nephrol Dial Transplant* 15:2-5

Friedlander RM, Gagliardini V, Hara H, Fink KB, Li W, MacDonald G, Fishman MC, Greenberg AH, Moskowitz MA, Yuan J (1997) Expression of a dominant negative mutant of interleukin-1 beta converting enzyme in transgenic mice prevents neuronal cell death induced by trophic factor withdrawal and ischemic brain injury. *J Exp Med* 185:933-940

Funk A, Blume A, Gohlke P, Dai WJ, Unger T, Culman J (2000) Effect of chronic inhibition of central AT1 receptors on the recovery from focal cerebral ischemia in normotensive rats. *J Hypertens* 18 (Supple 4):S92

Gagliardi RJ (2000) Neuroprotection, excitotoxicity and NMDA antagonists. *Arq Neuropsiquiatr* 58:583-588

Ganten D, Lang RE, Lehmann E, Unger T (1984) Brain angiotensin: on the way to becoming a well-studied neuropeptide system. *Biochem Pharmacol* 33:3523-3528

Garcia JH, Liu KF, Ho KL (1995a) Neuronal necrosis after middle cerebral artery occlusion in Wistar rats progresses at different time intervals in the caudoputamen and the cortex. *Stroke* 26:636-642

Garcia JH, Yoshida Y, Chen H, Li Y, Chopp M (1993) Progression from ischemic injury to infarct following middle-cerebral-artery occlusion in the rat. *Am J Pathol* 142:623-635

Garcia JH, Wagner S, Liu KF, Hu XJ (1995b) Neurological deficit and extent of neuronal necrosis attributable to middle cerebral artery occlusion in rats. *Stroke* 26:627-635

George R, Griffin JW (1994) Delayed macrophage responses and myelin clearance during Wallerian degeneration in the central nervous system: three dorsal radicotomy model. *Exp Neurol* 129:225-236

Geppetti P, Spillantini MG, Frilli S, Pietrini U, Fanciullacci M, Sicuteri F (1987) Acute oral captopril inhibits angiotensin converting enzyme activity in human cerebrospinal fluid. *J Hypertens* 5:151-154

Ginsberg MD, Pulsinelli WA (1994) The ischemic penumbra, injury thresholds, and the therapeutic window for acute stroke. *Ann Neurol* 36:553-554

Giulian D (1992) Microglia and disease of the nervous system. *Curr Top Neurol* 12:23-54

Giulian D (1997) Reative microglia and ischemic injury. In Welch KMA, Caplan LR, Reis DJ, Siesjö BK, Weir B, ed. *Primer on Cerebrovascular Diseases*. Academic Press, 117-124

Giulian D, Corpuz M, Chapman S, Mansouri M, Robertson C (1993) Reactive mononuclear phagocytes release neuron killing factors after stroke and trauma. *J Neurosci Res* 36:681-693

Gohlke P, Linz W, Schölkens BA, Wiemer G, Unger T (1996) Cardiac and vascular effects of long-term losartan treatment in stroke-prone spontaneously hypertensive rats. *Hypertension* 28:397-402

Gohlke P, Scholz A, Lehmann K, Unger T (1999) Lithium and the ACE inhibitor captopril act synergistically to prevent stroke in salt-loaded stroke-prone spontaneously hypertensive rats (SHRSP). *J Hypertens* 17(suppl.3):S142

Gohlke P, Urbach H, Scholkens B, Unger T (1989) Inhibition of converting enzyme in the cerebrospinal fluid of rats after oral treatment with converting enzyme inhibitors. *J Pharmacol Exp Ther* 249:609-616

Gohlke P, Von Kugelgen S, Jurgensen T, Kox T, Rascher W, Culman J, Unger T (2002) Effects of orally applied candesartan cilexetil on central responses to angiotensin II in conscious rats. *J Hypertens* 20:909-918

Gohlke P, Weiss S, Jansen A, Wienen W, Stangier J, Rascher W, Culman J, Unger T (2001) AT1 receptor antagonist telmisartan administered peripherally inhibits central responses to angiotensin II in conscious rats. *J Pharmacol Exp Ther* 298:62-70

Goodfriend TL, Elliott ME, Catt KJ (1996) Angiotensin receptors and their antagonists. *N Engl J Med* 334:1649-1654

Goodwin FK, Jamison KR (1990) Manic-Depressive Illness. New York: Oxford University Press

Gottron FJ, Ying HS, Choi DW (1997) Caspase inhibition selectively reduces the apoptotic component of oxygen-glucose deprivation-induced cortical neuronal cell death. *Mol Cell Neurosci* 9:159-169

Griendling KK, Lassegue B, Alexander RW (1996) Angiotensin receptors and their therapeutic implications. *Ann Rev Pharmacol Toxicol* 36:281-306

Hasgekar NN, Gokhale PP, Amin MK, Seshadri R, Lalitha VS (1996) Lithium inhibits growth in a murine neural precursor cell line. *Cell Biol Int* 20:781-786

Hashimoto R, Hough C, Nakazawa T, Yamamoto T, Chuang DM (2002) Lithium protection against glutamate excitotoxicity in rat cerebral cortical neurons: involvement of NMDA receptor inhibition possibly by decreasing NR2B tyrosine phosphorylation. *J Neurochem* 80:589-597

Hassan A, Markus HS (2000) Genetics and ischaemic stroke. *Brain* 123:1784-1812

Hengartner MO (2000) The Biochemistry of apoptosis. *Nature* 407:770-776

Hernandez-Presa M, Bustos C, Ortego M, Tunon J, Renedo G, Ruiz-Ortega M, Egido J (1997) Angiotensin-converting enzyme inhibition prevents arterial nuclear factor-kappa B activation, monocyte chemoattractant protein-1 expression, and macrophage infiltration in a rabbit model of early accelerated atherosclerosis. *Circulation* 95:1532-1541

Hernandez-Presa MA, Bustos C, Ortego M, Tunon J, Ortega L, Egido J (1998) ACE inhibitor quinapril reduces the arterial expression of NF-kappaB-dependent proinflammatory factors but not of collagen I in a rabbit model of atherosclerosis. *Am J Pathol* 153:1825-1837

Hickey WF, Vass K, Lassmann H (1992) Bone marrow-derived elements in the central nervous system: an immunohistochemical and ultrastructural survey of rat chimeras. *J Neuropathol Exp Neurol* 51:246-256

Hossmann KA (1994) Viability thresholds and the penumbra of focal ischemia. *Ann Neurol* 36:557-565

Inada Y, Ojima M, Itoh K, Shino A, Nishikawa K (1995) Effects of delapril on stroke, kidney dysfunction and cardiac hypertrophy in stroke-prone spontaneously hypertensive rats. *Drugs Exp Clin Res* 21:41-49

Inouye M, Yamamura H, Nakano A (1995) Lithium delays the radiation-induced apoptotic process in external granule cells of mouse cerebellum. *J Radiat Res* 36:203-208

Joje RS (1999) A bimodal model of the mechanism of action of lithium. *Mol Psychiatry* 4:21-25

Joje RS, Morrisett RA, Snead OC (1986) Characterization of lithium potentiation of pilocarpine induced status epilepticus in rats. *Exp Neurol* 91:471-480

Jordan FL, Thomas WE (1988) Brain macrophages: Questions of origin and interrelationship. *Brain Res Rev* 13:165-178

Kajstura J, Cigola E, Malhotra A, Li P, Cheng W, Meggs LG, Anversa P (1997) Angiotensin II induces apoptosis of adult ventricular myocytes in vitro. *J Mol Cell Cardiol* 29:859-870

Kaliszewski C, Fernandez LA, Wicke JD (1988) Differences in mortality rate between abrupt and progressive carotid ligation in the gerbil: role of endogenous angiotensin II. *J Cereb Blood Flow Metab* 8:149-154

Kato H, Kogure K, Liu XH, Araki T, Itoyama Y (1996) Progressive expression of immunomolecules on activated microglia and invading leukocytes following focal cerebral ischemia in the rat. *Brain Res* 734:203-212

Koizumi J, Yoshida Y, Nakazawa T, Ooneda G (1986) Experimental studies of ischemic brain edema, I: a new experimental model of cerebral embolism in rats in which recirculation can be introduced in the ischemic area. *Jpn J Stroke* 8:1-8

Kowala MC, Grove RI, Aberg Gm (1994) Inhibitors of angiotensin converting enzyme decrease early atherosclerosis in hyperlipidemic hamsters. Fosinopril reduces plasma cholesterol and captopril inhibits macrophage-foam cell accumulation independently of blood pressure and plasma lipids. *Atherosclerosis* 108:61-72

Kranzhofer R, Schmidt J, Pfeiffer CA, Hagl S, Libby P, Kubler W (1999) Angiotensin induces inflammatory activation of human vascular smooth muscle cells. *Arterioscler Thromb Vasc Biol* 19:1623-1629

Kyselovic J, Krenek P, Wibo M, Godfraind T (2001) Effects of amlodipine and lacidipine on cardiac remodelling and renin production in salt-loaded stroke-prone hypertensive rats. *Br J Pharmacol* 134:1516-1522

Laflamme N, Rivest S (1999) Effects of systemic immunogenic insults and circulating proinflammatory cytokines on the transcription of the inhibitory factor kappaB alpha within specific cellular populations of the rat brain. *J Neurochem* 73:309-321

Laragh JH, Sealey JE (1990) The renin-angiotensin-aldosterone system in hypertensive disorders: A key to two forms of arteriolar constriction and a possible clue to risk of vascular injury (heart attack and stroke) and prognosis. In Laragh JH, Brenner BM (eds). *Hypertension: Pathophysiology, Diagnosis, and Management*. New York, Raven Press Publishers, pp 1329-1348

Lee RM, Wang H, Smeda JS (1994) Effects of perindopril on hypertension and stroke prevention in experimental animals. *Can J cardiol* 10:33D-36D

Lees GJ (1993) The possible contribution of microglia and macrophages to delayed neuronal death after ischemia. *J Neurol Sci* 114:119-122

Lehmann K, Ritz E (1995) Angiotensin-converting enzyme inhibitors may cause renal dysfunction in patients on long-term lithium treatment. *Am J Kidney Dis* 25:82-87

Lehrmann E, Christensen T, Zimmer J, Diemer NH, Finsen B (1997) Microglial and macrophage reactions mark progressive changes and define the penumbra in the rat neocortex and striatum after transient middle cerebral artery occlusion. *J Comp Neurol* 386:461-476

Lenox RH, Manji HK (1998) Lithium. In: nemeroff CB, Schatzberg AF, editors. *American Psychiatric Press Textbook of Psychopharmacology*, 2nd Edition, Washington: American Psychiatric Press, pp 379-430

Leri A, Claudio PP, Li Q, Wang X, Reiss K, Wang S, Malhotra A, Kajstura J, Anversa P (1998) Stretch-mediated release of angiotensin II induces myocyte apoptosis by activating p53 that enhances the local renin-angiotensin system and decreases the Bcl-2-to-Bax protein ratio in the cell. *J Clin Invest* 101:1326-1342

Li D, Yang B, Philips MI, Mehta JL (1999) Proapoptotic effects of ANG II in human coronary artery endothelial cells: role of AT1 receptor and PKC activation. *Am J Physiol* 276:H786-792

Li H, Yuan J (1999) Deciphering the pathways of life and death. *Curr Opin Cell Biol* 11:261-266

Li R, Shen Y, El-Mallakh RS (1994) Lithium protects against ouabain-induced cell death. *Lithium* 5:211-216

Li Y, Chopp M, Jiang N, Yao F, Zaloga C (1995a) Temporal profile of in situ DNA fragmentation after transient middle cerebral artery occlusion in the rat. *J Cereb Blood Flow Metabol* 15:389-397

Li Y, Sharov VG, Jiang N, Zaloga C, Sabbah HN, Chopp M (1995b) Ultrastructural and light microscopic evidence of apoptosis after middle cerebral artery occlusion in the rat. *Am J Pathol* 146:1045-1051

Linnik MD, Zobrist RH, Hatfield MD (1993) Evidence supporting a role for programmed cell death in focal cerebral ischemia in rats. *Stroke* 24:2002-2009

Lipton P (1999) Ischemic cell death in brain neurons. *Physiol reviews* 79:1439-1443

Longa EZ, Weinstein PR, Carlson S, Cummins R (1989) Reversible middle cerebral artery occlusion without craniectomy in rats. *Stroke* 20:84-91

Lu R, Song L, Jope RS (1999) Lithium attenuates p53 levels in human neuroblastoma SH-SY5Y cells. *Neuroreport* 10:1123-1125

Mabuchi T, Kitagawa K, Ohtsuki T, Kuwabara K, Yagita Y, Yanagihara T, Hori M, Matsumoto M (2000) Contribution of microglia/macrophages to expansion of infarction and response of oligodendrocytes after focal cerebral ischemia in rats. *Stroke* 31:1735-1743

MacLeod AB, Vasdev S, Smeda JS (1997) The role of blood pressure and aldosterone in the production of hemorrhagic stroke in captopril-treated hypertensive rats. *Stroke* 28:1821-1829

Madiehe AM, Mampuru LJ, Tyobeka EM (1995) Induction of apoptosis in HL-60 cells by lithium. *Biochem Biophys Res Commun* 209:768-774

Manev H, Kharlamov A, Armstrong DM (1994) Photochemical brain injury in rats triggers DNA fragmentation, p53 and HSP72. *NeuroReport* 5:2661-2664

Manji HK, Moore GJ, Chen G (1999) Lithium at 50: have the neuroprotective effects of this unique cation been overlooked? *Biol Psychiatry* 46:929-940

Matsukawa T, Ichikawa I (1997) Biological functions of angiotensin and its receptors. *Ann Rev Physiol* 59:395-412

Matsunaga M, Yamamoto J, Hara A, Yamori Y, Ogino K (1975) Plasma renin and hypertensive vascular complications: an observation in the stroke-prone spontaneously hypertensive rat. *Jpn Circ J* 39:1305-1311

Mattson MP, Camandola S (2001) NF- κ B in neuronal plasticity and neurodegenerative disorders. *J Clin Invest* 107:247-254

Matussek N (1972) Biochemistry of depression. *J Neural Transm* 33:223-234

Meldrum B (1990) Protection against ischaemic neuronal damage by drugs acting on excitatory neurotransmission. *Cerebrovasc Brain Metab Rev* 2:27-57

Morrissey JJ, Klahr S (1997) Rapid communication. Enalapril decreases nuclear factor kappa B activation in the kidney with ureteral obstruction. *Kidney Int* 52:926-933

Nagaoka A, Iwatsuka H, Suzuoki Z, Okamoto K (1976) Genetic predisposition to stroke in spontaneously hypertensive rats. *Am J Physiol* 230:1354-1359

Nagasawa H, Kogure K (1989) Correlation between cerebral blood flow and histologic changes in a new rat model of middle cerebral artery occlusion. *Stroke* 20:1037-1043

Namura S, Zhu J, Fink K, Endres M, Srinivasan A, Tomaselli KJ, Yuan J, Moskowitz MA (1998) Activation and cleavage of caspase-3 in apoptosis induced by experimental cerebral ischemia. *J Neurosci* 18:3659-3668

Nishimura Y, Ito T, Saavedra JM (2000) Angiotensin II AT1 blockade normalizes cerebrovascular autoregulation and reduces cerebral ischemia in spontaneously hypertensive rats. *Stroke* 31:2478-2486

Nonaka S, Chuang DM (1998) Neuroprotective effects of chronic lithium on focal cerebral ischemia in rats. *Neuroreport* 9:2081-2084

Nonaka S, Hough CJ, Chuang DM (1998a) Chronic lithium treatment robustly protects neurons in the central nervous system against excitotoxicity by inhibiting N-methyl-D-aspartate receptor-mediated calcium influx. *Proc Natl Acad Sci U S A* 95:2642-2647

Nonaka S, Katsube N, Chuang DM (1998b) Lithium protects rat cerebellar granule cells against apoptosis induced by anticonvulsants, phenytoin and carbamazepine. *J Pharmacol Exp Ther* 286:539-547

Odaka C, Mizuochi T (2000) Angiotensin-converting enzyme inhibitor captopril prevents activation-induced apoptosis by interfering with T cell activation signals. *Clin Exp Immunol* 121:515-522

Okamoto K, Aoki K (1963) Development of a strain of spontaneously hypertensive rats. *Japan Circulation J* 27: 282-293

Okamoto K, Yamori Y, Nagaoka A (1974) Establishment of the stroke-prone spontaneously hypertensive rat (SHR). *Circ Res* 34-35(suppl I): I143-I153

Okamoto K, Yamori Y, Ooshima A, Tanaka T (1972) Development of substrains in spontaneously hypertensive rats; genealogy, isozymes and effects of hypercholesterolemic diet. *Japan Circulation J* 36:461-470

Okamoto M, Matsumoto M, Ohtsuki T, Taguchi A, Mikoshiba K, Yanagihara T, Kamada T (1993) Internucleosomal DNA cleavage involved in ischemia-induced neuronal death. *Biochem Biophys Res Commun* 196:1356-1362

Pascual T, Gonzalez JL (1995) A protective effect of lithium on rat behaviour altered by ibotenic acid lesions of the basal forebrain cholinergic system. *Brain Res* 695:289-292

Paulson OB, Vorstrup S, Andersen AR, Smith J, Godtfredsen J (1985) Converting enzyme inhibition resets cerebral autoregulation at lower blood pressure. *J Hypertens Suppl* Suppl 3:S487-S488

Paulson OB, Waldemar G, Andersen AR, Barry DI, Pedersen EV, Schmidt JF, Vorstrup S (1988) Role of angiotensin in autoregulation of cerebral blood flow. *Circulation* 77:I55-158

Paxinos G, Watson C (1986) *The Rat Brain in Stereotaxic Coordinates*. Second Edition. New York, Academic Press

- Perry VH, Andersson PB, Gordon S (1993)** Macrophages and inflammation in the central nervous system. *Trends Neurosci* 16:268-273
- Perry VH, Gordon S (1988)** Macrophages and microglia in the nervous system. *Topics Neurosci* 11:273-277
- Phillips MI (1987)** Functions of angiotensin in the central nervous system. *Annu Rev Physiol* 49:413-435
- Phillips MI, Summers C (1998)** Angiotensin II in central nervous system physiology. *Regul Pept* 78:1-11
- Plesnila N, Moskowitz MA (2000)** Caspase in cerebral ischemia. In: *Pharmacology of cerebral ischemia* (Krieglstein J and Klumpp S, eds), pp 137-143. Stuttgart, Germany: Medpharm Scientific
- Polidori C, Ciccocioppo R, Nisato D, Cazaubon C, Massi M (1998)** Evaluation of the ability of irbesartan to cross the blood-brain barrier following acute intragastric treatment. *Eur J Pharmacol* 352:15-21
- Portera-Cailliau C, Hedreen JC, Price DL, Koliastos VE (1995)** Evidence for apoptotic cell death in Huntington disease and excitotoxic animal models. *J Neurosci* 15:3775-3787
- Qin ZH, Wang Y, Nakai M, Chase TN (1998)** Nuclear factor- κ B contributes to excitotoxin-induced apoptosis in rat striatum. *Mol Pharmacol* 53:33-42
- Rabuffetti M, Sciorati C, Tarozzo G, Clementi E, Manfredi AA, Beltramo M (2000)** Inhibition of caspase-1-like activity by Ac-Tyr-Val-Ala-Asp-chloromethyl ketone induces long-lasting neuroprotection in cerebral ischemia through apoptosis reduction and decrease of proinflammatory cytokines. *J Neurosci* 20:4398-4404
- Ravati A, Junker V, Kouklei M, Ahlemeyer B, Culmsee C, Krieglstein J (1999)** Enalapril and moexipril protect from free radical-induced neuronal damage in vitro and reduce ischemic brain injury in mice and rats. *Eur J Pharmacol* 373:21-33

Richer C, Fornes P, Vacher E, Bruneval P, Giudicelli JF (1994) Trandolapril's protective effects in stroke-prone spontaneously hypertensive rats persist after treatment withdrawal. *Am J Cardiol* 73:26C-35C

Robertson GS, Xu DG, Nicholson DW (1998) Identification of neurons undergoing apoptosis following transient global and focal ischemia by immunohistochemical detection of conformationally active caspase-3. *Soc Neurosci Abstr* 24:1225

Saavedra JM, Ito T, Nishimura Y (2001) The role of angiotensin II AT1 receptors in the regulation of the central blood flow and brain ischemia. *JRAAS* 2:S102-S109

Savill J, Fadok V, Henson P, Haslett C (1993) Phagocyte recognition of cells undergoing apoptosis. *Immunol. Today* 14:131-136

Schielke GP, Yang GY, Shivers BD, Betz AL (1998) Reduced ischemic brain injury in interleukin-1 beta converting enzyme-deficient mice. *J Cereb Blood Flow Metab* 18:180-185

Schmid-Elsaesser R, Zausinger S, Hungerhuber E, Baethmann A, Reulen HJ (1998) A critical reevaluation of the intraluminal thread model of focal cerebral ischemia. *Stroke* 29:2162-2170

Schneider A, Martin-Villalba A, Weih F, Vogel J, Wirth T, Schwaninger M (1999) NF- κ B is activated and promotes cell death in focal cerebral ischemia. *Nat Med* 5:554-559

Schurr A, Rigor BM (1998) Brain anaerobic lactate production: a suicide note or a survival kit? *Dev Neurosci* 20:348-357

Shenoy UV, Richards EM, Huang XC, Sumners C (1999) Angiotensin II type 2 receptor-mediated apoptosis of cultured neurons from newborn rat brain. *Endocrinology* 140:500-509

Shibota M, Nagaoka A, Shino A, Fujita T (1979) Renin-angiotensin system in stroke-prone spontaneously hypertensive rats. *Am J Physiol* 236:H409-H416

Shionoiri H (1993) Pharmacokinetic drug interactions with ACE inhibitors. Clin Pharmacokinet 25:20-58

Silverstone T, Romans S (1996) Long term treatment of bipolar disorder. Drugs 51:367-382

Smeda J, Vasdev S, King SR (1999) Effect of poststroke captopril treatment on mortality associated with hemorrhagic stroke in stroke-prone rats. J Pharmacol Exp Ther 291:569-575

Smeda JS (1989) Hemorrhagic stroke development in spontaneously hypertensive rats fed a North American, Japanese-style diet. Stroke 20:1212-1218

Sparapani M, Virgili M, Ortali F, Contestabile A (1997) Effects of chronic lithium treatment on ornithine decarboxylase induction and excitotoxic neuropathology in the rat. Brain Res 765:164-168

Stier CT Jr, Adler LA, Levine S, Chander PN (1993) Stroke prevention by losartan in stroke-prone spontaneously hypertensive rats. J Hypertens Suppl 11:S37-S42

Stier CT Jr, Benter IF, Ahmad S, Zuo HL, Selig N, Roethel S, Levine S, Itskovitz HD (1989) Enalapril prevents stroke and kidney dysfunction in salt-loaded stroke-prone spontaneously hypertensive rats. Hypertension 13:115-121

Stier CT Jr, Chander P, Gutstein WH, Levine S, Itskovitz HD (1991) Therapeutic benefit of captopril in salt-loaded stroke-prone spontaneously hypertensive rats is independent of hypotensive effect. Am J Hypertens 4:680-687

Stier CT Jr, Benter IF, Levine S (1988) Thromboxane A2 in severe hypertension and stroke in stroke-prone spontaneously hypertensive rats. Stroke 19:1145-1150

Stoll G, Jander S, Schroeter M (1998) Inflammation and glial responses in ischemic brain lesions. Prog Neurobiol 56:149-171

Stoll G, Trapp BD, Griffin JW (1989) Macrophage function during Wallerian degeneration of the rat optic nerve: clearance of degenerating myelin and Ia expression. *J Neurosci* 9:2327-2335

Stoll M, Steckelings UM, Paul M, Bottari SP, Metzger R, Unger T (1995) The angiotensin AT₂-receptor mediates inhibition of cell proliferation in coronary endothelial cells. *J Clin Invest* 95:651-657

Streit WJ, Graeber MB, Kreutzberg GW (1988) Functional plasticity of microglia: A review. *Glia* 1:301-307

Swanson RA, Morton MT, Trsao-Wu G, Savalos RA, Davidson CM, Sharp FR (1990) A semiautomated method for measuring brain infarct volume. *J Cereb Blood Flow Metab* 10:290-293

Tamura A, Graham DI, McCulloch J, Teasdale GM (1981) Focal cerebral ischemia in the rat: 1. Description of technique and early neuropathological consequences following middle cerebral artery occlusion. *J. Cereb. Blood Flow Metab* 1:53-60

Tanaka M, Ohnishi J, Ozawa Y, Sugimoto M, Usuki S, Naruse M, Murakami K, Miyazaki H (1995) Characterization of angiotensin II receptor type 2 during differentiation and apoptosis of rat ovarian cultured granulosa cells. *Biochem Biophys Res Commun* 207:593-598

Tominaga T, Kure S, Narisawa K, Yoshimoto T (1993) Endonuclease activation following focal ischemic injury in the rat brain. *Brain Res* 608:21-26

Uhal BD, Gidea C, Bargout R, Bifero A, Ibarra-Sunga O, Papp M, Flynn K, Filippatos G (1998) Captopril inhibits apoptosis in human lung epithelial cells: a potential antifibrotic mechanism. *Am J Physiol* 275:L1013-1017

Unger T (2000) Neurohormonal modulation in cardiovascular disease. *Am Heart J* 139:S2-S8

Unger T, Badoer E, Ganten D, Lang RE, Rettig R (1988) Brain angiotensin: pathways and pharmacology. *Circulation* 77(Suppl 1):I40-I54

Unger T, Culman J, Gohlke P (1998) Angiotensin II receptor blockade and end-organ protection: pharmacological rationale and evidence. *J Hypertens Suppl* 16:S3-S9

Unger T, Ganten D, Lang RE (1983) Pharmacology of converting enzyme inhibitors: new aspects. *Clin Exp Hypertens A* 5:1333-1354

Vacher E, Fornes P, Domergue V, Richer C, Bruneval P, Giudicelli JF (1993) Quinapril prevents stroke both during and after the treatment period in stroke-prone spontaneously hypertensive rats. *Am J Hypertens* 6:951-959

van der Staay FJ, Augstein KH, Horvath E (1996) Sensorimotor impairments in rats with cerebral infarction, induced by unilateral occlusion of the left middle cerebral artery: strain differences and effects of the occlusion site. *Brain Res* 735:271-284

Velier JJ, Ellison JA, Kikly KK, Spera PA, Barone FC, Feuerstein GZ (1999) Caspase-8 and caspase-3 are expressed by different populations of cortical neurons undergoing delayed cell death after focal stroke in the rat. *J Neurosci* 19:5932-5941

Volonte C, Rukenstein A (1993) Lithium promotes short-term survival of PC12 cells after serum and NGF deprivation. *Lithium* 4:211-219

Volpe M, Camargo MJ, Mueller FB, Campbell WG Jr, Sealey JE, Pecker MS, Sosa RE, Laragh JH (1990) Relation of plasma renin to end organ damage and to protection of K⁺ feeding in stroke-prone hypertensive rats. *Hypertension* 15:318-326

Vraamark T, Waldemar G, Strandgaard S, Paulson OB (1995) Angiotensin receptor antagonist CV-11974 and cerebral blood flow autoregulation. *J Hypertens* 13:755-761

Wagner J, Drab M, Bohlender J, Amann K, Wienen W, Ganten D (1998) Effects of AT1 receptor blockade on blood pressure and the renin-angiotensin system in spontaneously hypertensive rats of the stroke prone strain. *Clin Exp Hypertens* 20:205-221

Wahl F, Allix M, Plotkine M, Boulu RG (1992) Neurological and behavioral outcomes of focal cerebral ischemia in rats. *Stroke* 23:267-272

Walther T, Olah L, Harms C, Maul B, Bader M, Hörtnagl H, Schultheiss HP, Mies G (2002) Ischemic injury in experimental stroke depends on angiotensin II. *FASEB J* 16:169-176

Wang R, Ibarra-Sunga O, Verlinski L, Pick R, Uhal BD (2000) Abrogation of bleomycin-induced epithelial apoptosis and lung fibrosis by captopril or by a caspase inhibitor. *Am J Physiol Lung Cell Mol Physiol* 279:L143-L151

Werner C, Hoffmann WE, Kochs E, Rabito SF, Miletich DJ (1991) Captopril improves neurological outcome from incomplete cerebral ischemia in rats. *Stroke* 22:910-914

Wienen W, Entzeroth M, van Meel JCA, Stangier J, Busch U, Ebner T, Schmid J, Lehmann H, Matzek K, Kempthorne-Rawson J, Gladigau V, Huel NH (2000) A review on telmisartan: a novel, long-acting angiotensin II-receptor antagonist. *Cardiovas Drug Reviews* 18:127-156

Wyllie AH, Kerr JF, Currie AR (1980) Cell death: The significance of apoptosis. *Int Rev Cytol* 68:251-306

Yamada T, Horiuchi M, Dzau VJ (1996) Angiotensin II type 2 receptor mediates programmed cell death. *Proc Natl Acad Sci USA* 93:156-160

Yuan P, Chen G, Manji HK (1999) Lithium activates the c-Jun NH₂-terminal kinases in vitro and in the CNS in vivo. *J Neurochem* 73:2299-2309.

Zhang Y, Pardridge WM (2001) Conjugation of brain-derived neurotrophic factor to a blood-brain barrier drug targeting system enables neuroprotection in regional brain ischemia following intravenous injection of the neurotrophin. *Brain Res* 889:49-56

Zhang ZG, Chopp M, Powers C (1997) Temporal profile of microglial response following transient (2h) middle cerebral artery occlusion. *Brain Res* 744:189-198

Acknowledgements

I especially thank Priv.-Doz. Dr. Peter Gohlke for his guidance, encouragement, and providing me the opportunity to perform this study. His critical review and patient proof-reading of my thesis is also greatly appreciated. I would like to thank Professor Albrecht Ziegler for his valuable support and advice.

I wish to express my sincere gratitude to all members in the Institute of Pharmacology who have been involved in this study. I deeply thank Dr. Juraj Culman for his valuable advice and constant support for this work. I would like to express my sincere appreciation to Dr. Annegret Blume and Dr. Stephan Brecht for their generous help on immunohistochemical methodologies. My sincere thanks also go to Ms. Jutta Finger and Mr. Jan Brdon for their kind help. I would like to acknowledge Professor Thomas Unger, who invited me to the institute and gave me the opportunity to start with the project, and to Professor Thomas Herdegen for the financial support and giving me the opportunity to finish my work.

I would like to thank PD Dr. Reinhold Kreutz, Institute of Clinical Pharmacology, University Clinic Benjamin Franklin, Berlin, for the determination of urinary albumin concentrations. My deepest thanks go to my family providing me with endless support, understanding and encouragement.

This work would not be possible without the financial support from Deutsches Institut für Bluthochdruckforschung (DIB) and from the Forschungszentrum Integrative Neurowissenschaften (FZIN).

Curriculum Vitae

Personal Data

Jihong Xu
born on July 20, 1969, Zhejiang, P. R. China
Nationality: Chinese

Education

11/1999-11/2002	Ph. D Study Institute of Pharmacology Christian-Albrechts-University of Kiel Germany
09/1991-07/1994	Graduate Study Department of Pharmacology Zhejiang Medical University P. R. China
1994	Master in Pharmacology
09/1987-07/1991	Undergraduate Study Department of Pharmaceutical Science Zhejiang Medical University P. R. China
1991	Bachelor of Science
1976-1987	Primary and High School in Zhejiang P. R. China

Work Experience

09/1994-08/1997	Research and Teacher Assistant Department of Pharmacology Zhejiang Medical University P. R. China
09/1997-11/1999	Lecturer Department of Pharmacology College of Medicine in Zhejiang University P. R. China

Publication List

XU J, CULMAN J, UNGER TH, GOHLKE P (2001). Telmisartan improves survival in salt-loaded stroke prone spontaneously hypertensive rats. *Dtsch Med Wschr* 126 (suppl. 3), S192.

GROTH W, XU J, GOHLKE P, BLUME A, UNGER T, CULMAN J (2002). Systemic treatment with AT1 receptor antagonists: Neurological outcome and infarction volume after focal brain ischemia in the rat. *J Hypertens* 20 (suppl. 4), S 147.

XU J, CULMAN J, BLUME A, UNGER T, GOHLKE P (2002). Effect of telmisartan and lithium on survival in salt-loaded stroke-prone spontaneously hypertensive rats (SHRSP). *J Hypertens* 20 (suppl. 4), S146.

GROTH W, GOHLKE P, XU J, BLUME A, UNGER TH, CULMAN J (2002). Neurological outcome and infarction volume after focal brain ischemia in normotensive rats: effects of systemic treatment with AT1 receptor antagonists. *Naunyn-Schmiedeberg's Arch Pharmacol* 365 (suppl. 1), R68.

XU J, CULMAN J, BLUME A, UNGER T, GOHLKE P (2002). Treatment with telmisartan and lithium of stroke-prone spontaneously hypertensive rats: survival study. *Naunyn-Schmiedeberg's Arch Pharmacol* 365 (suppl. 1), R67

XU J, CULMAN J, BLUME A, BRECHT S, GOHLKE P. Chronic treatment with a low dose of lithium protects the brain against ischemic injury by reducing apoptotic death. *Stroke* (submitted).